Cary D. Harbor
Vice President
Regulatory & Oversight

Palo Verde
Nuclear Generating Station
P.O. Box 52034
Phoenix, AZ 85072
Mail Station 7602
Tel: 623.393.7953

102-08633-CDH/MSC
July 26, 2023

U.S. Nuclear Regulatory Commission
ATTN: Document Control Desk
Washington, DC 20555-0001

Subject: **Palo Verde Nuclear Generating Station Units 1, 2, and 3**
Docket Nos. STN 50-528, 50-529, and 50-530
Renewed Operating License Number NPF-41, NPF-51, and NPF-74
License Renewal Pressurizer Surge Line Inspection

Reference: Safety Evaluation Report Related to the License Renewal of Palo Verde
Nuclear Generating Station, Units 1, 2, and 3 published as NUREG-1961,
dated April 2011 [Agencywide Documents Access and Management
System (ADAMS) Accession Number ML11095A011]

Consistent with the above reference, Arizona Public Service Company (APS) is
committed to manage the effects of environmentally assisted fatigue (EAF) of the
reactor coolant pressure boundary during the period of extended operation. Specifically,
when any monitored location fatigue usage factor including EAF projects to exceed 1.0,
corrective actions will be established using one or more of the following approaches:

1. Determine whether the scope of the enhanced Metal Fatigue of Reactor Coolant
   Pressure Boundary program must be enlarged to include additional affected
   reactor coolant pressure boundary locations. This determination will ensure that
   other locations do not approach design limits without an appropriate action.
2. Adjust fatigue monitoring methods to confirm continued conformance to the
   code limit.
3. Repair/modify the component.
4. Replace the component.
5. Perform a more rigorous analysis of the component to demonstrate that the
   design code limit will not be exceeded.
6. Modify plant operating practices to reduce the fatigue usage accumulation rate.
7. Perform a flaw tolerance evaluation and impose component-specific inspections,
   under ASME Section XI Appendices A or C (or their successors) and obtain
   required approvals from the regulatory agency.

For Palo Verde Nuclear Generating Station (PVNGS) Units 1, 2, and 3, monitored
locations on the pressurizer surge line are projected to exceed a cumulative usage
fatigue factor of 1.0 when considering the effects of EAF. APS intends to manage the
aging effects of EAF on the pressurizer surge line using approach seven described
above, namely periodic inspections performed at a frequency determined by a flaw

tolerance evaluation in accordance with ASME Section XI, Non-Mandatory Appendix L, *Operating Plant Fatigue Assessment*. Accordingly, the enclosure provides the description of the flaw tolerance evaluation and proposed inspections for NRC Staff review and approval.

A pre-submittal meeting for the pressurizer surge line inspection license renewal submittal was held between APS and the Nuclear Regulatory Commission (NRC) staff on May 25, 2023. Approval of the proposed method to manage aging due to EAF for the pressurizer surge line is requested by July 26, 2024. Once approved, the proposed method to manage aging due to EAF for the pressurizer surge line will be implemented within 120 days.

No new commitments are being made to the NRC by this letter.

Should you need further information regarding this letter, please contact Matthew S. Cox, Licensing Department Leader, at (623) 393-5753.

Sincerely,

Harbor, Cary (Z16762)

Digitally signed by Harbor, Cary (Z16762)
Date: 2023.07.26 15:42:19 -07'00'

CDH/MSC/cr

Enclosure: Proposed Method to Manage Environmentally Assisted Fatigue for the Pressurizer Surge Line

cc: R. J. Lewis   Acting NRC Region IV Regional Administrator
     S. P. Lingam   NRC NRR Project Manager for PVNGS
     L. N. Merker   NRC Senior Resident Inspector for PVNGS
     B. D. Goretzki   Arizona Department of Health Services – Bureau of
                        Radiation Control

ENCLOSURE

PROPOSED METHOD TO MANAGE ENVIRONMENTALLY ASSISTED FATIGUE FOR THE PRESSURIZER SURGE LINE

Submittal of Pressurizer Surge Line Inspection Program

ATTACHMENT(S):

Attachment 1: Structural Integrity Associates Report No. 2000645.402, *Flaw Tolerance Evaluation of the Palo Verde Units 1, 2, and 3 Surge Line Piping using ASME Code, Section XI, Appendix L*, Revision 0, dated March 2, 2023

PROPOSED METHOD TO MANAGE ENVIRONMENTALLY ASSISTED FATIGUE FOR THE PRESSURIZER SURGE LINE

1.0 BACKGROUND

Arizona Public Service Company (APS) license renewal application for Palo Verde Nuclear Generating Station (PVNGS) Units 1, 2, and 3 (Reference 1) describes the program (X.M1) for managing Metal Fatigue of the Reactor Coolant Pressure Boundary utilizing cycle counting and cumulative usage fatigue (CUF) factor tracking to ensure the actual plant experience remains bounded by design assumptions and calculation, including the effects of environmentally assisted fatigue (EAF), during the period of extended operation (PEO). As described in UFSAR Section 19.2.1, *Metal Fatigue of Reactor Coolant Pressure Boundar*y (Reference 6), when any monitored location usage factor including EAF are projected to exceed 1.0, corrective actions will be established using one or more of the following approaches:

1. Determine whether the scope of the enhanced Metal Fatigue of Reactor Coolant Pressure Boundary program must be enlarged to include additional affected reactor coolant pressure boundary locations. This determination will ensure that other locations do not approach design limits without an appropriate action.

2. Adjust fatigue monitoring methods to confirm continued conformance to the code limit.

3. Repair/modify the component.

4. Replace the component.

5. Perform a more rigorous analysis of the component to demonstrate that the design code limit will not be exceeded.

6. Modify plant operating practices to reduce the fatigue usage accumulation rate.

7. Perform a flaw tolerance evaluation and impose component-specific inspections, under ASME Section XI Appendices A or C (or their successors) and obtain required approvals from the regulatory agency.

As reflected in the Nuclear Regulatory Commission (NRC) Safety Evaluation Report (SER) for PVNGS, Units 1, 2, and 3 License Renewal Application (Reference 2), if an inspection program is proposed as the basis for aging management, the proposed aging management program (AMP) should ensure that (a) inspections will be performed for the specific component(s) or structure(s) in the evaluation, and (b) the inspection methods and frequencies in the proposed inspection program are applicable to the component(s), such that they may be used to demonstrate compliance with the requirement in 10 CFR 54.21(c)(1)(iii), which states:

The effects of aging on the intended function(s) will be adequately managed for the period of extended operation.

For PVNGS Units 1, 2, and 3, monitored locations on the pressurizer surge line are projected to exceed a CUF factor of 1.0 when considering the effects of EAF.

Consideration of the effects of EAF is required in the PEO. The bounding or sentinel location is the elbow immediately above the hot leg surge nozzle. At this location, the CUF factor considering the effects of EAF will exceed 1.0 upon entry into the PEO. For 60 years of operating cycles, the maximum projected EAF usage is 4.27 for Unit 1 (Reference 3), 4.66 for Unit 2 (Reference 4), and 5.86 for Unit 3 (Reference 5).

APS intends to manage the aging effects of EAF on the pressurizer surge line using approach seven described above, namely periodic inspections performed at a frequency determined by a flaw tolerance evaluation in accordance with ASME Section XI, Non-Mandatory Appendix L, *Operating Plant Fatigue Assessment*. Accordingly, Sections 2, 3 and 4 provide a description of the flaw tolerance evaluation, the inspection program, aging management program attributes, and implementation plan for NRC review and approval.

The current licensing basis analyses do not consider the effects of EAF. The pressurizer surge lines were analyzed as ASME Code Class 1 components to ASME Section III requirements. ASME Class 1 components are analyzed for metal fatigue per ASME NB-3600 and associated Code requirements. These analyses consider the design transients described in UFSAR Section 3.9.1.1, *Design Transients* (Reference 6). The pressurizer surge line analysis includes the effects of thermal stratification as required by NRC Bulletin 88-11, *Pressurizer Surge Line Thermal Stratification*, by incorporating the results of the Combustion Engineering Owners Group (CEOG) analysis CEN-387-NP, *Pressurizer Surge Line Flow Stratification Evaluation*, Revision 1-NP-A. This report consists of a generic bounding analysis for CEOG plants including PVNGS.

Design rules specified in NB-3200 were applied in the CEOG analysis. Since the originally specified set of design transients did not include any stratified flow loading conditions, the CEOG analysis developed a revised set of design basis transients based on test data acquired at PVNGS and other CEOG plants. One bounding set of transients were developed that could then be utilized by each CEOG plant. The analysis superimposed specified thermal stratification events for each assumed heatup and cooldown transient. The resulting fatigue analysis demonstrated that cumulative usage factor for locations on the pressurizer surge line was less than the Code limit of 1.0.

NUREG-1800, *Standard Review Plan for Review of License Renewal Applications for Nuclear Power Plants*, Revision 2 (Reference 7), Section 4.3.1, states:

> *The effects of fatigue for the initial 40-year reactor license period were studied and resolved under Generic Safety Issue (GSI)-78, "Monitoring of Fatigue Transient Limits for Reactor Coolant System and GSI-166, "Adequacy of Fatigue Life of Metal Components."*

These NRC studies concluded that conservatisms in the original fatigue calculations rendered a backfit of the environment fatigue data to operating plants unjustified. As such, the current license basis fatigue calculations are not required to address or consider EAF. For the PEO, explicit consideration of EAF is required and is the subject of this ASME Section XI, Non-Mandatory Appendix L, flaw tolerance evaluation specific to PVNGS pressurizer surge lines.

2.0   FLAW TOLERANCE EVALUATION DESCRIPTION

The proposed pressurizer surge line inspections are based on the flaw tolerance approach described in ASME Section XI, Non-Mandatory Appendix L. Appendix L has been approved by the ASME Code and has been implemented and used successfully for managing fatigue for extended plant operation in several pressurized water reactors (Refer to Section 5.0 of this enclosure).

PVNGS Units 1, 2, and 3 surge line is 12-inch nominal pipe size, schedule 160, ASME SA-376 or SA-312 Grade TP304 pipe and SA-403 Grade WP304 elbows.

A fatigue flaw tolerance evaluation was performed specifically for PVNGS to assess the operability of the pressurizer surge line by using inspections and the ASME Section XI, Appendix L, methodology to determine the successive inspection interval for the pressurizer surge line with a postulated inside diameter (ID) surface-connected reference flaws (Reference 8). From a survey of the stresses, load cycles and calculated crack growth in the pressurizer surge line, the bounding locations were identified and evaluated in detail.

The bounding locations for determining the successive inspection interval are the butt welds on a horizontally oriented elbow approximately mid-length between the pressurizer and the hot leg (welds 30B and 30E in Table 1). From a comparison of geometry, material properties, and applicable loads, the evaluation of the bounding location is also applicable to the other pipe and weld locations on the pressurizer surge line.

A detailed evaluation was also performed for the pressurizer surge line hot leg elbow base metal, which is the EAF sentinel location for the pressurizer surge line. That evaluation utilizing crack growth and flaw tolerance methodology that take guidance from Section XI, Appendix L and Appendix C, and other industry references, determined that the successive inspection interval is bounded by the pressurizer surge line elbow butt welds, and thus will be performed at the same interval (Reference 8).

The terminal ends of the pressurizer surge line at the pressurizer nozzle and hot leg nozzle do not project to greater than a CUF factor of 1.0 considering EAF and thus are not within the scope of this Appendix L submittal. However, PVNGS already performs periodic examinations of the full structural weld overlays (WOLs) on these nozzles. The successive examination interval of these two (2) WOLs is consistent (i.e., 10 years) with that determined for the pressurizer surge line welds and base metal elbows within this ASME Appendix L submittal.

The results of the crack growth and flaw tolerance evaluations for the weld locations are presented in Table 1 and elbow base metal in Table 2. The technical analysis of the flaw tolerance evaluation is provided in Reference 8.

Weld ID	Paths	Semi-Elliptical Axial Flaw					360-Degree Circumferential Flaw			
		Flaw size in 10 Years			Allowable a/t	N, years	Flaw size in 10 Years		Allowable a/t	N, years
		a, inch	c, inch	a/t			a, inch	a/t		
20B	P1	0.2336	0.5972	0.1781	0.75	≥100	0.2500	0.1906	0.2523	22
	P2	0.2321	0.5963	0.1769	0.75	≥100	0.2513	0.1915	0.2523	21
	P3	0.2443	0.6037	0.1862	0.75	≥100	0.2660	0.2027	0.2523	**17**
	P4	0.2332	0.5966	0.1778	0.75	≥100	0.2475	0.1886	0.2523	22
20E	P1	0.2575	0.6158	0.1963	0.75	≥100	0.2466	0.1879	0.3155	34
	P2	0.2324	0.5978	0.1772	0.75	≥100	0.2702	0.2059	0.3155	24
	P3	0.2537	0.6128	0.1934	0.75	≥100	0.3173	0.2418	0.3155	**15**
	P4	0.2603	0.6183	0.1984	0.75	≥100	0.3296	0.2512	0.3155	**14**
27	P1	0.2302	0.5953	0.1755	0.75	≥100	0.2505	0.1909	0.4282	52
	P2	0.2304	0.5954	0.1756	0.75	≥100	0.2474	0.1885	0.4282	57
	P3	0.2274	0.5930	0.1733	0.75	≥100	0.2474	0.1885	0.4282	57
	P4	0.2316	0.5962	0.1765	0.75	≥100	0.2833	0.2159	0.4282	29
30B	P1	0.2635	0.6213	0.2008	0.75	99	0.2487	0.1896	0.3117	32
	P2	0.2455	0.6068	0.1871	0.75	≥100	0.2474	0.1886	0.3117	34
	P3	0.2447	0.6057	0.1865	0.75	≥100	0.2474	0.1886	0.3117	34
	P4	0.2469	0.6074	0.1882	0.75	≥100	0.3236	0.2466	0.3117	**14**
30E	P1	0.2623	0.6203	0.1999	0.75	≥100	0.2485	0.1894	0.2957	29
	P2	0.2456	0.6068	0.1872	0.75	≥100	0.2661	0.2028	0.2957	23
	P3	0.2471	0.6076	0.1883	0.75	≥100	0.3191	0.2432	0.2957	**13**
	P4	0.2490	0.6091	0.1898	0.75	≥100	0.3206	0.2444	0.2957	**13**
50B	P1	0.2389	0.6009	0.1821	0.75	≥100	0.2464	0.1878	0.4238	56
	P2	0.2357	0.5994	0.1796	0.75	≥100	0.2537	0.1934	0.4238	49
	P3	0.2511	0.6102	0.1914	0.75	≥100	0.2487	0.1896	0.4238	52
	P4	0.2471	0.6074	0.1884	0.75	≥100	0.2978	0.2270	0.4238	25
50E	P1	0.2437	0.6042	0.1858	0.75	≥100	0.2468	0.1881	0.4314	57
	P2	0.2358	0.5994	0.1797	0.75	≥100	0.2474	0.1886	0.4314	57
	P3	0.2517	0.6107	0.1918	0.75	≥100	0.2482	0.1891	0.4314	55
	P4	0.2469	0.6073	0.1882	0.75	≥100	0.2999	0.2286	0.4314	25
60B	P1	0.2415	0.6029	0.1841	0.75	≥100	0.2539	0.1935	0.4512	51
	P2	0.2373	0.6000	0.1808	0.75	≥100	0.2522	0.1922	0.4512	55
	P3	0.2385	0.6009	0.1818	0.75	≥100	0.2488	0.1896	0.4512	60
	P4	0.2304	0.5949	0.1756	0.75	≥100	0.2808	0.2141	0.4512	30
60E	P1	0.2317	0.5964	0.1766	0.75	≥100	0.2543	0.1938	0.4207	47
	P2	0.2315	0.5959	0.1764	0.75	≥100	0.2609	0.1989	0.4207	38
	P3	0.2453	0.6052	0.1870	0.75	≥100	0.2504	0.1909	0.4207	51
	P4	0.2406	0.6022	0.1834	0.75	≥100	0.2584	0.1969	0.4207	40

Table 1: PVNGS Pressurizer Surge Line Fatigue Crack Growth Results-Welds

Notes for Table 1:
1. The postulated initial axial flaw depth is determined from Table IWB-3410-1 using a flaw aspect ratio of 0.167 and a component thickness of 1.312 inches, resulting is an initial flaw depth of 0.1885 inches and flaw length of 1.131.
2. The postulated initial circumferential flaw depth is 0.1885 inches with a 360-degree circumferential extent.

3. The allowable flaw a/t from ASME Section XI, Appendix C, Table C-5310-5 for circumferential flaws and Table C-5410-1 for axial flaws.
4. Per Appendix L, if the allowable operating period is equal to or greater than 10 years, the successive inspection schedule shall be equal to the examination interval listed in the PVNGS ASME Section XI Schedule of Inservice Inspection (ISI) program, or 10 years.

Table 2: PVNGS Pressurizer Surge Line Fatigue Crack Growth Results-Elbow Base Metal					
	Semi-Elliptical Axial Flaw (Flank)				
Location (Elbow Flank)	Flaw size in 10 years			Allowable a/t	N, years
	a, inch	C, inch	a/t		
Elbow 60	0.3520	0.7192	0.2683	0.75	50
Elbow 30	0.2982	0.6548	0.2273	0.74	72

Notes for Table 2:
1. The postulated initial axial flaw depth is determined from Table IWB-3410-1 using a flaw aspect ratio of 0.167 and a component thickness of 1.312 inches, resulting is an initial flaw depth of 0.1885 inches and flaw length of 1.131.
2. Allowable flaw sizes: depth-to-thickness ratio (a/t) from ASME Section XI, Appendix C, Table C-5410-1.
3. Inspection interval of pressurizer surge line elbow base metal will be the same as the inspection schedule for the Table 1 welds (i.e., 10 years).

3.0 INSPECTION ATTRIBUTES

The attributes of the pressurizer surge line inspection program, consistent with the attributes delineated in NUREG-1800, Revision 2 (Reference 7), are discussed below:

1. Scope of the Program

   The pressurizer surge line welds listed in Table 3 will be examined in accordance with ASME Section XI, and will use acceptance criteria of Section XI, IWB for Class 1 welds. In addition, the elbow base metal for the pressurizer surge line elbows will be examined in accordance with ASME Code, Section XI procedures capable of detecting thermal fatigue with acceptance criteria from ASME Section III, NB-2500. The aging effect managed with these inspections is cracking due to EAF. Figure 1 provides the location of the pressurizer surge line welds and elbows.

| Table 3: PVNGS Pressurizer Surge Line-Inspection Summary			
Weld/Elbow No.	Last Examination Performed & Results	Allowable Operating Period per ASME Appendix L Analysis (Note 1)	Proposed Inspections Type/Frequency
20B	U1-Ultrasonic (UT) Spring 2022 (1R23) U2-UT Spring 2023 (2R24) U3-UT Fall 2022 (3R23) *Inspections identified no detectable flaws*	Greater than 10 years	Volumetric Once in 10 years
20E	U1-UT Spring 2022 (1R23) U2-UT Spring 2023 (2R24) U3-UT Fall 2022 (3R23) *Inspections identified no detectable flaws*	Greater than 10 years	Volumetric Once in 10 years
27	U1-UT Spring 2022 (1R23) U2-UT Spring 2023 (2R24) U3-UT Fall 2022 (3R23) *Inspections identified no detectable flaws*	Greater than 10 years	Volumetric Once in 10 years
30B	U1-UT Spring 2022 (1R23) U2-UT Spring 2023 (2R24) U3-UT Fall 2022 (3R23) *Inspections identified no detectable flaws*	Greater than 10 years	Volumetric Once in 10 years

Table 3: PVNGS Pressurizer Surge Line-Inspection Summary			
Weld/Elbow No.	Last Examination Performed & Results	Allowable Operating Period per ASME Appendix L Analysis (Note 1)	Proposed Inspections Type/Frequency
30E	U1-UT Spring 2022 (1R23) U2-UT Spring 2023 (2R24) U3-UT Fall 2022 (3R23) *Inspections identified no detectable flaws*	Greater than 10 years	Volumetric Once in 10 years
50B	U1-UT Spring 2022 (1R23) U2-UT Spring 2023 (2R24) U3-UT Fall 2022 (3R23) *Inspections identified no detectable flaws*	Greater than 10 years	Volumetric Once in 10 years
50E	U1-UT Spring 2022 (1R23) U2-UT Spring 2023 (2R24) U3-UT Fall 2022 (3R23) *Inspections identified no detectable flaws*	Greater than 10 years	Volumetric Once in 10 years
60B	U1-UT Spring 2022 (1R23) U2-UT Spring 2023 (2R24) U3-UT Fall 2022 (3R23) *Inspections identified no detectable flaws*	Greater than 10 years	Volumetric Once in 10 years
60E	U1-UT Spring 2022 (1R23) U2-UT Spring 2023 (2R24) U3-UT Fall 2022 (3R23) *Inspections identified no detectable flaws*	Greater than 10 years	Volumetric Once in 10 years
Surge line elbow (Elbow 60)	U1-UT Spring 2022 (1R23) U2-UT Spring 2023 (2R24) U3-UT Fall 2022 (3R23) *Inspections identified no detectable flaws*	Greater than 10 years (Note 2)	Volumetric Once in 10 years (Note 2)
Surge line elbow (Elbow 30)	U2-UT Spring 2023 (2R24) *Inspections identified no detectable flaws*	Greater than 10 years (Note 2)	Volumetric Once in 10 years (Note 2)

Notes for Table 3:
1. The inspection frequency as determined by ASME Code Section XI, Appendix L, analysis is more than 10 years. In accordance with the requirements of Appendix L Table-3420-1, the pressurizer surge line welds will be examined at a 10 year interval.
2. The inspection frequency for the pressurizer surge line elbow base metal as determined by equivalent or similar to ASME Code Section XI, Appendix L, methodology is more than 10 years. Pressurizer surge line elbows will have base metal examinations performed at the same interval/frequency as the pressurizer surge line welds.

Figure 1: Monitored Pressurizer Surge Line Welds and Elbows
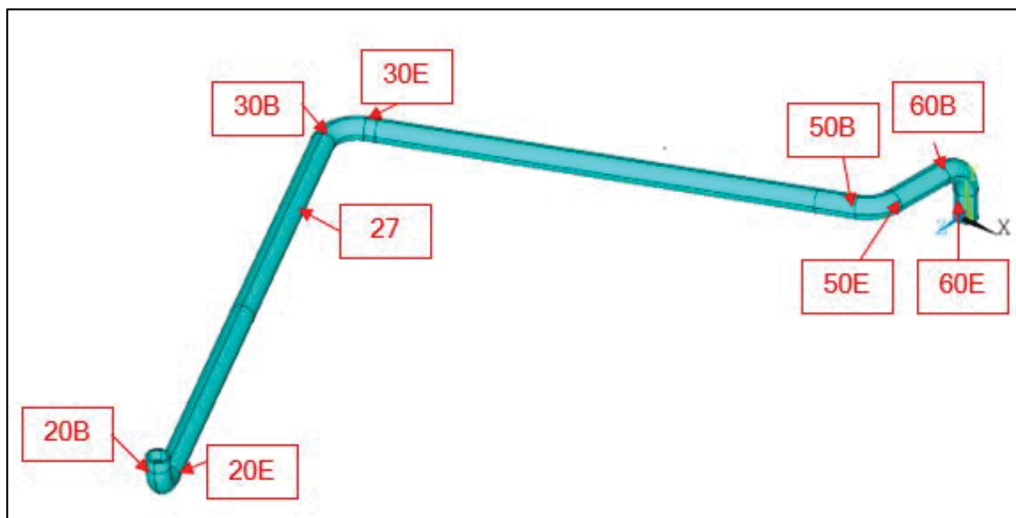
During the PEO, examinations of the pressurizer surge line piping welds and the base metal of the pressurizer surge line elbows base metal will be performed at a ten-year inspection interval in accordance with the PVNGS Inservice Inspection (ISI) Program. The pressurizer surge line welds have been examined in PVNGS Units 1, 2, and 3, and were absent of flaws larger than the applicable ASME acceptance standards, as required for applicability of ASME Section XI, Appendix L. Additionally, the sentinel elbow base metal component have been examined in PVNGS Units 1, 2, and 3, and were absent of flaws larger than the applicable ASME, Section III, acceptance standards, which supports the use of guidance from ASME Section XI, Appendix L.

Examinations results are evaluated by qualified individuals in accordance with ASME Section XI and Section III, as applicable, acceptance criteria. Components with indications that meet these acceptance criteria are considered acceptable for continued service.

2. Preventive Actions

    There are no specific preventive actions under these inspections to prevent the effects of aging.

3. Parameter(s) Monitored or Inspected

    Future ISI examinations for the pressure surge line elbow welds and pressurizer surge line elbow base metal are planned to be volumetric examinations at the frequency of 10 years.

4. Detection of Aging Effects

    The degradation of the monitored pressurizer surge line components is determined by volumetric examinations in accordance with the requirements of the PVNGS ISI program. The frequency and scope of examinations are sufficient to ensure that the aging fatigue effects are detected before the integrity of the pressurizer surge line would be compromised.

    The pressurizer surge line is subject to a thermal degradation per the site N-716-1, *Alternative Classification and Examination Requirements, Section XI, Division 1*, risk informed program documented in MN756-A00031, *Palo Verde ASME Code Case N-716-1 Program Updated (2022)*, and the ISI program manuals, 4INT-ISI-1,2,3, *4th Inspection Interval Inservice Inspection Program Summary Manual – PVGS Unit 1, 2, and 3*. Examinations are conducted using performance demonstration initiative procedure for austenitic material and MRP-36 trained examiners. Examination volume of the welds include extended exam volumes as addressed in MRP-36 and base metal exams used scanning techniques consistent with MRP-36 training.

    In preparation for the initial pressurizer surge line thermal fatigue examinations, flawed samples were used to train examiners for detection of thermal fatigue. In addition to scanning flawed samples, examiners who had previous MRP-36 training reviewed the training material along with any newly trained MRP-36 examiners.

5. <u>Monitoring and Trending</u>

The frequency and scope of the examinations are sufficient to ensure that the EAF effects are detected before the intended function of the pressurizer surge line is compromised. Volumetric examinations will be performed in accordance with the inspection intervals based on the results of the postulated flaw tolerance evaluations performed in accordance with or based on guidance from the ASME Section XI, Appendix L, methodology.

Flaws identified in the pressurizer surge line components will be evaluated by engineering to assess the effect of EAF and determine impacts on the EAF analysis. Records of the examination procedures, results of activities, examination databases, and corrective actions taken or recommended will be maintained in accordance with the requirements of PVNGS ISI Program and ASME Section XI.

6. <u>Acceptance Criteria</u>

Acceptance standards for the ISI examinations of the pressurizer surge line welds are identified in Section XI, Subsection IWB for Class 1 components. Table IWB-3410 identifies the acceptance standards listed in IWB-3500. Acceptance standards for pressurizer surge line elbow base metal are identified in Section III, NB-2500. Flaws found in the pressurizer surge line components that are revealed by the volumetric examinations require additional flaw evaluation per the requirements of ASME Section XI or replacement.

Flaws that exceed the acceptance criteria will be entered into the PVNGS corrective action program. Acceptance for continued service with flaws that do not meet the applicable acceptance standards will be corrected by repair, replacement or analytical flaw evaluation performed in accordance with or guidance from ASME Section XI, Appendices A or C, and other industry references as applicable.

Repairs or replacements will be performed in accordance with ASME Section XI, Subsection IWA-4000, as described in PVNGS procedure, *Repair/Replacement-ASME Section XI*.

7. <u>Corrective Actions</u>

Condition Reports are generated in accordance with the PVNGS corrective action program for flaws that exceed the acceptance criteria. Components with examination results that do not meet applicable acceptance criteria are subject to acceptance by analytical flaw evaluation and/or acceptance by repair or replacement in accordance with subsection IWA-4000. Evaluation of flaws in elbow base metal will utilize guidance from Section XI, Appendices A and C, and other Industry references as applicable.

8. <u>Confirmation Process</u>

When degradation is identified in pressurizer surge line components, an engineering evaluation is performed to determine if the components are

acceptable for continued service or if repair or replacement is required. The engineering evaluation includes probable causes, the extent of degradation, the nature and frequency of additional examinations, and whether repair or replacement is required.

Repairs or replacements will be performed in accordance with ASME Section XI, Subsection IWA-4000, as described in PVNGS procedure, *Repair/Replacement-ASME Section XI*.

9. Administrative Controls

The PVNGS ISI Program will document the EAF inspection requirements for the PVNGS pressurizer surge lines under the ASME Section XI, ISI Program. Site Quality Assurance procedures, review and approval processes, and administrative controls are implemented in accordance with the requirements of Appendix B of 10 CFR Part 50 and will continue to be applicable for the PEO.

PVNGS procedures utilized include:

1) *Condition Reporting Process*

2) *Repair/ Replacements-ASME Section XI*

10. Operating Experience

The PVNGS pressurizer surge line welds and sentinel pressurizer surge line elbow base metal were examined ultrasonically during each Unit's most recent refueling outage (Unit 1-Spring 2022, Unit 3-Fall 2022, Unit 2-Spring 2023). No reportable flaws were identified in any of the examinations. The programmatic operating experience activities described in relevant station procedures ensure adequate evaluation of operating experience on an ongoing basis to address age-related degradation and aging management of the pressurizer surge lines.

There have been no incidents of thermal fatigue cracking in the pressurizer surge line piping of U.S. Pressurized Water Reactor (PWR) plants. However, the effects of high thermal cycles and environmental fatigue are recognized as potential contributors to plant aging (Reference 9). There are numerous industry programs in place to identify, monitor and mitigate the effects of thermal cycling and thermal fatigue cracking in PWRs (e.g., see References 10 and 11), and these lessons and guidelines have been applied to the PVNGS pressurizer surge lines as demonstrated by the combination of fatigue monitoring and inspections of the pressurizer surge lines in order to manage the effects of fatigue for extended plant operation.

The proposed inspections to examine the pressurizer surge line components at the specified interval as shown in Table 3, provides reasonable assurance that potential environmental effects of fatigue will be managed such that the pressurizer surge lines will continue to perform their intended function for the extended PEO in PVNGS Units 1, 2, and 3.

Corrective actions, confirmation process and administrative controls for license renewal are in accordance with the PVNGS Quality Assurance Program pursuant to 10 CFR Part 50, Appendix B, which governs structures, systems, and components subject to an aging management review.

4.0 IMPLEMENTATION PLAN

Upon NRC approval (within 120 days) of the PVNGS pressurizer surge line EAF management approach, the appropriate inspection procedure(s) will be updated accordingly.

5.0 PRECEDENT

The proposed method to manage aging due to EAF for the pressurizer surge line is similar to the following applications that have been approved by the NRC:

- Turkey Point, Units 3 and 4, License Renewal Commitment, Submittal of Pressurizer Surge Line Welds Inspection Program (ADAMS Accession Numbers ML12152A156 and ML13141A595).

- St. Lucie, Units 1 and 2 – License Renewal Commitment, Submittal of Pressurizer Surge Line Welds Inspection Program (ADAMS Accession Numbers ML15314A160 and ML16235A138).

- Arkansas Nuclear One, Unit 2, License Renewal Pressurizer Surge Line and Safety Injection Nozzle Inspection (ADAMS Accession Number ML18144A970 and ML19074A028).

6.0 REFERENCES

1. Palo Verde License Renewal Application dated December 11, 2008 and updated through Amendment 31

2. NRC Safety Evaluation Report Related to the License Renewal of Palo Verde Nuclear Generating Station, Units 1, 2, and 3 published as NUREG-1961, dated April 2011 (ADAMS Accession Number ML11095A011)

3. Structural Integrity Report FP-PV-321, Palo Verde 2022 Unit 1 FP4 Update Through 04/30/22-RFO 23, dated August, 2022

4. Structural Integrity Report FP-PV-320, Palo Verde Unit 2 FP4 Update Through 10/30/21-RFO 23, dated April, 2022

5. Structural Integrity Report FP-PV-319, Palo Verde 2021 Unit 3 FP4 Update Through 04/30/21-RFO 22, dated November, 2021

6. Palo Verde Nuclear Generating Station (PVNGS) Units 1, 2, and 3 Updated Final Safety Analysis Report (UFSAR) Revision 22, dated June 2023.

7. NUREG-1800, Revision 2, Standard Review Plan for Review of License Renewal Applications for Nuclear Power Plants, dated December 2010

8. Structural Integrity Report 2000645.402 R0, Flaw Tolerance Evaluation of the Palo Verde Units 1, 2, and 3 Surge Line Piping using ASME Code Section XI, Appendix L, dated March 2, 2023 [Provided as Attachment 1 of this enclosure].
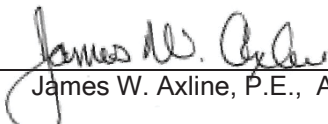
9. Third International Conference on Fatigue of Reactor Components, EPRI/USNRC/CSNI, Seville, Spain, 3-6 October, 2004.

10. Materials Reliability Program: Lessons Learned From PWR Thermal Fatigue Management Training (MRP-83), EPRI, Palo Alto, CA: 2002. 1003666.

11. Materials Reliability Program: Fatigue Management Handbook (MRP-235, Revision 2), EPRI, Palo Alto, CA. 2015. 3002005510.

ENCLOSURE
PROPOSED METHOD TO MANAGE ENVIRONMENTALLY ASSISTED
FATIGUE FOR THE PRESSURIZER SURGE LINE

Attachment 1

Structural Integrity Associates Report No. 2000645.402, *Flaw Tolerance*
Evaluation of the Palo Verde Units 1, 2, and 3 Surge Line Piping using ASME
*Code, Section XI, Appendix L***, Revision 0, dated March 2, 2023**

Flaw Tolerance Evaluation of the Palo Verde Units 1, 2, and 3 Surge Line Piping using ASME Code, Section XI, Appendix L

Prepared For:

Palo Verde Generating Station, Units 1, 2, & 3
Arizona Public Service Company
5801 S. Wintersburg Road
Tonopah, AZ

Contract Number 500636760

Structural Integrity Associates, Inc.
San Jose, California

Prepared by: _James W. Axline_   Date: 3/2/2023
James W. Axline, P.E., Associate

Reviewed by: _Dominguez_   Date: 3/2/2023
Garivalde S. Dominguez, Senior Engineer

Approved by: _R. A. Mattson_   Date: 3/2/2023
Richard A. Mattson, P.E., Senior Associate

REGISTERED PROFESSIONAL ENGINEER
JAMES W. AXLINE
M 17802
EXP. 9/30/2023
MECHANICAL
STATE OF CALIFORNIA

REVISION CONTROL SHEET

Report Number:	2000645.402			
Title:	Flaw Tolerance Evaluation of the Palo Verde Units 1, 2, and 3 Surge Line Piping using ASME Code, Section XI, Appendix L			
Client:	Arizona Public Service			
SI Project Number: 2000645.00		**Quality Program:** ☒ Nuclear ☐ Commercial		

SECTIONS	PAGES	REVISION	DATE	COMMENTS
All	All	0	3/2/2023	Initial Issue

Structural Integrity Associates, Inc.®

TABLE OF CONTENTS

LIST OF TABLES

LIST OF FIGURES

1.0 INTRODUCTION

Palo Verde Generating Station (PVGS), Units 1, 2, and 3 has committed to managing the fatigue of the Reactor Coolant System (RCS) Pressure Boundary, including the effects of Environmentally Assisted Fatigue (EAF), in accordance with its 60-year license renewal commitments. In support of the fatigue management program, PVGS has requested an alternative ASME Boiler and Pressure Vessel (B&PV) Code, Section XI, Appendix L flaw evaluation at the critical locations on the pressurizer surge line where the fatigue cumulative fatigue usage factor, when EAF is considered, will exceed acceptance criteria.

A flaw tolerance evaluation in accordance with the 2013 Edition of the ASME B&PV Code, Section XI, Nonmandatory Appendix L [1] was performed in this project to manage environmentally assisted fatigue at the critical locations of the PVGS Units 1, 2, and 3 pressurizer surge lines. The evaluation determined both that the provisions of Appendix L are met, and the required successive examination interval at these locations.

PVGS already performs periodic examinations of the full structural weld overlays (WOL) on the hot leg surge nozzle and pressurizer surge nozzle. The successive examination intervals of these two (2) WOL's are addressed separately and are not included in this report. The two WOL nozzle welds on the surge line are not subject to NRC approval per the PVGS License Renewal Commitment for Metal Fatigue, since the cumulative fatigue usage factors considering EAF (U_{en}) are projected to remain less than 1.0

Details of the determination of inspection intervals for these two WOL's are contained in Reference [2] and Reference [3]. The crack growth duration service life of the postulated flaws in the two weld overlaid nozzle ends of the surge line piping are greater than 10 years.

The Appendix L flaw tolerance evaluation is contained in References [4] through [7], and focuses on the surge line piping alone, and not the RCS piping, as the RCS pipe welds are addressed separately. The limiting Appendix L locations are shown in Table 6-3. The crack growth duration service life of the postulated flaws in the surge line piping elbows and butt welds are greater than 10 years.

2.0 TECHNICAL APPROACH

The evaluation was performed in accordance with the requirements of the 2013 Edition of the ASME B&PV Code, Section XI, Appendix L [1]. Effective 8/17/2017, the latest ASME B&PV Code edition approved by the NRC is the 2013 Edition, which includes Section XI, Appendix L. Code Case (CC) N-809 [8], which includes the latest crack growth data, has been approved by ASME. Although Code Case N-809 has not been officially endorsed by the NRC, the NRC has reviewed and approved the use of CC N-809 in precedent license renewal commitments pertaining to fatigue of surge line welds for Turkey Point (Submittal: ML12152A156 and Approval: ML1314A595) and St. Lucie (Submittal: ML15314A160 and Approval: ML16235A138). Both evaluations used the same crack growth models and data, which were published at an EPRI conference prior to ASME approval of the Code Case.

All butt weld locations on the surge line, excluding the pressurizer and hot leg surge nozzles that have been weld overlaid on all three Units, are evaluated. The pressurizer and hot leg surge nozzle weld overlays are addressed separately.

The methodology used to determine the successive inspection schedule consists of the following principal tasks:

- Determine the loads [4] and stresses [5, 6] at the critical locations in the surge line (all butt welds) (Sections 3.0 and 4.0).

- Use the stresses at the critical locations to determine the allowable flaw depths for various service levels [7] (Section 5.0).

- Postulate hypothetical flaws at the critical locations. Select appropriate crack models to simulate the postulated flaws [6]. Both axial and circumferential flaws will be considered. (Section 6.0).

- Use the stresses determined at the critical locations and the selected crack models to compute stress intensity factors for all the applicable normal and upset condition loads. Perform fatigue crack growth (FCG) analyses with the resulting stress intensity factors to determine the end-of-evaluation-period flaw size and/or determine the time (allowable

operating period) necessary for the postulated initial flaw to grow to the allowable flaw depth [6] (Section 6.0).

However, other work on assessment of EAF for the surge line piping components has identified that a location on the hot leg elbow body has the highest fatigue usage (F_{en}). The elbows in the surge line were evaluated to determine the successive examination interval in Reference [6], and the conclusion of this evaluation is that the FCG of the postulated flaw at the elbow flanks (elbow 30 and elbow 60 locations) showed that it will take a significantly greater duration before the postulated flaw grows to the allowable size, compared to the bounding flaw at the butt weld 30E location. Thus, examination of the butt welds and the surge line elbows at the examination interval determined by the butt weld is conservative.

The following Sections 2.1 and 2.2 provide a high-level technical overview of the heat transfer, fluid dynamics, and transient definitions used in the development of the loads for assessment at the various locations.

2.1   Heat Transfer Coefficients

As described in the following, heat transfer coefficients for specific locations on the surge line are calculated based on surge flow during thermal transients. These coefficients are needed for the thermal transient analysis (Section 4.0).

The thermal transient loads are based on Reference [4] and consist of heat transfer coefficients and bulk fluid temperatures as a function of time. Heat transfer coefficients are applied to the inside surface of the elbows and piping. The outside surfaces of the surge line are covered with 3 inches of insulation [9, Appendix D, page 3-12]. All outside surfaces of the pressurizer surge line piping are conservatively assumed to be perfectly insulated. The heat transfer coefficients (HTC) are calculated as follows:

$$\text{HTC} = 2167 \frac{(\text{flow rate}/1{,}000{,}000)^{0.8}}{(D_i/12)^{1.8}} \tag{2-1}$$

where: flow rate = Inside pipe flow rate, lb/hr

$\quad\quad\quad\quad D_i$ = Inside diameter of surge piping (inch) = 10.126 in [10]

The equation above is based on Reference [11, Section 3.3], where a conservative value of temperature of 656°F is used. Table 2-5 lists the heat transfer coefficients under different flow rates.

2.2   Thermal Stratification and Thermal Anchor Movement

Thermal stratification can potentially occur during each transient if the required flow rate and temperature conditions are mutually satisfied. If the flow rate is high enough, then an insurge or outsurge will sweep the line, preventing thermal stratification. If the flow rate operates in a sufficiently low flow regime and there is a temperature difference between the pressurizer and RCS hot leg, then a thermally stratified interface may develop due to the buoyancy caused by the density differences of the fluid above and below the fluid flow boundary layer. When the low flow rate changes but remains within the flow regime necessary to maintain stratification conditions, the stratified interface may move up or down, resulting in local stress perturbations.

For each transient definition, the surge flow rate history, in addition to pressurizer water and hot leg temperatures, are provided. It is desirable to use these parameters to determine if stratification exists at each point in time during the transient, and if so to also determine the stratified interface level and the top and bottom surge line temperatures.

The stratification phenomena are driven by the difference in temperature between the pressurizer and the hot leg. This temperature effect is observed in the surge line pipe. This analysis defines the difference in temperature to be located at exactly ½ the vertical distance through the pipe cross-section, where vertical is the global y-axis (see Figure 2-3). The static thermal solutions for the stratification conditions are combined with the anchor displacements for a combined stress result.

In the thermal stratification event, the temperature of the top half of the surge line is considered as the hot part (T_{top}) while the bottom half is considered as the cold part (T_{bottom}).

For the high-pressure stratification events, T_{top} is equal to 653°F (consistent with the high pressure insurge/outsurge events defined in Table 2-1) and T_{bottom} is equal to 653°F - ΔT. For the low-pressure stratification events, T_{top} is 440°F (consistent with the low pressure insurge/outsurge events defined in Table 2-1) and the lower pipe temperature is equal to 440°F - ΔT. Finally, the hot standby events are treated as high pressure events [12]. This

generates nine (S1 through S9) different stratification conditions. Table 2-4 shows the definitions of stratification for various events [12].

The thermal anchor displacements are applied to the cut-boundaries of the model, and the temperature distributions from the stratification thermal solutions are also applied for a combined stress result. In calculating the scaling factors for the thermal anchor displacements, the T used in Equation 4-1 is equal to T_{bottom} while the T used in Equation 4-2 is equal to T_{top}. Table 4-3 shows the scaled anchor point displacements which are combined with the thermal stratification results.

Thermal stratification is also applied to transients Trans18 and Trans19. The temperature distribution in the inside surface of the surge line such as T_{top} and T_{bottom} are dependent on the flow rate of the insurge and outsurge (insurge flow rates are positive and outsurge flow rates are negative). Based on experience and engineering judgement, the following are assumed in the stratified conditions for Trans18 and Trans19:

If the flow rate is less than -70,000 lb/hr, the event is considered as full outsurge, where

$$T_{top} = T_{bottom} = T_{PZR}. \tag{2-2}$$

If the flow rate is greater than 22,000 lb/hr, the event is considered as full insurge, where

$$T_{top} = T_{bottom} = T_{HL}. \tag{2-3}$$

Elsewhere, if the flow rate is between -70,000 lb/hr and 22,000 lb/hr, the event is considered as stratified outsurge, where

$$T_{top} = T_{PZR}, \quad T_{bottom} = T_{HL}. \tag{2-4}$$

T_{PZR} and T_{HL}, defined in Reference [4, Table 5], are the pressurizer temperature and hot leg temperature, respectively. Using the relations above, the transient definitions of Trans18 and Trans19 are summarized in Table 2-3.

Table 2-1: Thermal Transient Definitions [1]

Transient ID	Description	Time, sec	Temp, °F	Temp. rate, °F/hr	Pressure, psia	Flow Rate lb/hr	Annual Cycles
Tran1	Plant Heatup	0	70		15	43200	1.398 [3]
		16560	540	102	2250	43200	
Tran2	Plant Cooldown	0	540		2250	43200	1.390 [3]
		16560	70	-102	15	43200	
Tran3	Loss of Flow, Loss of Load	0	621.2		2250	0	0.531 [3]
		100	551.2	-2520	[2]	0	
Tran6	Plant Unloading, 10% Step Down	0	653		2250	108000	2.695 [3]
		0	593		2250	108000	
Tran7	Plant Unloading, 10% Step Up	0	593		2250	108000	2.695 [3]
		0	653		2250	108000	
Tran9	Leak Test, 2250 psia, Up	0	160		400	0	0.042 [3]
		10800	400	80	2250	0	
Tran10	Leak Test, 2250 psia, Down	0	400		2250	0	0.042 [3]
		10800	160	-80	400	0	
Tran11	Insurge/Outsurge Heatup, ΔT = 300°F	0	440		381	43200	19.4 [4]
		180	140	-6000	381	43200	
		3780	140	0	381	43200	
		3960	440	6000	381	43200	
Tran12	Insurge/Outsurge Heatup, ΔT = 250°F	0	440		381	43200	52.3 [4]
		150	190	-6000	381	43200	
		1050	190	0	381	43200	
		1200	440	6000	381	43200	
Tran13	Insurge/Outsurge Heatup, ΔT = 150°F	0	440		381	43200	35.93 [4]
		300	290	-1800	381	43200	
		600	290	0	381	43200	
		900	440	1800	381	43200	
Tran14	Insurge/Outsurge Heatup, ΔT = 100°F	0	653		2250	43200	69.17 [4]
		600	553	-600	2250	43200	
		660	553	0	2250	43200	
		1260	653	600	2250	43200	
Tran15	Insurge/Outsurge Cooldown, ΔT = 250°F	0	440		381	43200	7.4 [4]
		500	190	-1080	381	43200	
		1400	190	0	381	43200	
		1900	440	1080	381	43200	
Tran16	Insurge/Outsurge Cooldown, ΔT = 150°F	0	440		381	43200	3.7 [4]
		300	290	-1800	381	43200	
		600	290	0	381	43200	
		900	440	1800	381	43200	
Tran17	Insurge/Outsurge Cooldown, ΔT = 100°F	0	653		2250	43200	6.73 [4]
		200	553	-1800	2250	43200	
		260	553	0	2250	43200	
		460	653	1800	2250	43200	

Notes:
1. This table is based on Table 5 and Table 7 of Reference [4].
2. Maximum pressure of 2550 psia occurs at 60 seconds, minimum pressure of 1650 psia occurs at 100 seconds.
3. The annual cycles are derived from Table 5 of Reference [4].
4. The annual cycles are derived from Table 7 of Reference [4].

Table 2-2: Reactor Trip Transient Definitions [1]

Transient ID	Description	Time, sec	Temp, °F	Temp. rate, °F/hr	Pressure, psia	Flow Rate, lb/hr	Annual Cycles
Tran4	Reactor Trip	0	621		2280	108000	3.06
		35	621		2400	108000	
		40	621		2280	108000	
		130	618	-120	2195	108000	
		220	615	-120	2214	108000	
		640	572	367	2305	108000	
		1200	572		2280	108000	

Note:
1. This table is based on Table 5 of Reference [4].

Table 2-3: 5% Loading and 5% Unloading Transients Definitions [1]

Transient ID	Description	Time, sec	T_{top} [2,3], °F	T_{bottom} [2,3], °F	T_{top} rate, °F/hr	T_{bottom} rate, °F/hr	Pressure, psia	Flow Rate, lb/hr [4]	Annual Cycles
Trans18	5% Loading	0	653	572			2280	0	250
		50	652	652	-72	5760	2265	-108000	
		75	651	572	-144	-11520	2257	9000	
		100	573	573	-11232	144	2266	126000	
		225	580	580	202	202	2313	126000	
		300	583	583	144	144	2313	126000	
		975	617	617	181	181	2313	126000	
		1050	621	621	192	192	2313	108000	
		1350	621	621			2280	36000	
		1500	653	621	768		2280	0	
Trans19	5% Unloading	0	653	621			2280	0	250
		75	621	621	-1536	0	2314	93600	
		150	649	649	1344	1344	2283	-108000	
		300	649	649			2222	-108000	
		525	650	650	16	16	2222	-108000	
		1050	651	651	7	7	2256	-108000	
		1125	651	572		-3792	2253	-54000	
		1200	651	572			2250	0	
		1425	651	572			2250	0	
		1500	651	572			2280	0	

Notes:
1. This table is based on Table 5 of Reference [4].
2. T_{top} and T_{bottom} are temperature at top half portion of the surge line and bottom half portion of the surge line as depicted in Figure 2-3.
3. T_{top} and T_{bottom} are determined using Equations 2-2, 2-3, and 2-4 in Section 2.2.
4. Positive flow means 'insurge' while negative flow rate means 'outsurge'.

Table 2-4: Stratification Load Case Descriptions

Stratification ID (used in pc-CRACK)	Stratification ID (used from Reference [4])	Description	Annual Cycles [1]
S1	S1L	Heatup, ΔT = 340°F, Low Pressure	11.8
		Cooldown, ΔT = 340°F, Low Pressure	
S2	S2L	Heatup, ΔT = 250°F, Low Pressure	5.55
		Cooldown, ΔT = 250°F, Low Pressure	
S3	S3L	Heatup, ΔT = 200°F, Low Pressure	9.53
		Cooldown, ΔT = 200°F, Low Pressure	
S4	S4L	Heatup, ΔT = 150°F, Low Pressure	26
		Cooldown, ΔT = 150°F, Low Pressure	
S5	S1H	Heatup, ΔT = 340°F, High Pressure	2.67
		Cooldown, ΔT = 340°F, High Pressure	
S6	S2H	Heatup, ΔT = 250°F, High Pressure	2.4
		Cooldown, ΔT = 250°F, High Pressure	
S7	S3H	Heatup, ΔT = 200°F, High Pressure	3.93
		Cooldown, ΔT = 200°F, High Pressure	
S8	S4H	Heatup, ΔT = 150°F, High Pressure	16.33
		Cooldown, ΔT = 150°F, High Pressure	
S9	S5	Heatup, ΔT = 90°F, Hot Standby	2923.7
		Cooldown, ΔT = 90°F, Hot Standby	

Note: 1. Number of cycles are obtained from Table 6 of Reference [4].

Table 2-5: Heat Transfer Coefficients [1]

Flow Rate, lb/hr	HTC, BTU/hr-ft²-°F
≤ 43,200	238
54,000	285
93,600	442
108,000	495
117,000	529
126,000	561

Note: 1. This table is based on Table 5 of Reference [5].
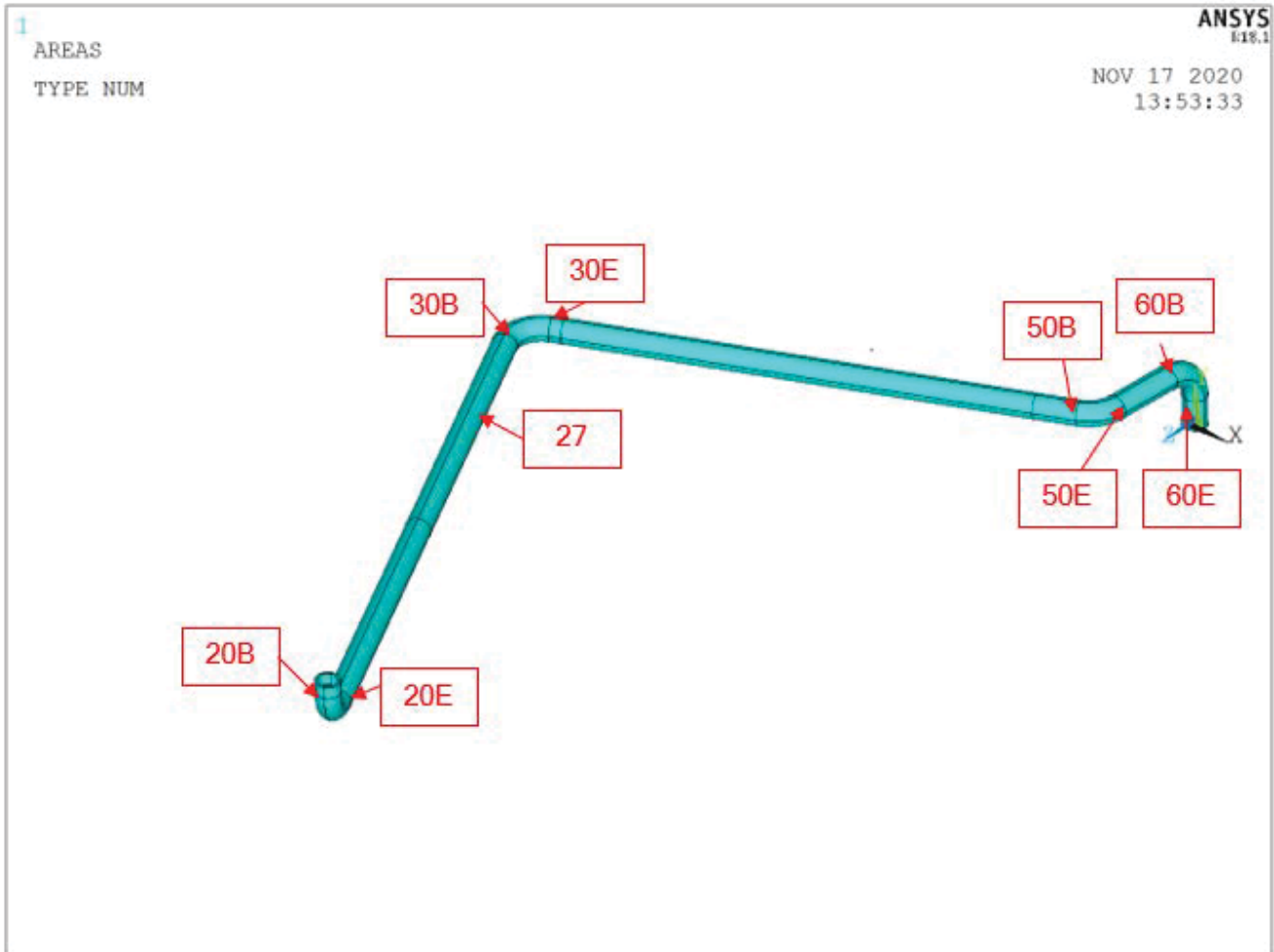
Figure 2-1. Pressurizer Surge Line Weld Locations

This figure is based on Figure 1 of Reference [5].
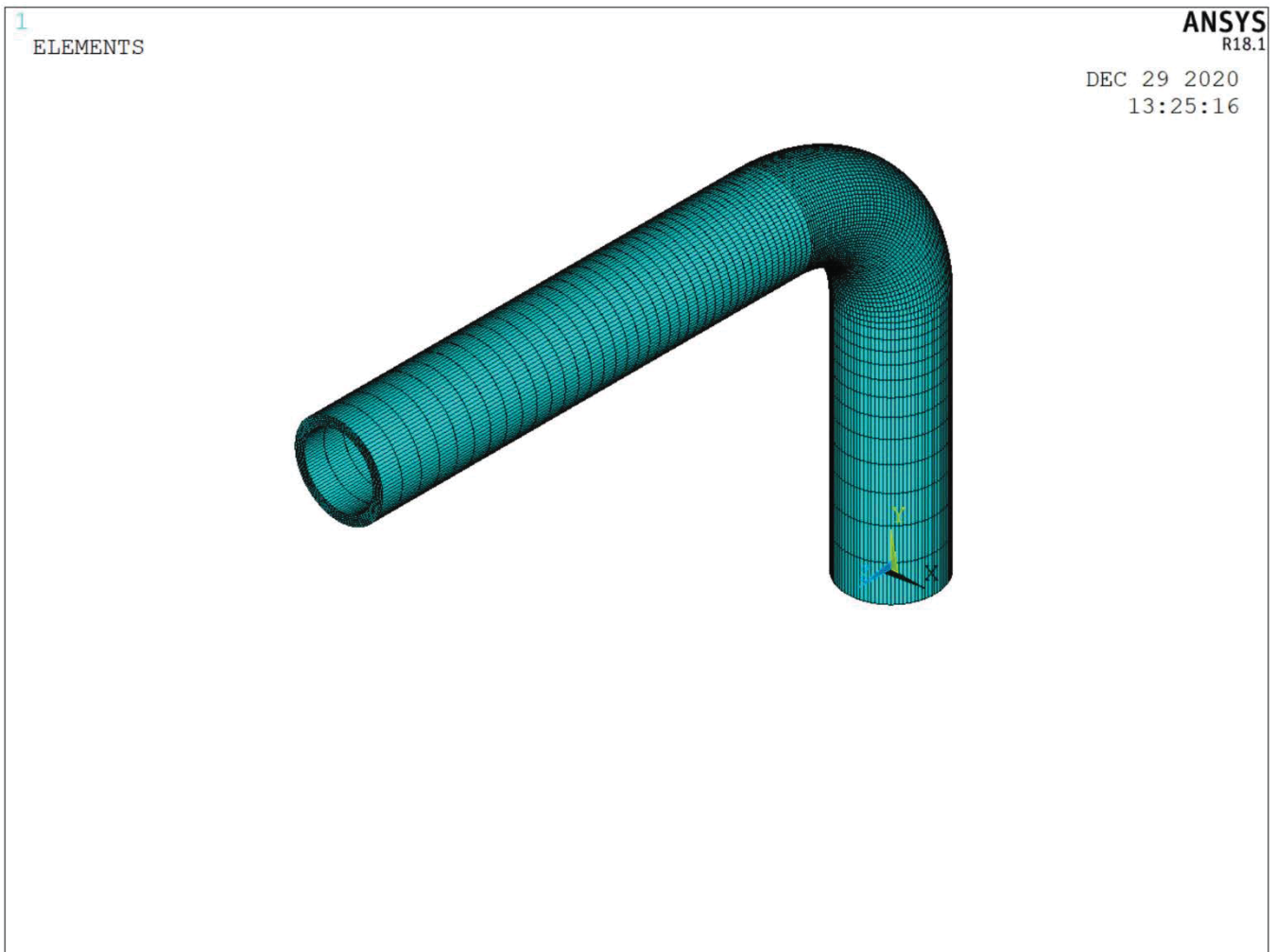
Figure 2-2. Surge Line Elbow Finite Element Model

This figure is based on Figure 2 of Reference [5].
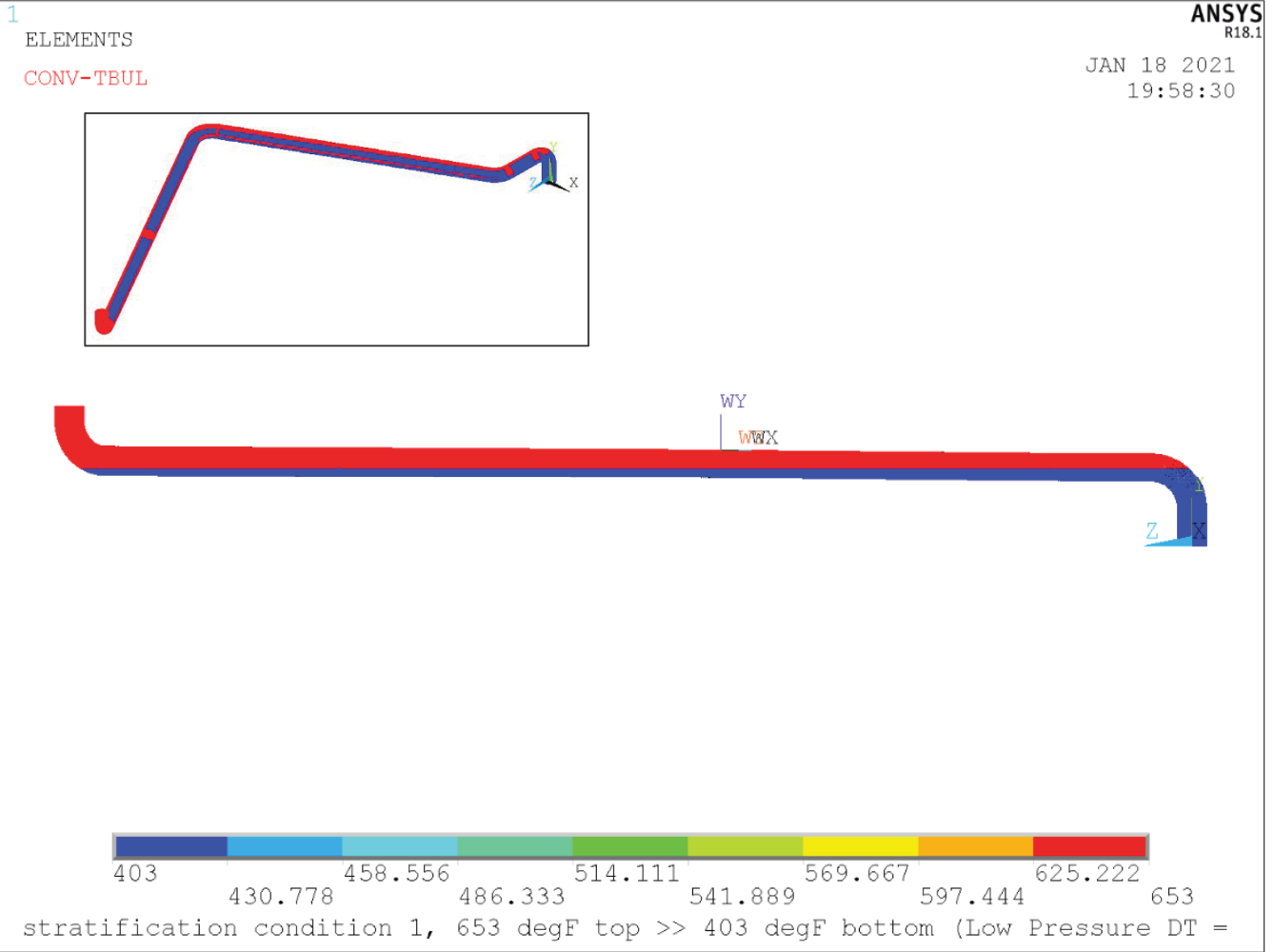
(side view)

Figure 2-3. Regions of Applied Temperature for Stratification Load (in °F)

This figure is based on Figure 6 of Reference [5].

3.0 DESIGN INPUTS AND ASSUMPTIONS

The following are design inputs for the allowable flaw size determination, along with the source of design inputs used.

3.1 Piping Dimensions

The piping dimensions for the surge line are for a 12" Schedule 160 pipe [5]:

Surge Line Outside Diameter:	12.75 inches
Surge Line Thickness:	1.312 inches

3.2 Operating Conditions

The normal operating conditions for the surge line are [4]:

Maximum Normal Operating Pressure:	2299 psig
Maximum Normal Operating Temperature:	655 °F

The upset conditions for the surge line are [4]:

Maximum Upset Pressure:	2535 psig
Maximum Upset Temperature:	661 °F

Faulted Condition Pressure [4]: 2299 psig

661 °F is conservatively used for the analysis of all service levels.

3.3 Piping Loads

The piping loads required for the evaluation are the three moment components (torsion and two bending moments). The moments for each load case are combined using the square-root-sum-of-the-squares (SRSS) method. Some welds are skewed relative to the global surge line coordinate system [5], so a local coordinate system is used to define moments at welds where applicable (see Table 3-1, Note 2). For the allowable flaw size calculation, axial forces are not included as specified in ASME B&PV Code, Section XI, Appendix C, C-2500 [1] (only bending moments and pressure are considered).

3.3.1 Load Cases

Table 3-1 tabulates the following piping moments for each surge line location [7]
- Deadweight
- Thermal Expansion
- Operating Basis Earthquake (OBE)
- OBE SAM (OBE Seismic Anchor Movement)
- Safe Shutdown Earthquake (SSE)
- SSE SAM (SSE Seismic Anchor Movement)
- LOCA (Loss of Coolant Accident)

Discussion of additional load cases listed below is contained in Section 4.0.

- Internal Pressure
- Thermal Transients
- Thermal Stratification – Insurge/Outsurge
- Thermal Anchor Movements

These loadings are used for both the allowable flaw size determination (Section 5.0) and the fatigue crack growth evaluation (Section 6.0).

3.4 Thermal Transients for Fatigue Crack Growth Analysis

The most significant transients occur during heatups and cooldowns.

The thermal transients shown in Table 2-1 are analyzed using the finite element model (FEM) shown in Figure 4-1. Table 2-1 tabulates the pressure and temperature history of the surge line transients and insurge and outsurge events, which also includes the rate of change in temperature and annual cycles for each transient [4, Table 5]. Hydrostatic test is not included in the stress analysis since its impact on fatigue crack growth is negligible, as it is a low frequency event. The bounding Reactor Trip Transient, including the pressure and temperature history and annual cycles, is summarized in Table 2-2.

The 5% Loading Up and 5% Loading Down transients (Trans18 and Trans19) are defined in Transient Group E and F of Reference [4, Table 5]. The transient definitions for the 5% Loading Up and 5% Loading Down transients are tabulated in Table 2-3. The details of the temperature distributions of the aforementioned transients are discussed in Section 2.2.

3.5   Analysis Parameters and Approaches

The following are analysis parameters and approaches used in this report:

1. The ambient containment temperature is set at 120°F. This is conservatively selected as a lower bound value of the outer pipe wall temperature during stratified conditions.

2. Since the piping system is insulated, the outside surfaces are conservatively modeled to be adiabatic, such that the component is treated as perfectly insulated.

3. OBE loads are input in the analysis as applied at normal operating conditions.

4. The stress-free reference temperature for the thermal stress calculation is modeled to be 70°F, which is judged to be a reasonable temperature at installation and is used for thermal strain calculations.

5. The surge line welds are conservatively evaluated as shielded metal arc welds (SMAW) since the selection of SMAW (a flux welding process) is conservative as it has more stringent requirements for allowable flaw size determination.

6. The crack face pressure loading is assumed as a uniform membrane stress in pc-CRACK [13].

7. Full structural weld overlays were applied at the pressurizer surge nozzle-to-pipe and hot leg surge nozzle welds for all three (3) Units. As such, the stress paths at these locations are excluded in the crack growth evaluation.

Table 3-1: Piping Load Cases [1,2]

Node[3,4]	Load Case	M_x (ft-lb)	M_y (ft-lb)	M_z (ft-lb)	M_{SRSS} (in-kip)
20B	Deadweight	-2251	6	1706	34
	Thermal	-6887	159231	-519	1913
	OBE	5097	3597	3494	86
	OBE SAM	1097	3040	979	41
	SSE	9522	6045	6523	156
	SSE SAM	2404	6890	2174	91
	LOCA	16952	14353	8821	287
20E†	Deadweight	349	8	-958	12
	Thermal	13415	141915	9553	1714
	OBE	756	2382	3855	55
	OBE SAM	242	2650	486	32
	SSE	1433	4008	7323	102
	SSE SAM	538	6007	836	73
	LOCA	1493	10386	10018	174
27†	Deadweight	-349	-42	-2898	35
	Thermal	-13415	93028	95	1128
	OBE	756	1920	3877	53
	OBE SAM	242	3100	95	37
	SSE	1433	3170	7326	97
	SSE SAM	538	7044	211	85
	LOCA	1493	10619	8687	166
30B†	Deadweight	-349	-49	-1140	14
	Thermal	-13416	146498	2286	1766
	OBE	756	2839	776	36
	OBE SAM	242	3653	155	44
	SSE	1433	4809	1452	63
	SSE SAM	538	8312	278	100
	LOCA	1493	12854	4385	164
30E†	Deadweight	448	-43	1446	18
	Thermal	3003	147845	-12704	1781
	OBE	1000	1498	1100	25
	OBE SAM	183	9401	238	113
	SSE	1898	2585	2078	46
	SSE SAM	315	21377	523	257
	LOCA	2465	15556	3855	195

Table 3-1 – Piping Load Cases [1, 2] (concluded)

Node[3, 4]	Load Case	M_x (ft-lb)	M_y (ft-b)	M_z (ft-b)	M_{SRSS} (in-kip)
50B†	Deadweight	-447	-74	-2047	25
	Thermal	-3002	75699	-22745	949
	OBE	1000	1342	505	21
	OBE SAM	183	12308	2242	150
	SSE	1898	2244	906	37
	SSE SAM	315	27962	5088	341
	LOCA	2465	18640	6389	238
50E	Deadweight	223	80	811	10
	Thermal	16286	-80868	19533	1017
	OBE	785	1549	806	23
	OBE SAM	1256	9108	2066	113
	SSE	1479	2581	1502	40
	SSE SAM	2837	20695	4678	257
	LOCA	4020	15126	5508	199
60B	Deadweight	1080	-84	-811	16
	Thermal	-21331	67628	-19533	883
	OBE	2872	1916	806	43
	OBE SAM	1606	6189	2066	81
	SSE	5376	3155	1502	77
	SSE SAM	3633	14067	4678	183
	LOCA	11122	14191	5508	226
60E	Deadweight	-1031	86	809	16
	Thermal	1518	-60615	12520	743
	OBE	4445	2709	1061	64
	OBE SAM	4158	12733	5207	172
	SSE	8190	4459	1886	114
	SSE SAM	9441	28925	11823	392
	LOCA	13191	23717	12494	359

Notes:

1. This table is based on Table 1 of Reference [7].
2. All moments evaluated in global coordinates unless otherwise indicated.
3. † Indicates moments evaluated in local coordinates where X = Axial,
   Y = Vertical (on horizontal run), and Z = Lateral
4. B indicates Beginning of elbow, E for End of elbow.

Table 3-2: Piping Interface Loads[4, 5]

Location, Node	Load Type[1]	FX[2, 3], lbf	MY[2], ft-lbf	MZ[2], ft-lbf	SRSS(MY, MZ), inch-kip
Weld 20B	Deadweight	-1	6	1706	20.5
	OBE	1164	3597	3494	60.2
	OBE SAM	584	3040	979	38.3
	Total OBE	1748	6637	4473	98.5
Weld 20E	Deadweight	-6	8	-958	11.5
	OBE	1679	2382	3855	54.4
	OBE SAM	1028	2650	486	32.3
	Total OBE	2707	5032	4341	86.7
Weld 27	Deadweight	6	-42	-2898	34.8
	OBE	966	1920	3877	51.9
	OBE SAM	1028	3100	95	37.2
	Total OBE	1994	5020	3972	89.1
Weld 30B	Deadweight	6	-49	-1140	13.7
	OBE	732	2839	776	35.3
	OBE SAM	1030	3653	155	43.9
	Total OBE	1762	6492	931	79.2
Weld 30E	Deadweight	-2	-43	1446	17.4
	OBE	838	1498	1100	22.3
	OBE SAM	6160	9401	238	112.8
	Total OBE	6998	10899	1338	135.2
Weld 50B	Deadweight	2	-74	-2047	24.6
	OBE	541	1342	505	17.2
	OBE SAM	6160	12308	2242	150.1
	Total OBE	6701	13650	2747	167.3
Weld 50E	Deadweight	1	80	811	9.8
	OBE	556	1549	806	21.0
	OBE SAM	4836	9108	2066	112.1
	Total OBE	5392	10657	2872	133.0
Weld 60B	Deadweight	-1	-84	-811	9.8
	OBE	629	1916	806	24.9
	OBE SAM	4836	6189	2066	78.3
	Total OBE	5465	8105	2872	103.2
Weld 60E	Deadweight	1	86	809	9.8
	OBE	762	2709	1061	34.9
	OBE SAM	4836	12733	5207	165.1
	Total OBE	5598	15442	6268	200.0

Notes:
1. Total OBE = OBE + OBE SAM.
2. FX is the axial force in the local direction of the pipe. MY and MZ are the in-plane moments in the local direction of the pipe, respectively. Values from [7, 14].
3. Negative values of FX are considered 0 for the FCG calculation since their compressive nature does not contribute as a crack driving force.
4. Values shown in the table are the magnitudes to be used in scaling the unit load analysis. SSE and LOCA loadings are not included (see Section 6.2).
5. This table is based on Table 1 of Reference [6].

4.0 STRESS ANALYSIS

A three-dimensional (3-D) finite element model for the surge line piping [5] is developed using the **ANSYS** finite element analysis (FEA) software package [15] to perform the stress analysis [6]. The following is the order in which the FEA was conducted:

- Develop a finite element model of the surge line piping, as shown in Figure 4-1 (Weld numbers shown in Figure 4-2).
- Perform thermal transient analyses to obtain the temperature history for the applicable normal plant transients.
- Perform thermal transient analyses to obtain the steady-state temperature for the applicable stratification events.
- Perform stress analyses using temperature results from thermal transient definitions [5]. These stress analyses include the appropriate internal pressure and thermal anchor movements (TAMs) at the corresponding temperature time steps.
- Perform stress analysis for the Mechanical Piping Loads.
- Review stress results and select stress extraction paths for locations in the base metal and the welds, and store them in computer files.

The following Sections 4.1 through 4.9 provide a high-level technical overview of the finite element modeling, displacement loadings, materials, and analyses performed for assessment of the various locations.

4.1   Finite Element Model

For the thermal transient and thermal stratification analyses and pressure analysis, a 3-D finite element model of the pressurizer surge line is used, which was previously developed in Reference [5, Figure 1] using **ANSYS** APDL [15]. The model is a SOLID45 brick model which includes the surge line piping between the terminal nozzles on the reactor coolant system hot leg and the pressurizer. Figure 4-1 shows the FEM of the pressurizer surge line with the global coordinate system.

For the structural analyses that involve mechanical loadings at the junction between the surge line elbow and the straight piping, a 3-D FEM of a section of an elbow is used, which was previously developed in Reference [12, Figure 1] using **ANSYS** APDL [15]. The model is a SOLID45 brick model which also includes straight pipe attached at each end of the elbow to eliminate discontinuity effects on the stress when mechanical loads are being applied. Figure 2-2 shows the FEM of the surge line elbow with the global coordinate system. Reference [12] used the elbow model to represent the hot leg elbow. In this calculation, the 3-D FEM of a section of the elbow is used to represent all the elbow locations of the surge line, and the resulting stresses from the unit loads on this model will be scaled to the actual mechanical piping loads (deadweight, thermal expansion, and OBE) at the elbows.

Temperature dependent material properties, summarized in Table 4-4, from Reference [10], are used for the thermal transient and thermal stratification analyses. For the unit pressure and structural analyses, material properties at 70°F are employed in the FEM.

The loads that are considered in the stress analysis using the pressurizer surge line FEM are as follows:

- Internal Pressure
- Thermal Transients
- Thermal Stratification – Insurge/Outsurge
- Thermal Anchor Movements

The FEM from Figure 4-1 is used to calculate the mechanical piping loads using the unit loads as 1000 lb for axial load and 1000 lb-inch for the two in-plane bending moments. The resulting

stresses that are scaled to the actual piping loads in the subsequent fatigue crack growth analyses are deadweight, thermal expansion, and OBE.

For the fatigue crack growth analysis, the loads are limited to operating conditions such as Service Levels A and B, as the crack driving force. Loads such as SSE, LOCA and other design basis loads are not considered, as they are Service Level C and D loads.

A three-dimensional model is constructed using 8-node structural solid **ANSYS** SOLID45 elements. The thermal equivalent element type for the thermal transient analyses is SOLID70.

4.2   Thermal Anchor Movements

The thermal displacements [11], shown in Table 4-2, are applied on either end of the surge line as two separate load cases, and a steady state stress analysis is performed for each. To calculate the thermal anchor movements, two **ANSYS** runs are performed: (a) the first thermal displacement run is simulated by applying the boundary conditions at the pressurizer end and the displacements are applied to the hot leg end, (b) the second thermal displacement run is simulated by applying the boundary conditions at the hot leg end and the displacements are applied to the pressurizer end. The surge line is maintained at a uniform and stress-free temperature of 70°F.

In the first run, thermal anchor displacements were applied at the hot leg surge nozzle end of the surge line, while keeping the pressurizer surge nozzle end fixed in the axial and circumferential directions, and stress analysis was performed. Figure 4-4 shows the displacement vector sum contour plot for anchor displacements applied at the hot leg surge nozzle end. All the top nodes of the spring hanger locations are fixed in all three orthogonal directions.

Similarly, in the second run, thermal displacements were applied at the pressurizer surge nozzle end of the surge line, while keeping the hot leg surge nozzle end fixed in the axial and circumferential directions, and stress analysis was performed. Figure 4-5 shows the displacement vector sum contour plot for anchor displacements applied at the pressurizer end. All the top nodes of the spring hanger locations are fixed in all three orthogonal directions.

Anchor displacements are applied in the **ANSYS** model global Cartesian coordinate system (CSYS 0), which is aligned with the coordinate system of the design piping isometric drawings

[16]. The measured anchor displacements are scaled based on the operating temperatures of the pressurizer and hot leg. The displacement values, and therefore resulting stresses, have been scaled according to the following equations, using 70°F as the stress-free reference temperature.

Thermal Scale Factor for Hot Leg Side, TSF_{HL}:

$$TSF_{HL} = \frac{T_{hot\ leg} - 70}{553 - 70}$$

(4-1)

where $T_{hot\ leg}$ is the temperature of the hot leg.

Thermal Scale Factor for Pressurizer Side, TSF_{PRZ}:

$$TSF_{PRZ} = \frac{T_{Pzr} - 70}{653 - 70}$$

(4-2)

where T_{Pzr} is the temperature of the pressurizer.

The stress results from the anchor displacement analysis are scaled to all other transient temperatures.

4.3   Material Properties

The material for the surge line is [17]:

Surge Line Butt Welds   SA-376,* Type 304 (18Cr-8Ni)

The yield strength and tensile strength for SA-376, Type 304 from the ASME Code are [18]:

Yield Strength at 650°F:	18 ksi
Yield Strength at 661°F:	17.912 ksi
Yield Strength at 700°F:	17.6 ksi
Tensile Strength at 650°F:	59.2 ksi
Tensile Strength at 661°F:	59.2 ksi
Tensile Strength at 700°F:	59.2 ksi

*Note – SA-376 and SA-312 have identical material properties.

4.4 Thermal/Mechanical Stress Analysis

Stress analyses are performed for thermal transients, mechanical piping loads, and internal pressure. For thermal transients, thermal analyses are performed to determine the transient temperature distribution for each transient in Section 2.0. The temperature distribution is then used as input to perform a stress analysis for each transient. Evaluations of Thermal Anchor Movements are performed in a separate stress analysis, which are scaled based on the temperature of the corresponding transient.

A unit (1000 psig) internal pressure analysis was performed on a full model of the surge line with constant material properties at 70°F. The pressure stress result was scaled based on the actual pressure for each corresponding transient. Figure 4-6 shows the applied loading for the unit pressure stress analysis.

Stresses from thermal transients, TAM's, and pressure were later combined in the crack growth evaluation in Section 6.6, together with the stratification loads and mechanical piping loads.

Table 4-1 tabulates the temperature and pressure time histories for the bounding thermal transients, and lists the transients evaluated along with the event naming convention used in ANSYS.

The stresses due to deadweight loading will be combined with the individual transient stresses in the crack growth calculation (Section 6.0), which will define the load combinations evaluated.

4.5 Mechanical Boundary Conditions

At each terminal end of the surge line piping, the displacements are constrained in both the axial and the circumferential directions, as shown in Figure 4-3. These boundary conditions prevent global translation or rotation of the anchor points/piping ends while still allowing thermal expansion in the radial direction to prevent any artificially introduced stresses from a complete fixity. Snubbers are also modeled as shown based on Reference [12].

Since the entire surge line piping system is modeled using FEA, this will automatically account for piping interface loads (moments and forces) induced by thermal expansion during thermal stratification. However, it is necessary to also account for dead weight, thermal expansion, thermal anchor movements, and seismic loads.

The structural boundary conditions for the elbow FEM are discussed below.

4.6   Unit Pressure Loads

Figure 4-6 shows the applied loading for unit pressure stress analysis and Figure 4-7 shows the stress intensity due to applied internal pressure.

4.7   Elbow Mechanical Loads

The three-dimensional model of the elbow is used for the mechanical load simulations. Displacement and rotational boundary conditions are applied at one end of the elbow while the other end is left unconstrained. A pilot node was also employed at the unconstrained end of the elbow where the mechanical loads are applied.

A 1000 lb axial force, FY, and 1000 in-lb in-plane, MX, and in-plane, MZ, moments are applied at the unconstrained end of the elbow.

The results of the mechanical load analyses will be scaled based on actual piping loads such as Deadweight, Thermal, and OBE as needed in the subsequent analyses.

4.8   Stress Paths

The hoop and axial stresses in and around the surge line welds as illustrated in Figure 2-1 are reviewed in detail to determine limiting locations.

4.8.1   Thermal Load Cases

For thermal loads, two cases are used for the selection of the critical stress paths as follows:

(a) representative for thermal transient and insurge/outsurge events
(b) representative for thermal stratification.

For the thermal transient, Transient 12 (insurge and outsurge event) (see Table 2-1) is used for the selection because it has the largest temperature rate of change with 52.3 annual cycles [4, Table 7]. For the selection of stress paths due to thermal stratification, stratification load, S6, is selected as it has a large temperature difference ($\Delta T=250°F$), although it is not the highest ΔT. It is noted that this is not the selection of the only loading for thermal stratification. All cases are

run with the appropriate cycle counts (see Table 2-4). This transient S6, which is representative of thermal stratification, is only used to select paths for the full analysis.

The aforementioned thermal load cases are used for the determination of the critical paths by reviewing the axial and circumferential (hoop) stress at the weld locations [16, 17, 19].

4.8.2 *Path Locations based on Thermal Transients and Stratification*

Figure 4-8 through Figure 4-16 show the critical stress path locations based on thermal transients and stratification. The stress paths are based on the maximum stress at the inside diameter (ID) surface. In cases where the maximum stress is not at the ID surface, such as the axial stress from the stratification load case for Welds 60B and 60E, the bounding stress paths are selected based on the through-wall stress distributions.

The definition of the paths is as follow:

Path 1: Maximum hoop stress from the representative thermal transient
Path 2: Maximum axial stress from the representative thermal transient
Path 3: Maximum hoop stress from the representative thermal stratification load case
Path 4: Maximum axial stress from the representative thermal stratification load case

Figure 4-17 and Figure 4-18 show the region of interest in the elbow and the location of the stress paths evaluated for mechanical loads. The definition of the paths is as follows:

- Generated from stress analysis under axial force; FX Paxial_a and Paxial_h are paths based on maximum axial stress and maximum hoop stress, respectively.

- Generated from stress analysis under bending moment; MX, loading, Pmom_a and Pmom_h are paths based on maximum axial stress and maximum hoop stress, respectively.

4.9   Hoop Stress and Axial Stress Distributions

Hoop stress and axial stress were plotted for Weld 20B, 20E, 30B, 30E, 60B, and 60E. The stress plots are based on Transient 11 (TRAN 11, see Table 4-1) which is the load combination that generates the most severe effect upon crack growth. The maximum total stress distributions are combinations of pressure, deadweight, thermal transient and thermal expansion, thermal anchor movement, and weld residual stress. The maximum total hoop stress distributions are

shown in Figure 4-19 through Figure 4-24, while the maximum total axial stress distributions are shown in Figure 4-25 through Figure 4-30. The total stresses at normal operating conditions are depicted in Figure 4-31 through Figure 4-36 for hoop stress and in Figure 4-37 through Figure 4-42 for axial stress. In the aforementioned figures, the maximum axial stress occurs at Weld 30E while the maximum hoop stress occurs at Weld 30B.

Appendix B of Reference [6] provides an analysis of the elbow flank at nodes 60 and 30 which demonstrated that the butt welds provide the most limiting service fatigue life.

Table 4-1: Transient Events

Transient	ANSYS ID	Pressure[1] (ksig)		Temperature[1] (°F)			Annual Cycles[1]	Rise Time[4], sec.
		Max.	Min.	Max.	Min.	Ave.		
Plant Heatup	Tran1	2.235	0.000	540	70	305	1.398	16356
Plant Cooldown	Tran2	2.235	0.000	540	70	305	1.39	16008
Loss of Flow, Loss of Load	Tran3	2.535	1.685	621	551	586	0.531	100
Reactor Trip - Revised Transient[2]	Tran4	2.385	2.180	621	572	597	3.06	600
Plant Unloading, 10% Step Down	Tran6	2.235	2.235	653	593	623	2.695	29
Plant Unloading, 10% Step Up	Tran7	2.235	2.235	653	593	623	2.695	1303
Leak Test, 2250 psia, Down	Tran9	2.235	0.385	400	160	280	0.042	10800
Leak Test, 2250 psia, Up	Tran10	2.235	0.385	400	160	280	0.042	10080
I/O Heatup, ΔT = 300°F	Tran11	0.366	0.366	440	140	290	19.4	2350
I/O Heatup, ΔT = 250°F	Tran12	0.366	0.366	440	190	315	52.3	2320
I/O Heatup, ΔT = 150°F	Tran13	0.366	0.366	440	290	365	35.93	2100
I/O Heatup, ΔT = 100°F	Tran14	2.235	2.235	653	553	603	69.17	1989
I/O Cooldown, ΔT = 250°F	Tran15	0.366	0.366	440	190	315	7.4	2300
I/O Cooldown, ΔT = 150°F	Tran16	0.366	0.366	440	290	365	3.7	2100
I/O Cooldown, ΔT = 100°F	Tran17	2.235	2.235	653	553	603	6.73	2000
5% Loading - New Transient[3]	Trans18	2.298	2.242	653	572	613	250	4389
5% Unloading - New Transient[3]	Trans19	2.299	2.207	651	572	612	250	822

Notes:
1. Values are extracted from Table 2 of Reference [5] except for Tran4, Trans18, and Trans19.
2. Values are extracted from Table 3 of Reference [5].
3. Values are extracted from Table 4 of Reference [5].
4. Values are extracted from the **SI-TIFFANY** report file. The bounding (maximum) rise times between the transient events for each stress path are conservatively used.

Table 4-2: Anchor Displacement Analysis Load Cases

ΔX (inches)	ΔY (inches)	ΔZ (inches)	Description
-0.957	0.512	0	Thermal displacements at Hot Leg Surge Nozzle (represents hot leg temperature going from 70°F to 553°F)
-0.001	-0.141	0	Thermal displacements at Pressurizer end at 70°F (represents pressurizer bulk temperature going from 70°F to 653°F)

Note: Values are extracted from Table 6 of Reference [5].

Table 4-3: Scaled Anchor Displacements for the Thermal Stratification Analyses

Stratification Conditions	Anchor Displacements (in)		
	ΔX (inches)	ΔY (inches)	ΔZ (inches)
Low Pressure - Pressurizer Side T_{TOP} = 440°F	-0.0006	-0.0900	0
High Pressure - Pressurizer Side T_{TOP} = 653°F	-0.0010	-0.1410	0
Low Pressure – Hot Leg Side			
ΔT=340, 440 - 340 = T_{BOT} = 100°F	-0.0594	0.0318	0
ΔT=250, 440 - 250 = T_{BOT} = 190°F	-0.2378	0.1272	0
ΔT=200, 440 - 200 = T_{BOT} = 240°F	-0.3368	0.1802	0
ΔT=150, 440 - 150 = T_{BOT} = 290°F	-0.4359	0.2332	0
High Pressure – Hot Leg Side			
ΔT=340, 653 - 340 = T_{BOT} = 313°F	-0.4815	0.2576	0
ΔT=250, 653 - 250 = T_{BOT} = 403°F	-0.6598	0.3530	0
ΔT=200, 653 - 200 = T_{BOT} = 453°F	-0.7589	0.4060	0
ΔT=150, 653 - 150 = T_{BOT} = 503°F	-0.8579	0.4590	0
ΔT=90, 653 - 90 = T_{BOT} = 563°F	-0.9768	0.5226	0

Note: Values are extracted from Table 8 of Reference [5].

Table 4-4: Surge Line Material Properties [1]

Temperature, T, °F	Young's Modulus, E (10⁶), psi	Mean Coefficient of Thermal Expansion, α, (10⁻⁶), in/in/°F	Conductivity[2], k, Btu/hr-ft-°F	Diffusivity, d, ft²/hr	Specific Heat, C_p, Btu/lbm-°F
70	28.3	8.5	8.6	0.151	0.116
100	28.1	8.6	8.7	0.152	0.117
150	27.9	8.8	9.0	0.154	0.120
200	27.6	8.9	9.3	0.156	0.122
250	27.3	9.1	9.6	0.158	0.124
300	27.0	9.2	9.8	0.160	0.125
350	26.8	9.3	10.1	0.162	0.127
400	26.5	9.5	10.4	0.165	0.129
450	26.2	9.6	10.6	0.167	0.130
500	25.8	9.7	10.9	0.170	0.131
550	25.6	9.8	11.1	0.172	0.132
600	25.3	9.8	11.3	0.174	0.133
650	25.1	9.9	11.6	0.177	0.134
700	24.8	10.0	11.8	0.179	0.135

Notes:
1. This table is based on Table 2 of Reference [10].
2. Converted to Btu/sec-inch-°F **ANSYS** input files.
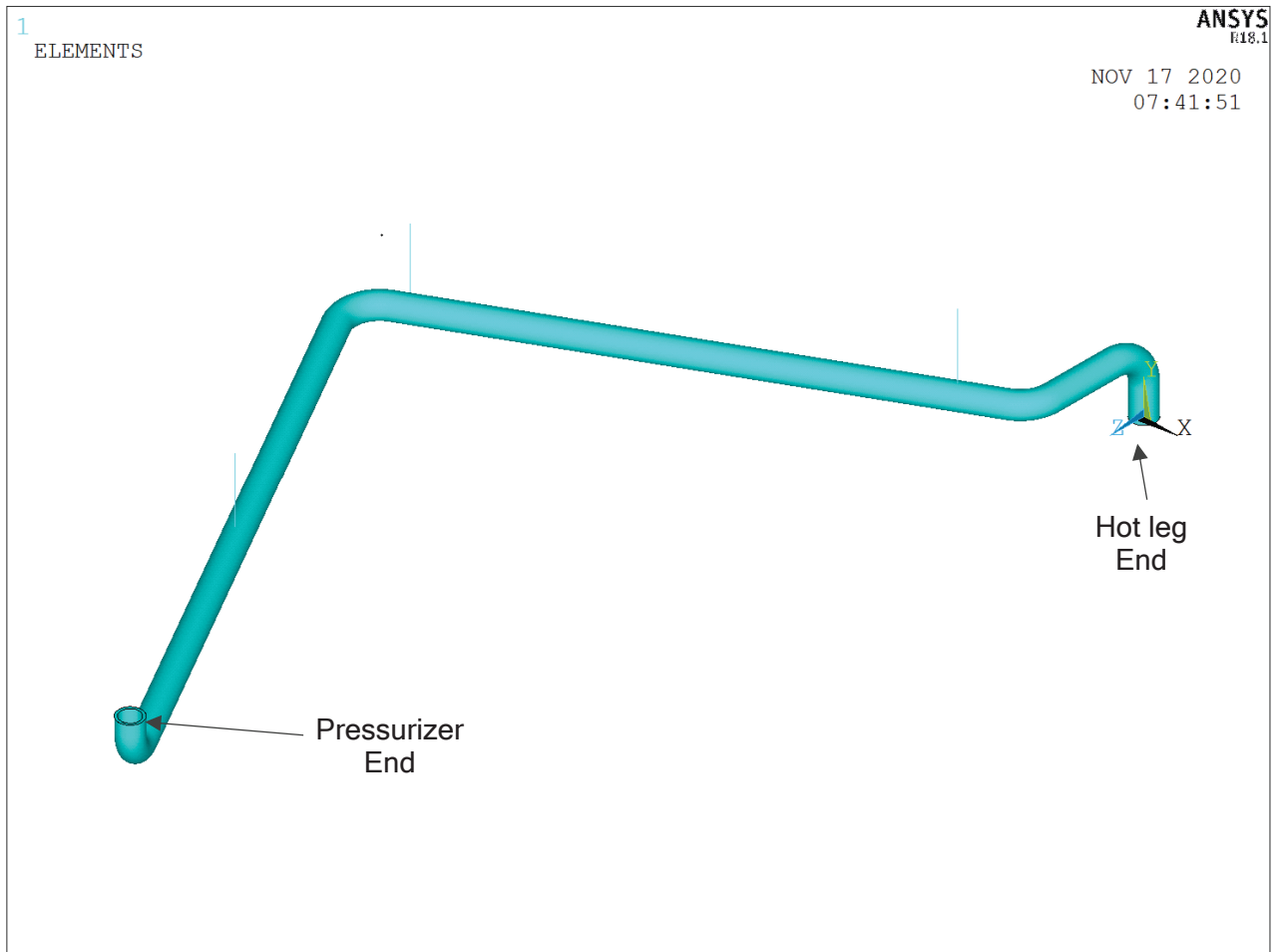
Figure 4-1. Pressurizer Surge Line Finite Element Model

This figure is based on Figure 1 of Reference [5].
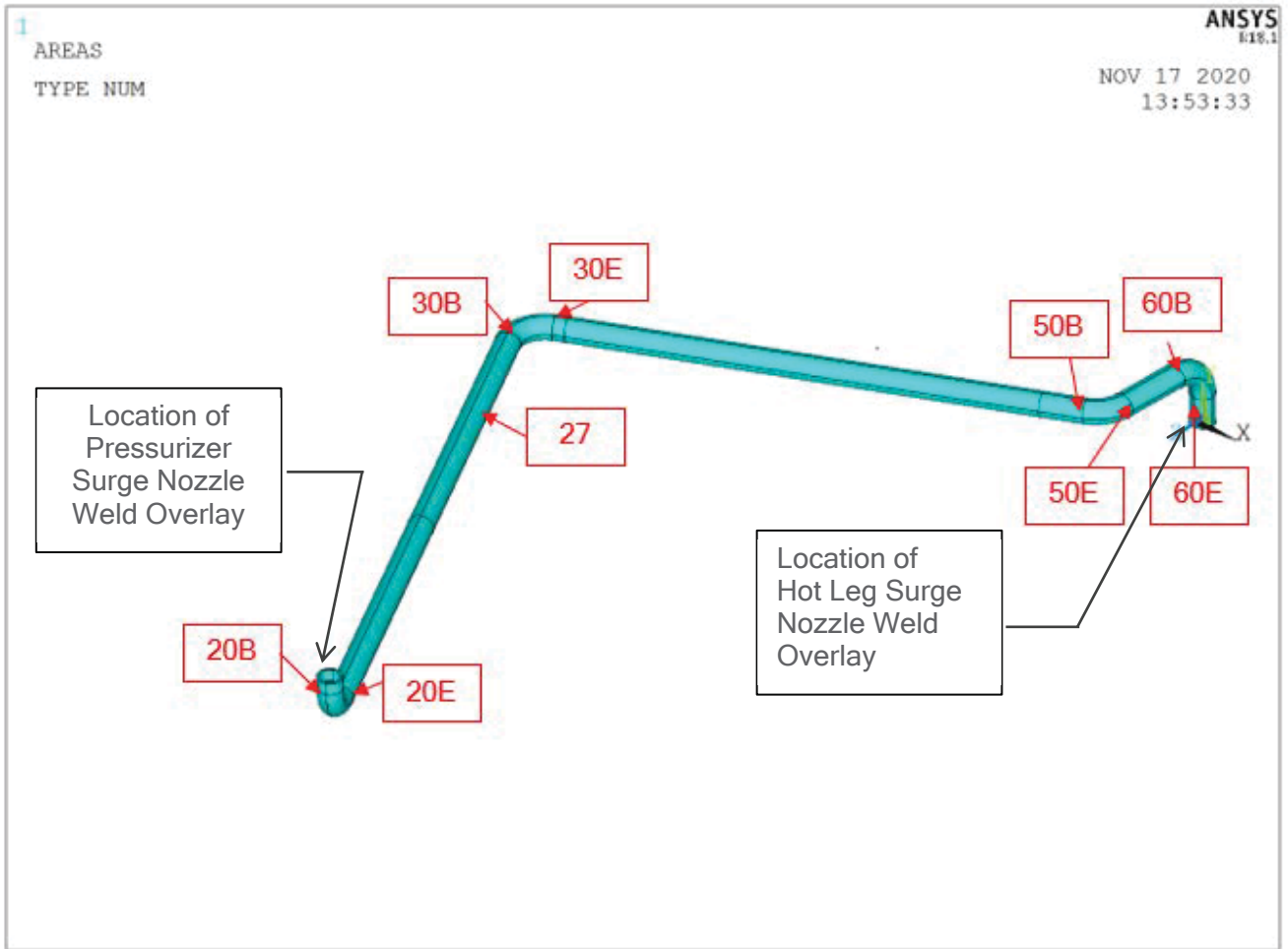
Local Coordinate System: A = Axial, B = Vertical (on horizontal run), C = Lateral

Figure 4-2. Pressurizer Surge Line Weld Locations

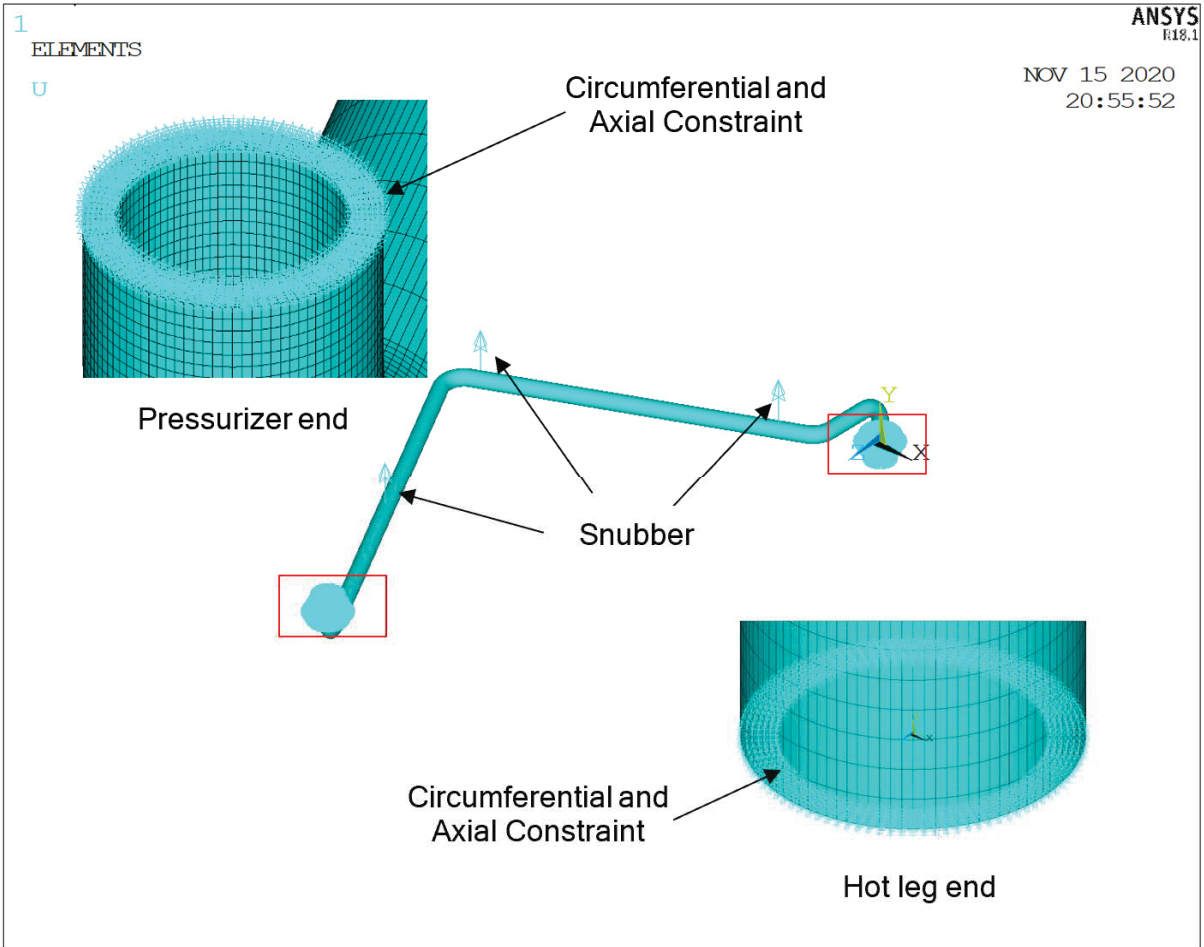*(Bounding FEM)*

This figure is based on Figure 1 of Reference [6].

Figure 4-3. Pressurizer Surge Line Structural Boundary Conditions

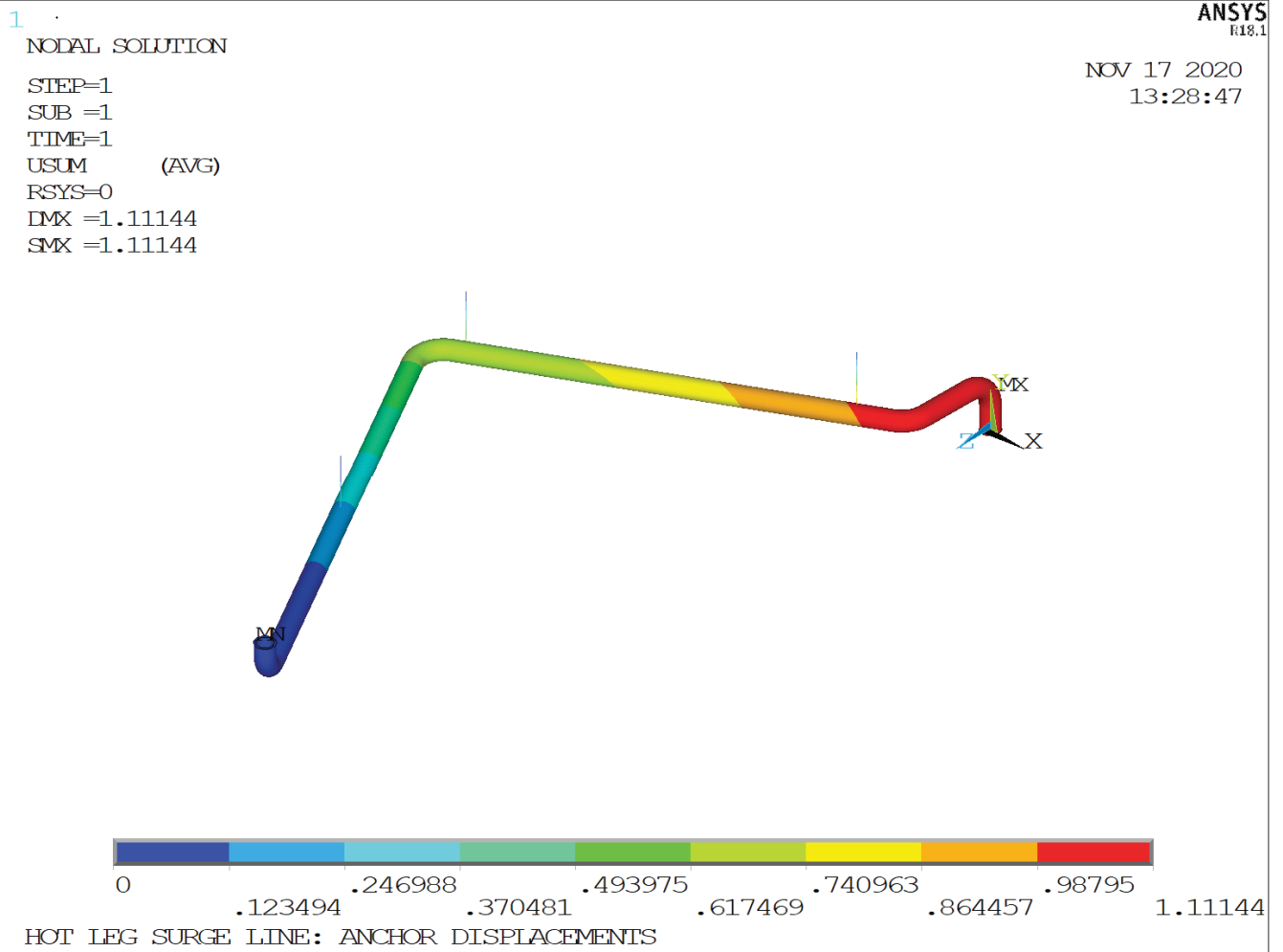*(Bounding FEM)*

This figure is based on Figure 3 of Reference [5].

Figure 4-4. Displacement Vector Sum Contour Plot for Thermal Displacements Applied at the Hot Leg Surge Nozzle End (in inches)

(Bounding FEM)

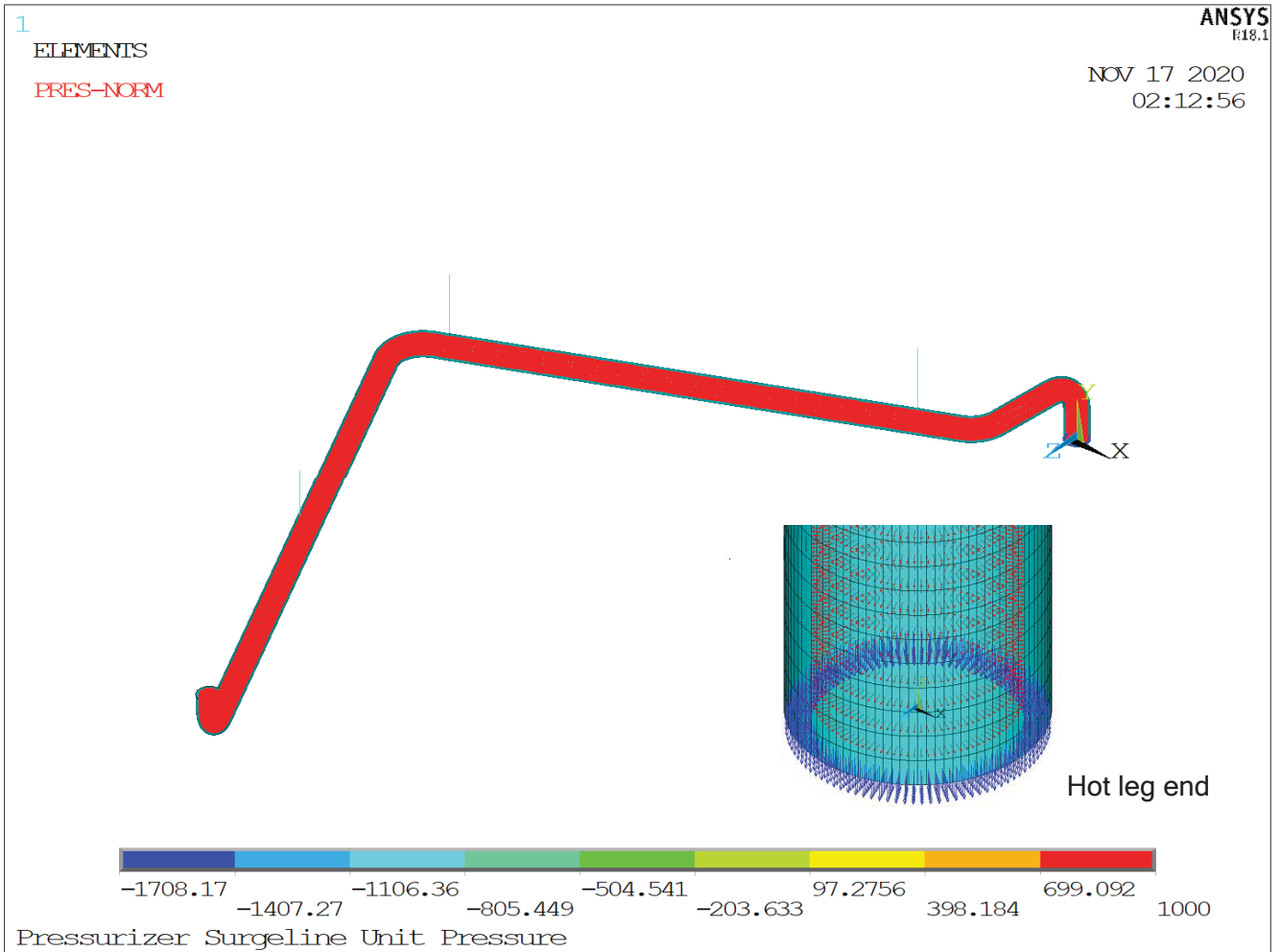This figure is based on Figure 4 of Reference [5].
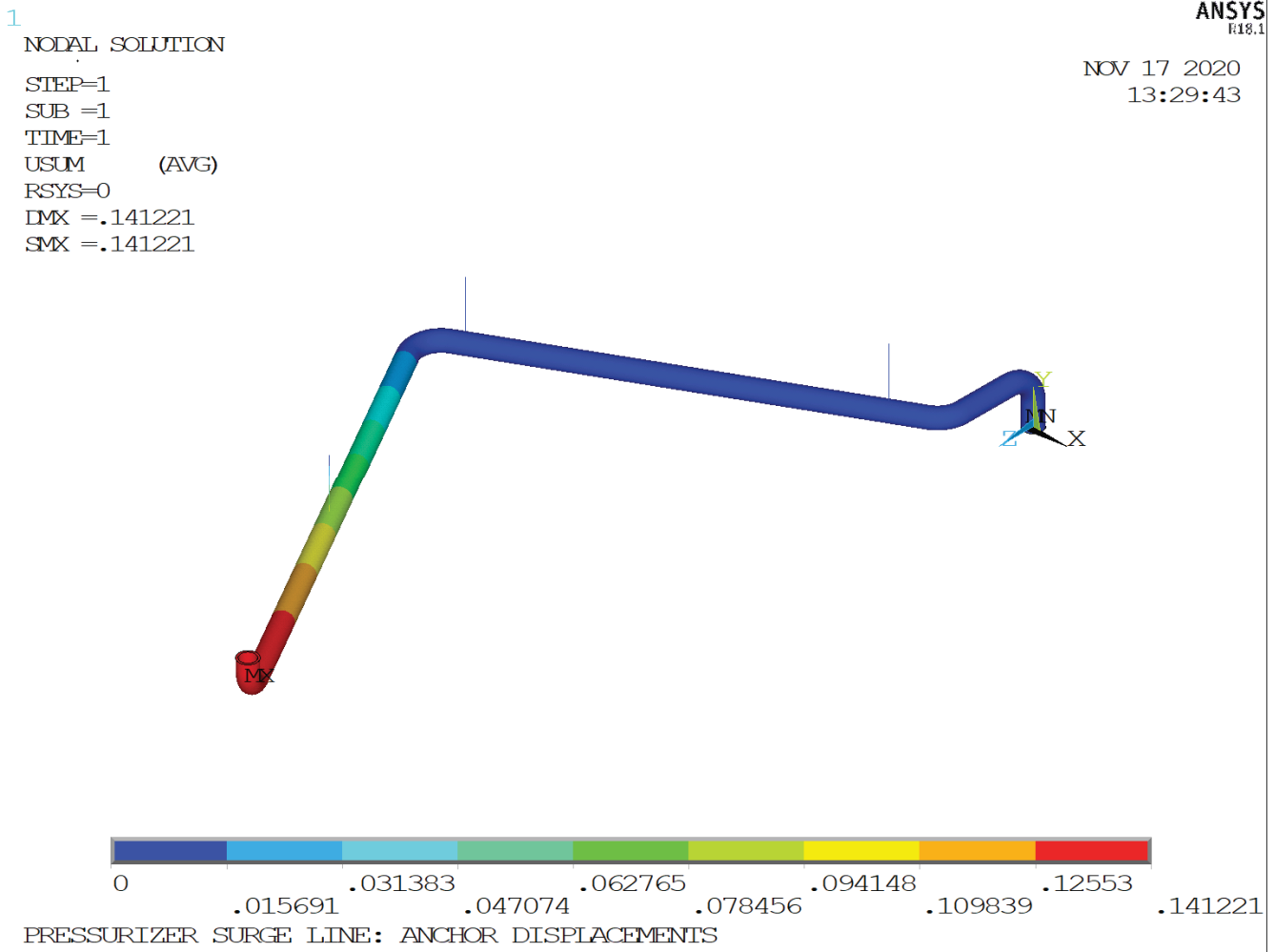
Figure 4-5. Displacement Vector Sum Contour Plot for Thermal Displacements Applied at the Pressurizer Surge Nozzle End (in inches)

(Bounding FEM)

This figure is based on Figure 5 of Reference [5].

Figure 4-6. Applied Loading for Unit Pressure Stress Analysis

(Units for pressure is in psi.)

(Bounding FEM)

This figure is based on Figure 7 of Reference [5].
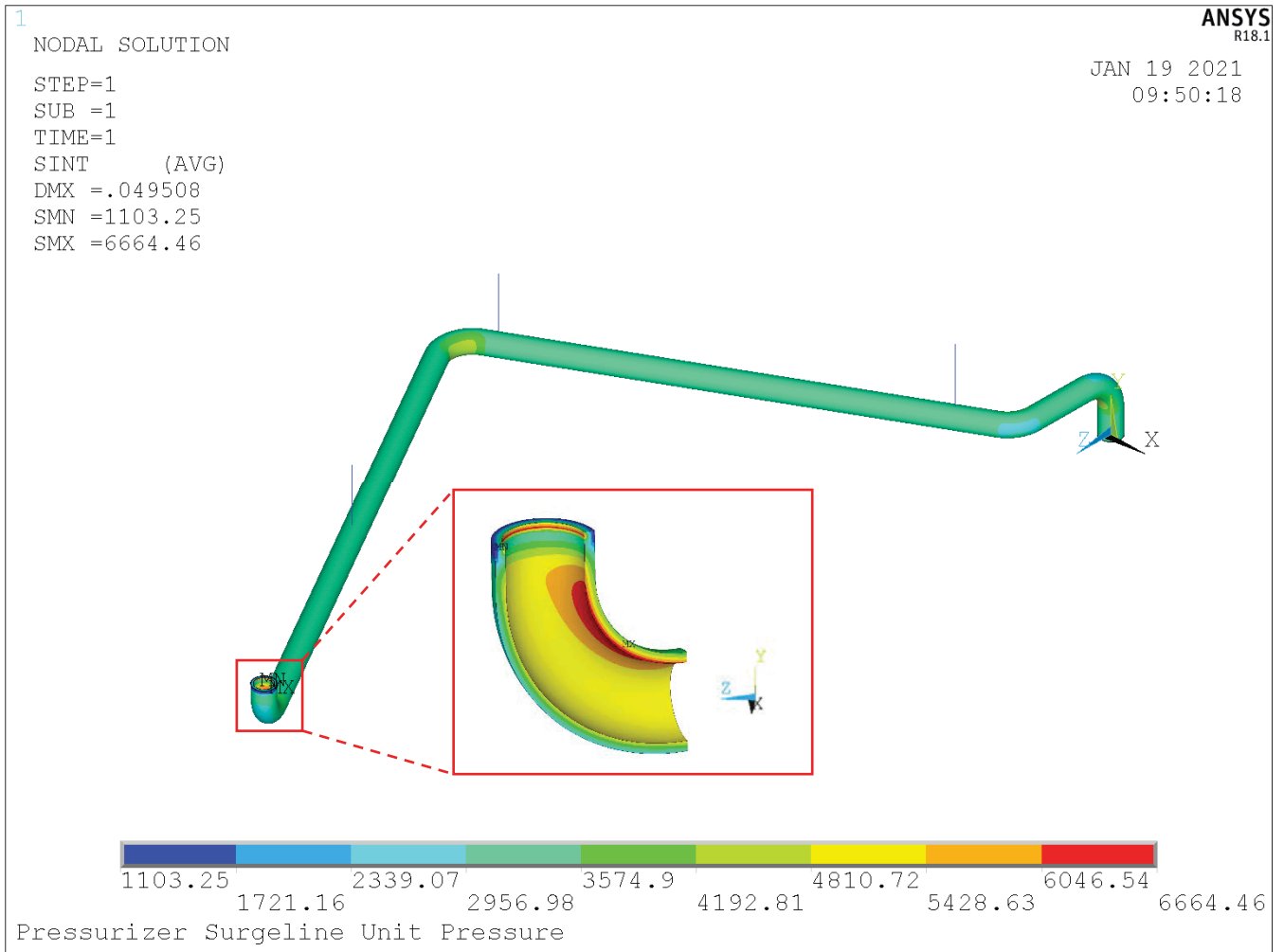
Figure 4-7. Stress Intensity Contour Plot for Unit Pressure Stress Analysis (in psi)

(Bounding FEM)

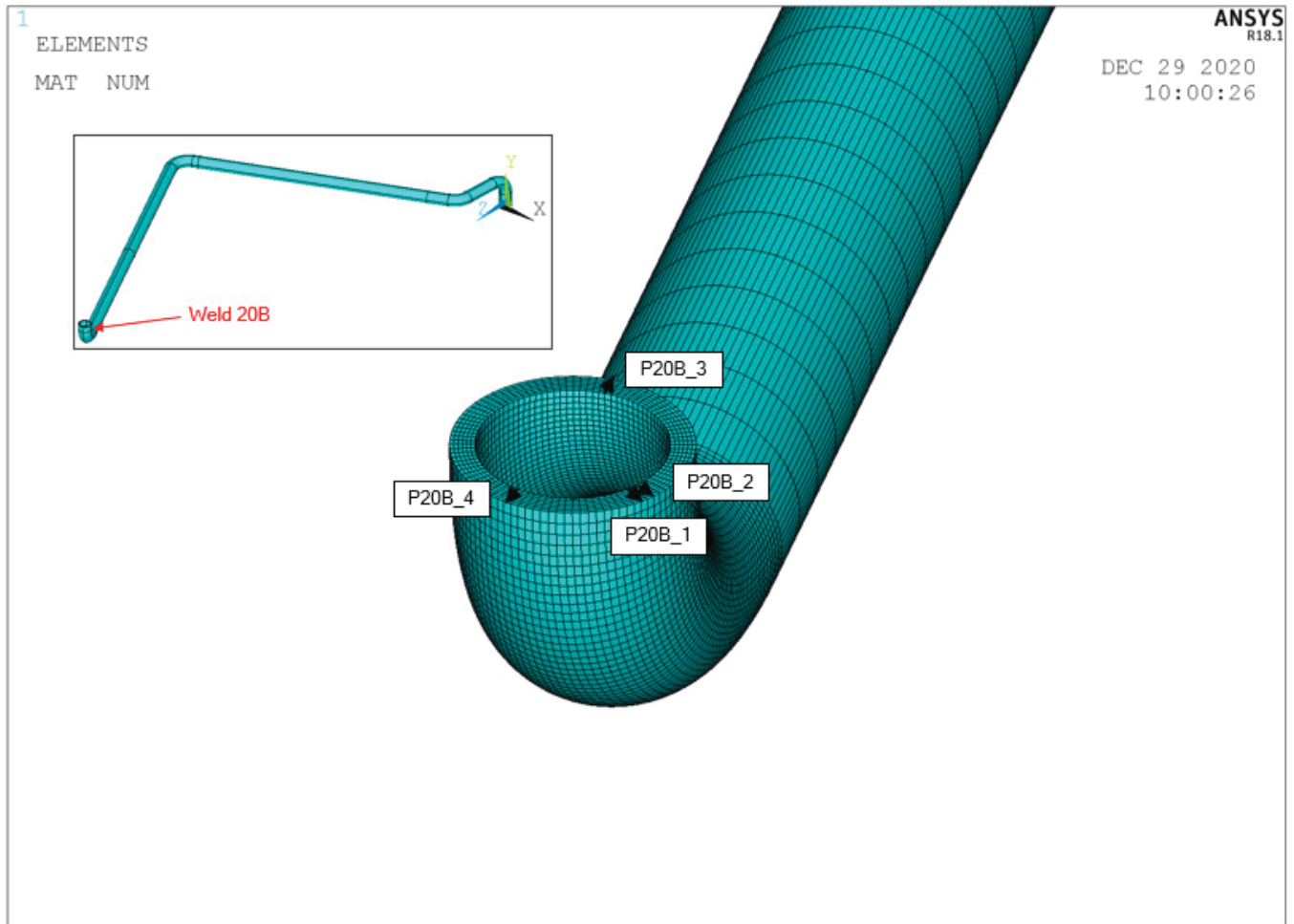This figure is based on Figure 8 of Reference [5].

Figure 4-8. Weld 20B Critical Paths

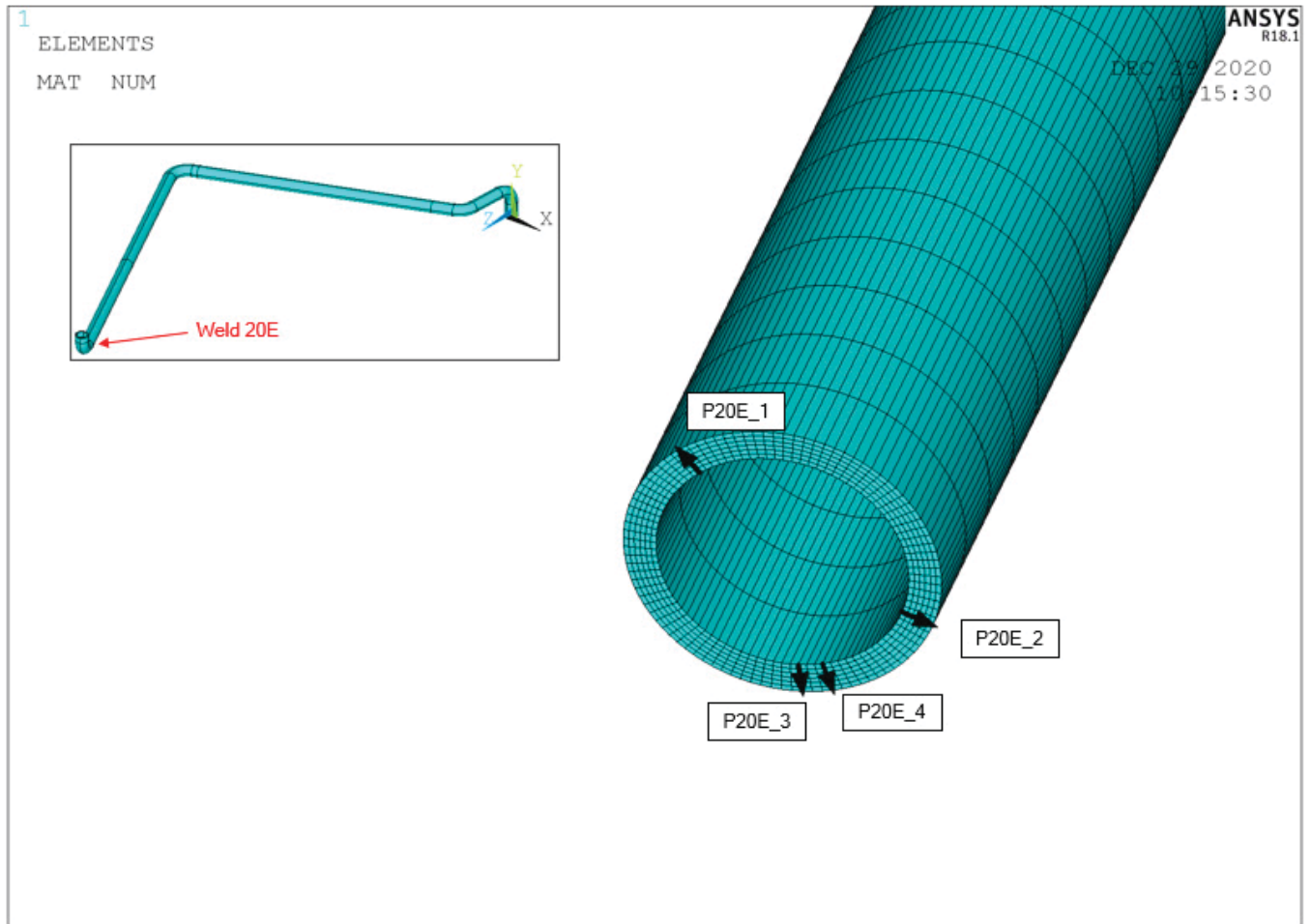This figure is based on Figure 13 of Reference [5].

Figure 4-9. Weld 20E Critical Paths

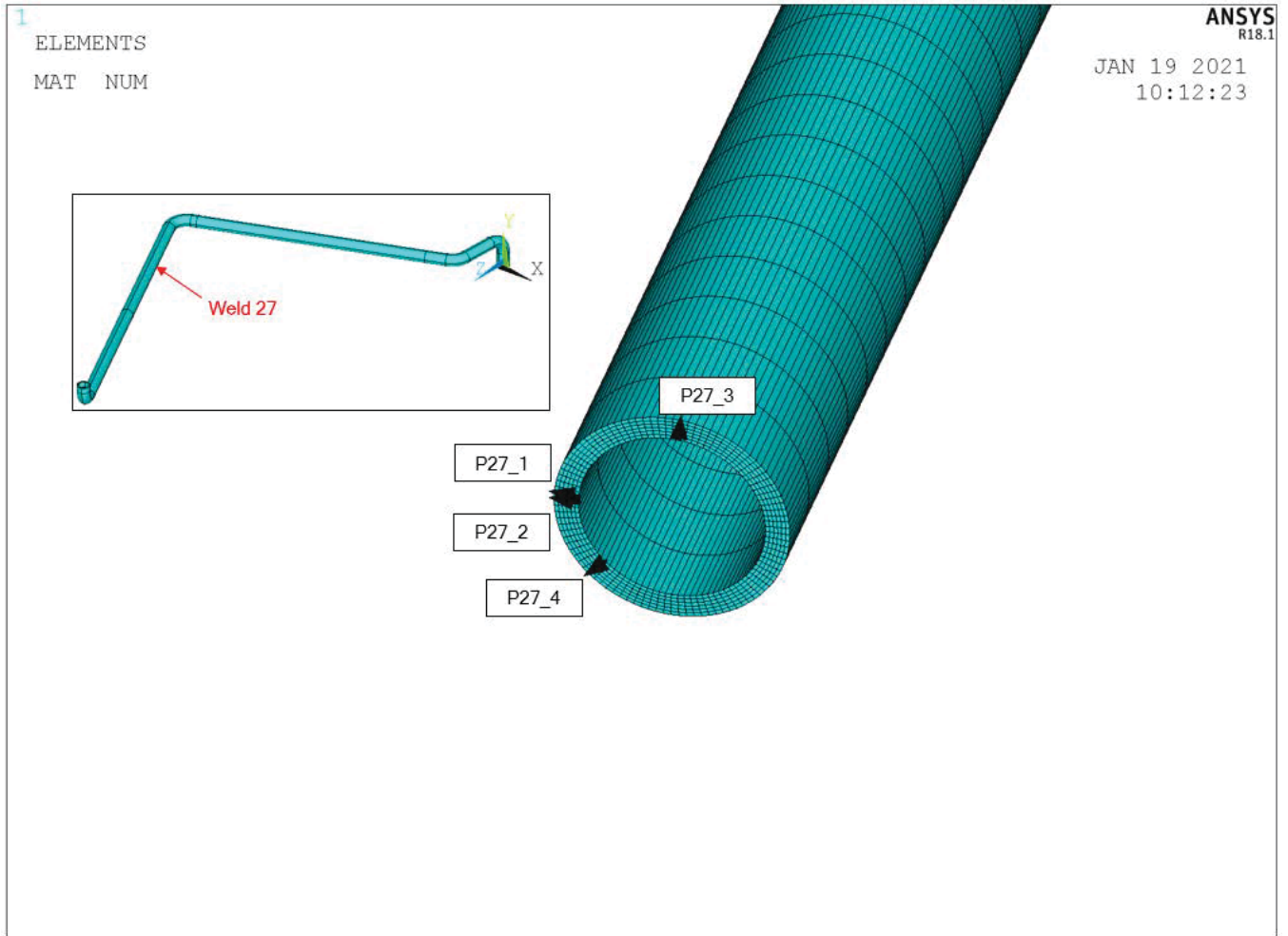This figure is based on Figure 14 of Reference [5].

Figure 4-10. Weld 27 Critical Paths

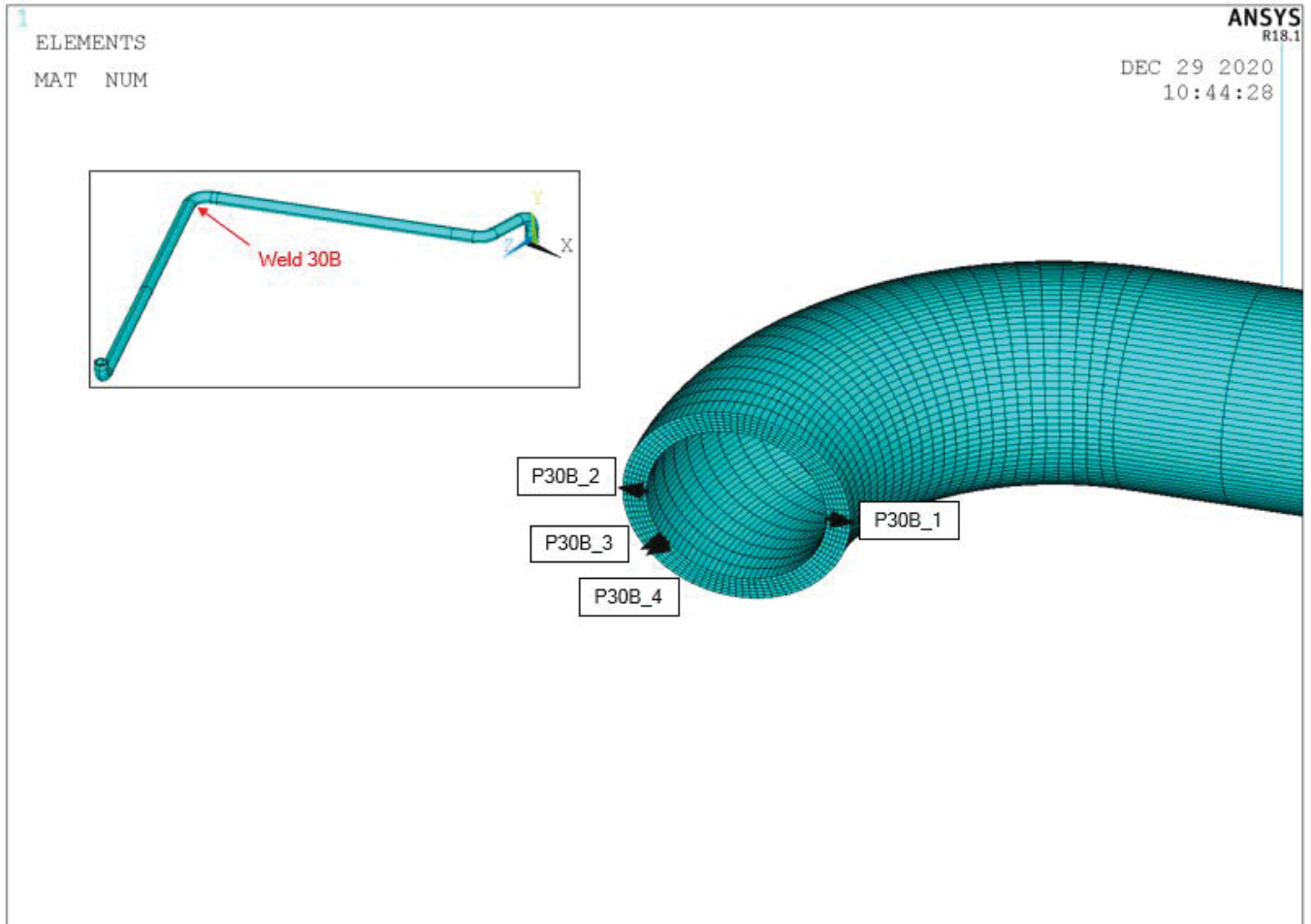This figure is based on Figure 15 of Reference [5].

Figure 4-11. Weld 30B Critical Paths

This figure is based on Figure 16 of Reference [5].

Figure 4-12. Weld 30E Critical Paths

This figure is based on Figure 17 of Reference [5].

Figure 4-13. Weld 50B Critical Paths

This figure is based on Figure 18 of Reference [5].

Figure 4-14. Weld 50E Critical Paths

This figure is based on Figure 19 of Reference [5].

Figure 4-15. Weld 60B Critical Paths

This figure is based on Figure 20 of Reference [5].
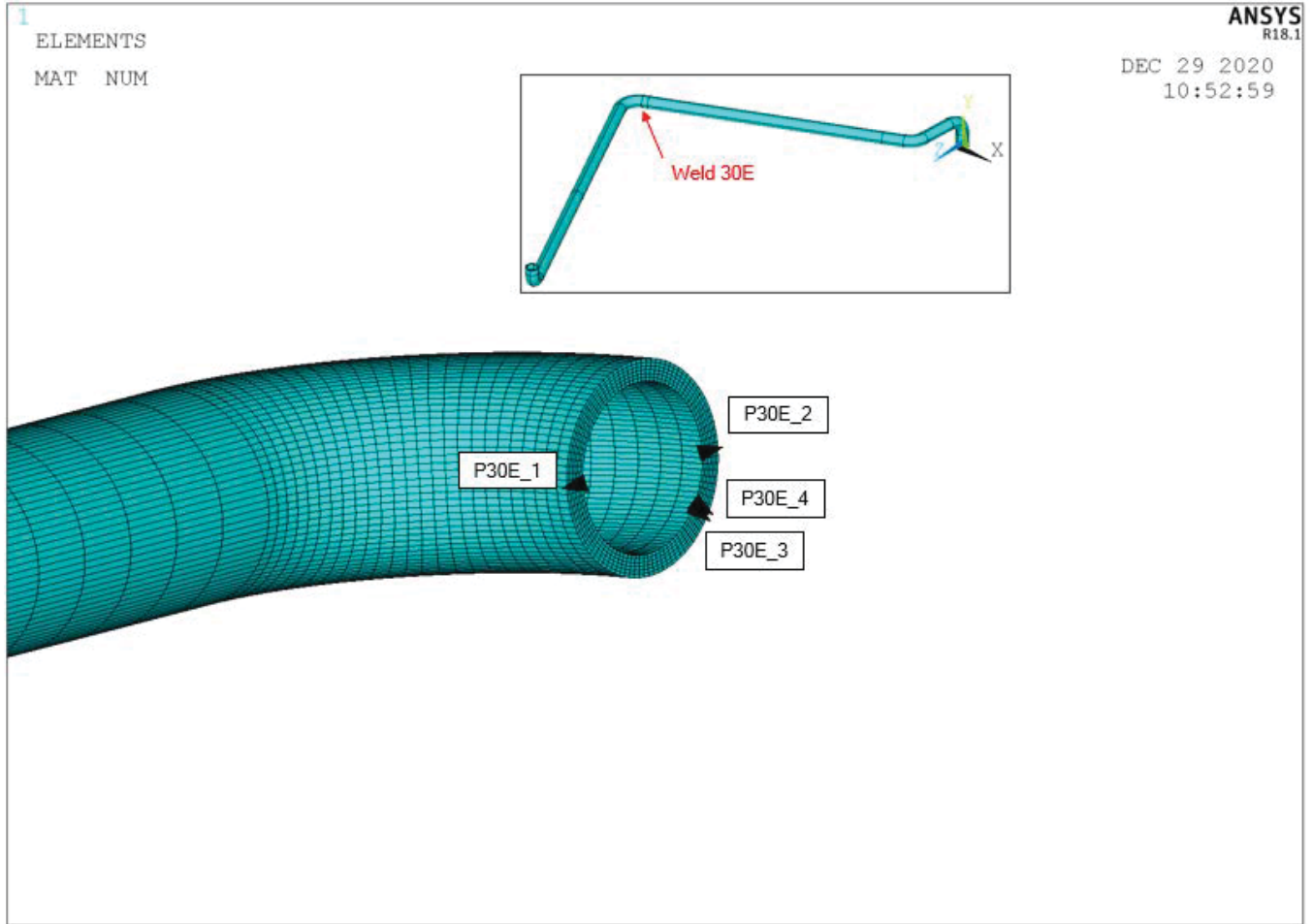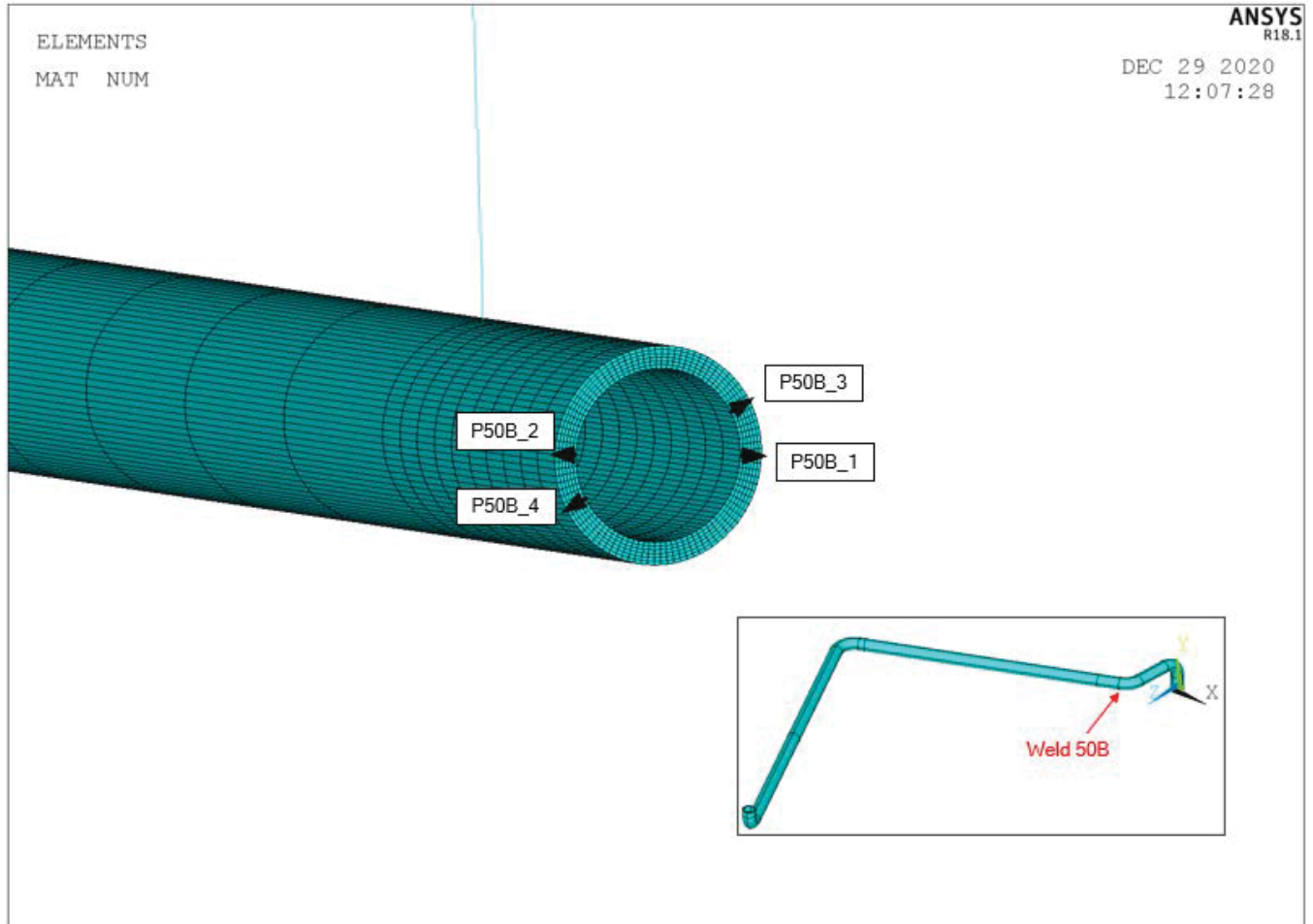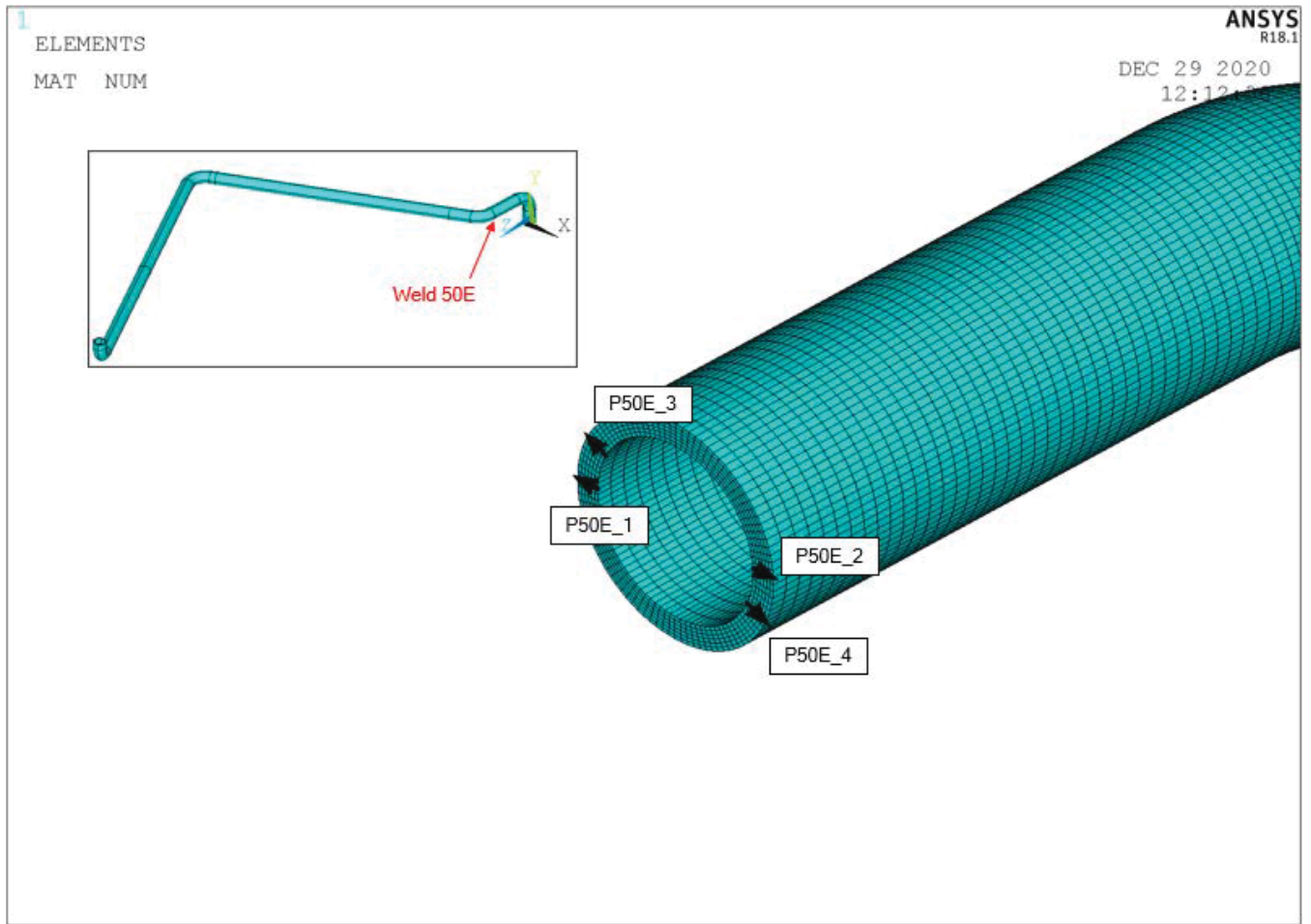
Figure 4-16. Weld 60E Critical Paths
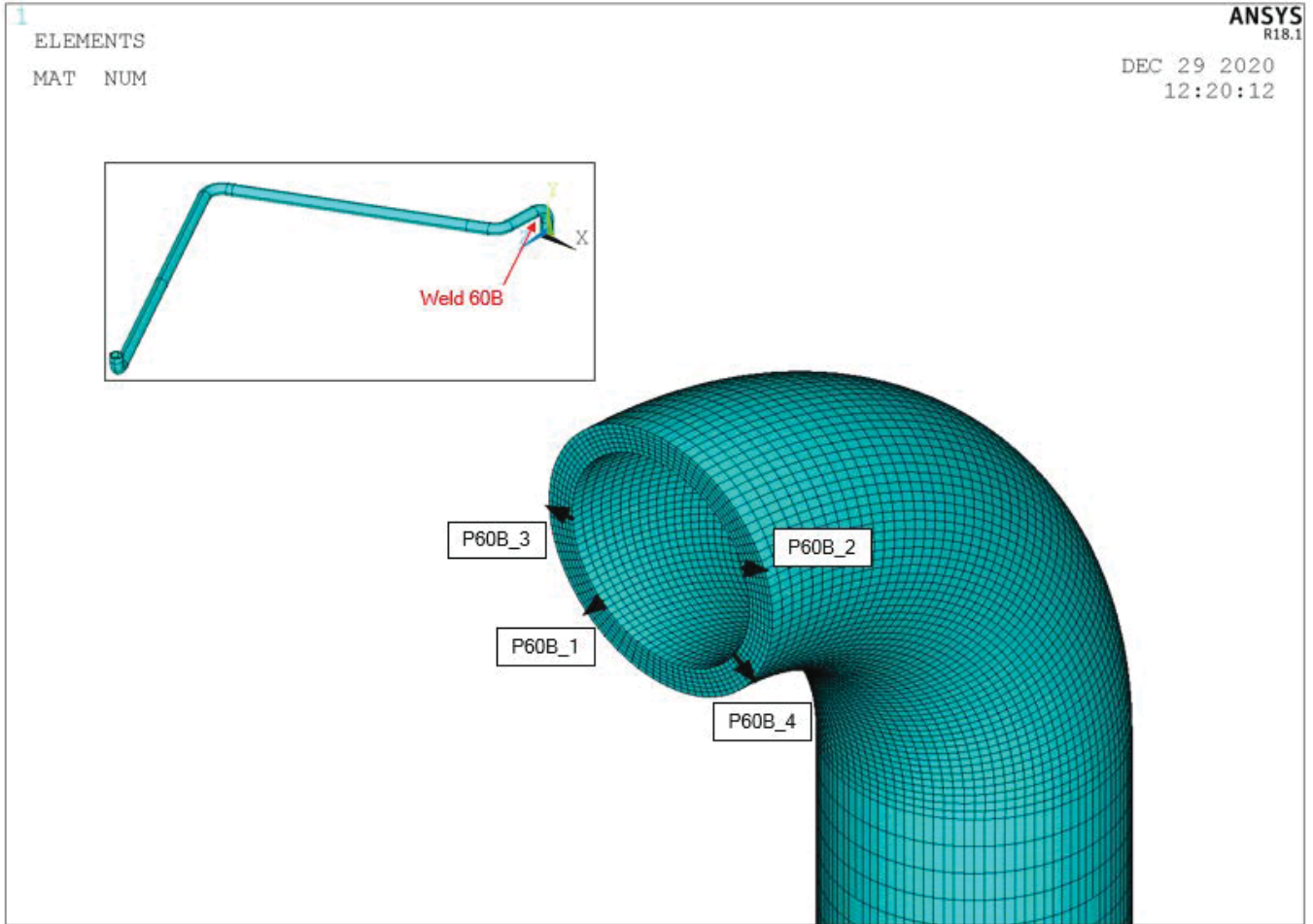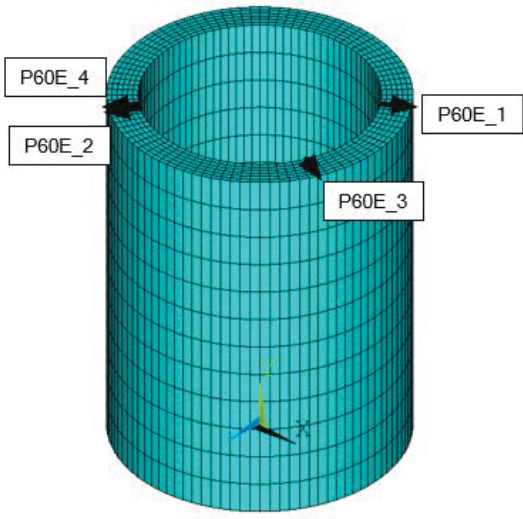
This figure is based on Figure 21 of Reference [5].
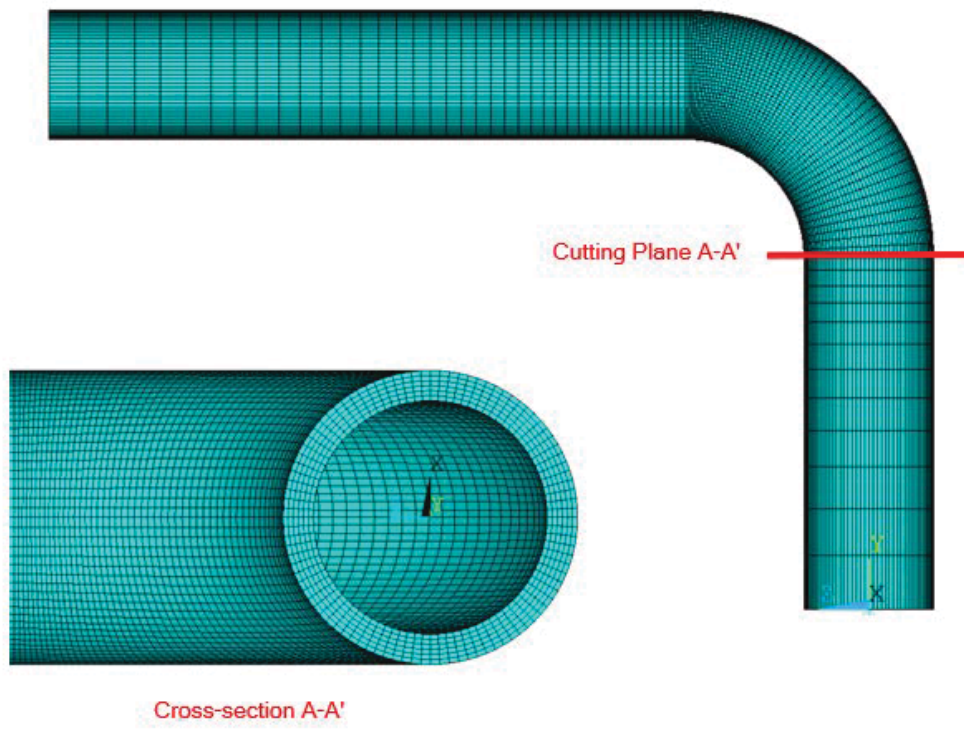
Figure 4-17. Elbow Mechanical Load Stress Analyses Region of Interest

This figure is based on Figure 22 of Reference [5].
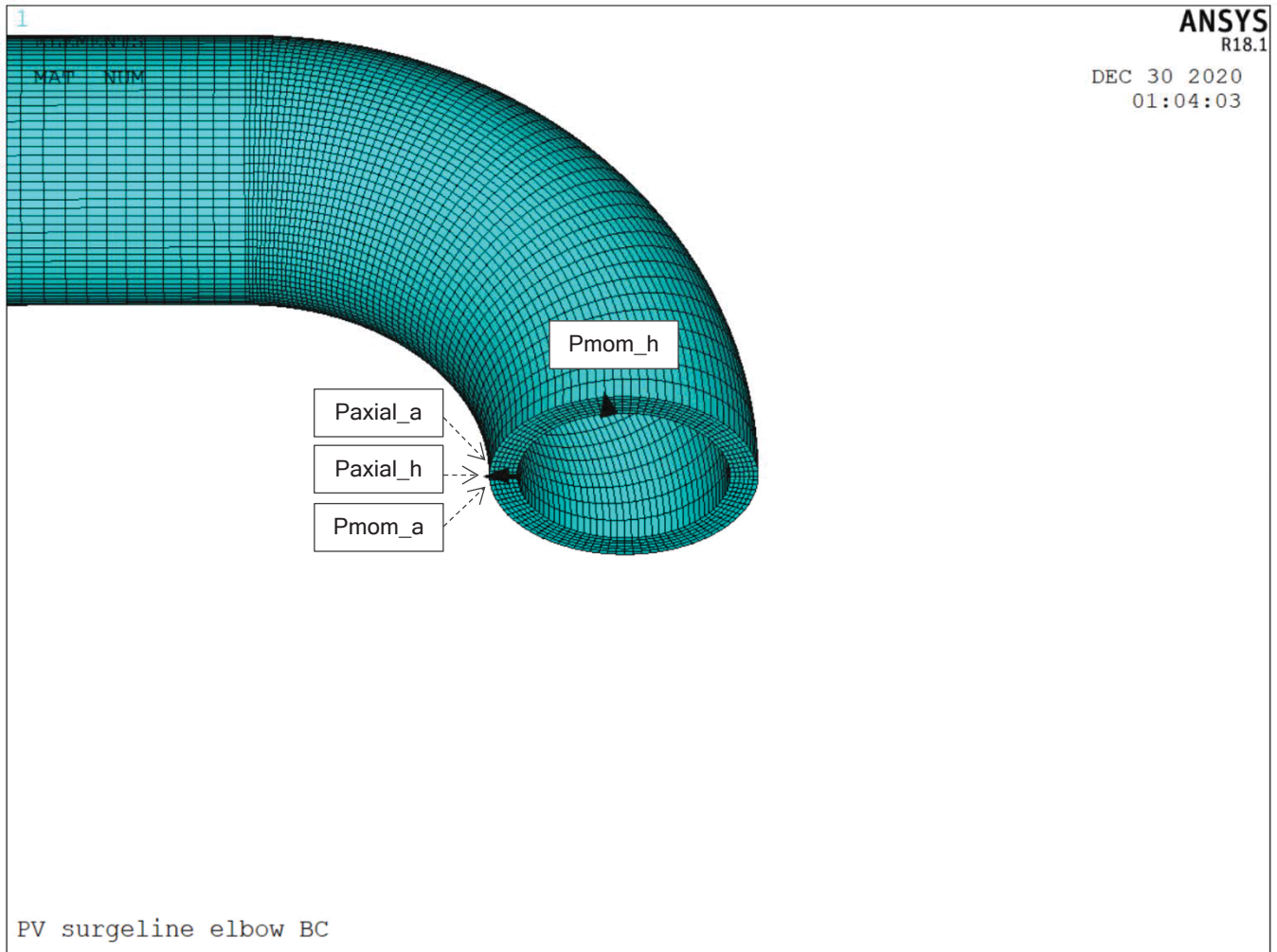
Figure 4-18. Elbow Critical Stress Path Locations due to Mechanical Loads

Note:

Generated from stress analysis under axial force, FY, loading. Paxial_a and Paxial_h are paths based on maximum axial stress and maximum hoop stress, respectively.

Generated from stress analysis under bending moment, MX, loading. Pmom_a and Pmom_h are paths based on maximum axial stress and maximum hoop stress, respectively.

Paxial_a, Paxial_h and Pmom_a have the same path location.

This figure is based on Figure 23 of Reference [5].

Figure 4-19. Maximum Hoop Stress at Weld 20B

Figure 4-20. Maximum Hoop Stress at Weld 20E

Notes:
Figures above were obtained from Reference [6]
** - Maximum total stress is the sum of the stress plotted in the figure.
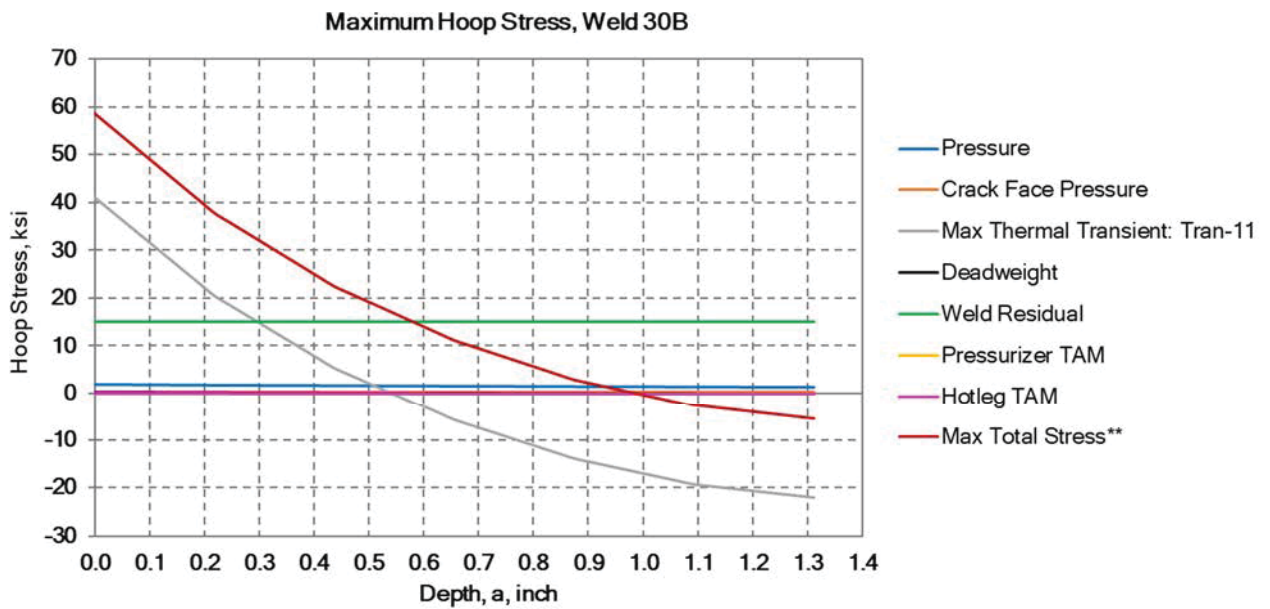
Figure 4-21. Maximum Hoop Stress at Weld 30B
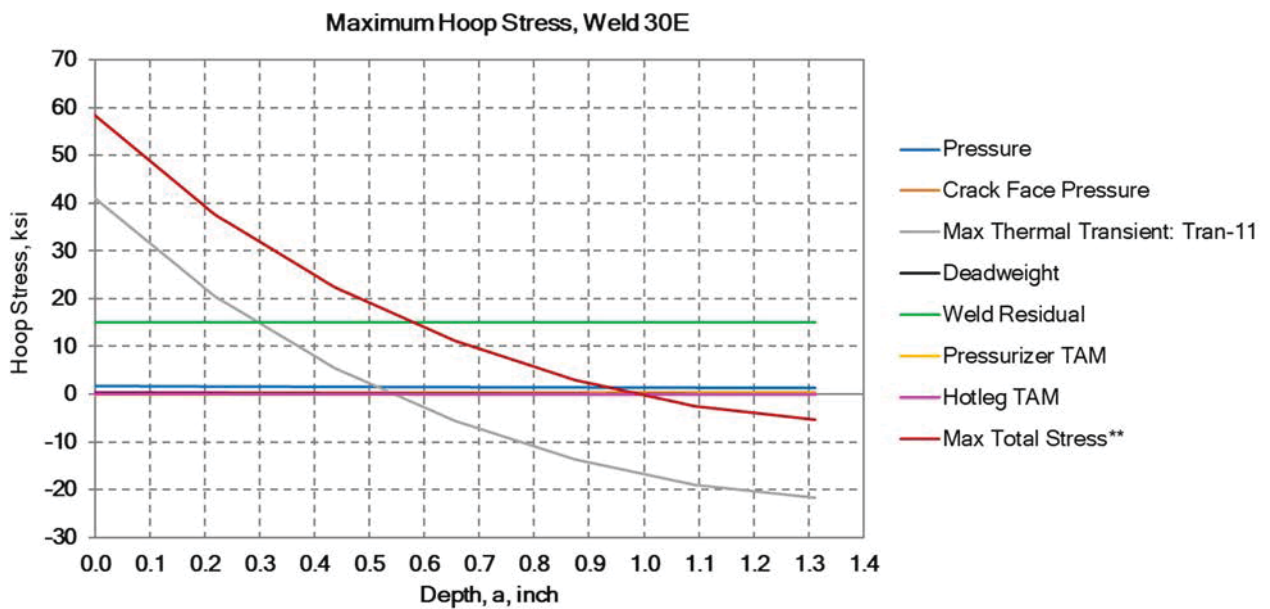
Figure 4-22. Maximum Hoop Stress at Weld 30E

Notes:
Figures above were obtained from Reference [6]
** - Maximum total stress is the sum of the stress plotted in the figure.
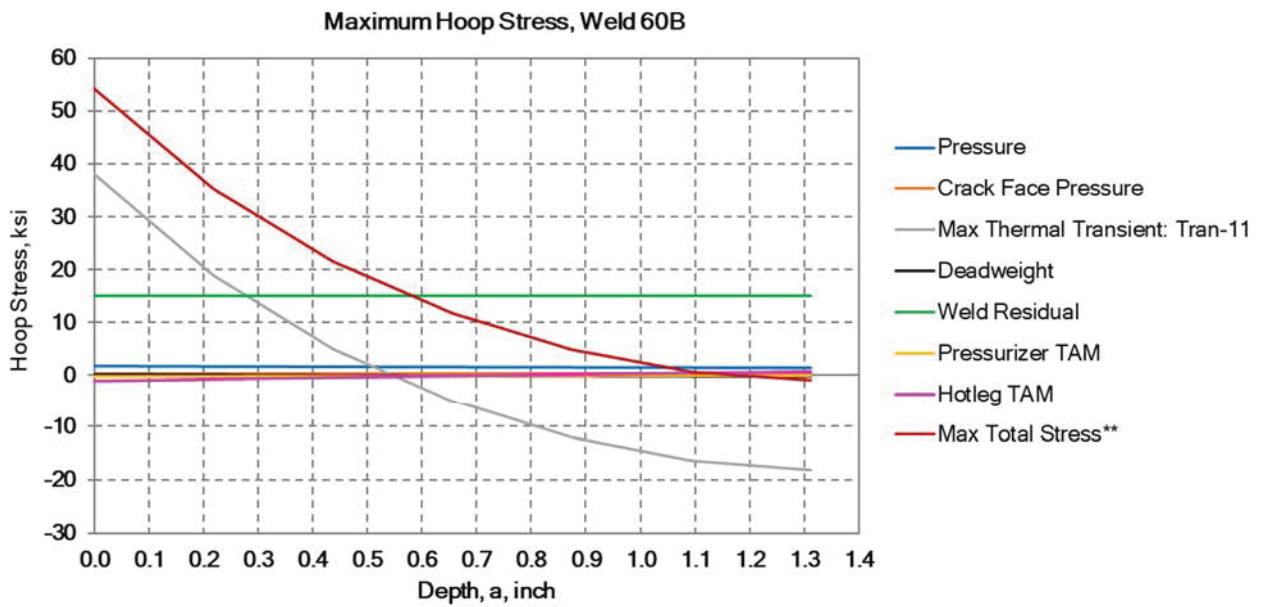
Figure 4-23. Maximum Hoop Stress at Weld 60B
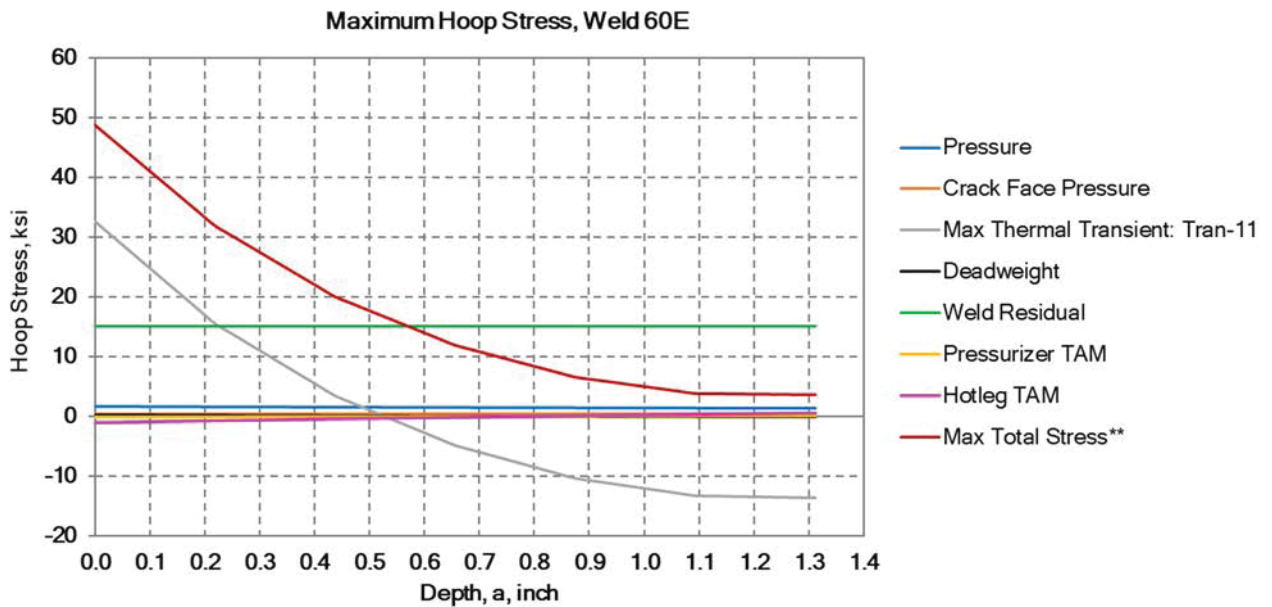
Figure 4-24. Maximum Hoop Stress at Weld 60E

Notes:
Figures above were obtained from Reference [6]
** - Maximum total stress is the sum of the stress plotted in the figure.
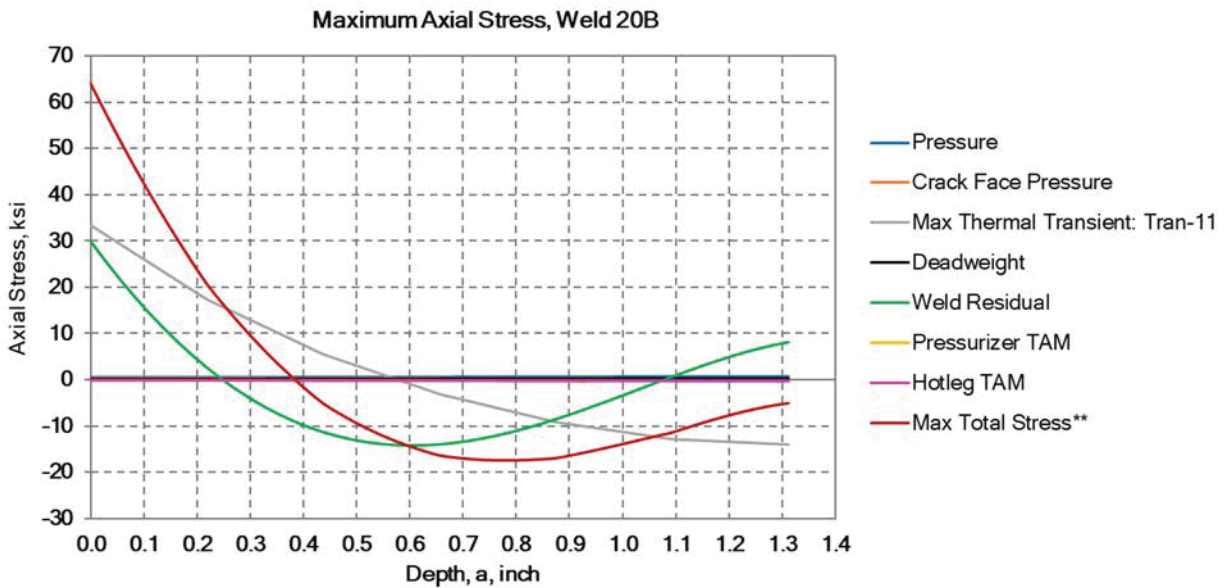
Figure 4-25. Maximum Axial Stress at Weld 20B
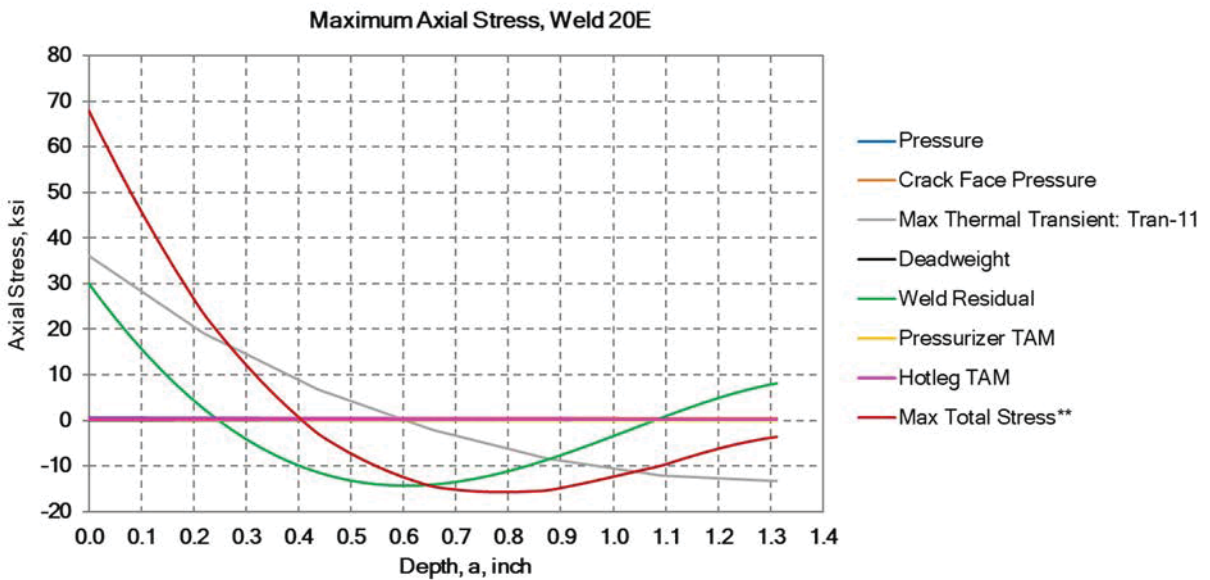
Figure 4-26. Maximum Axial Stress at Weld 20E

Notes:
Figures above were obtained from Reference [6]
** - Maximum total stress is the sum of the stress plotted in the figure.
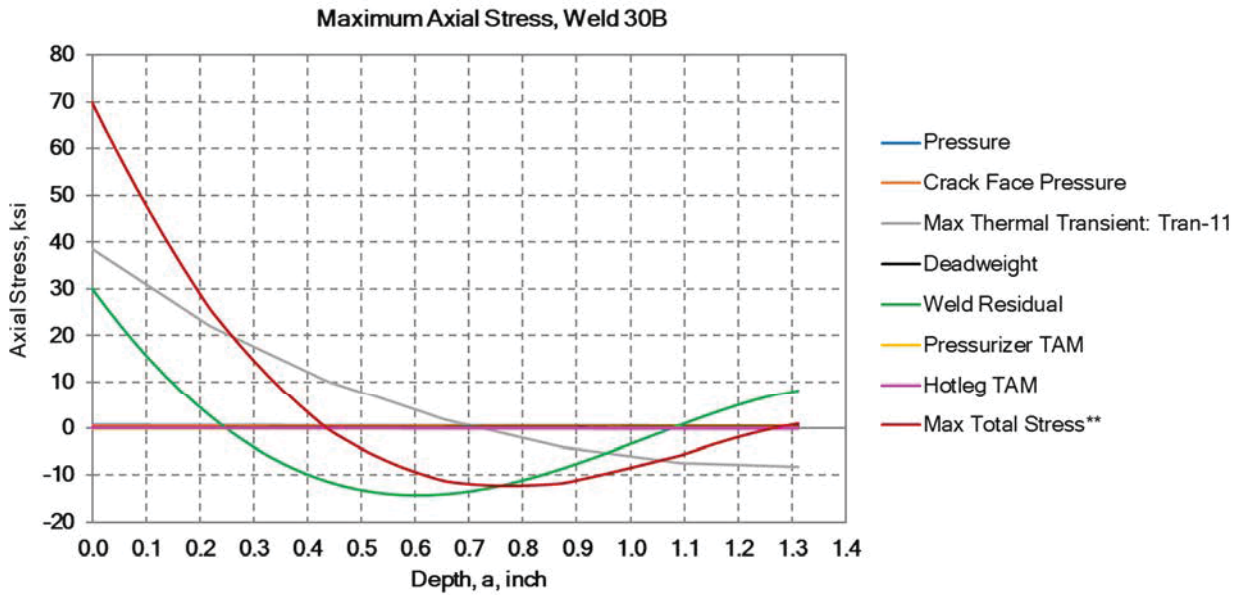
Figure 4-27. Maximum Axial Stress at Weld 30B
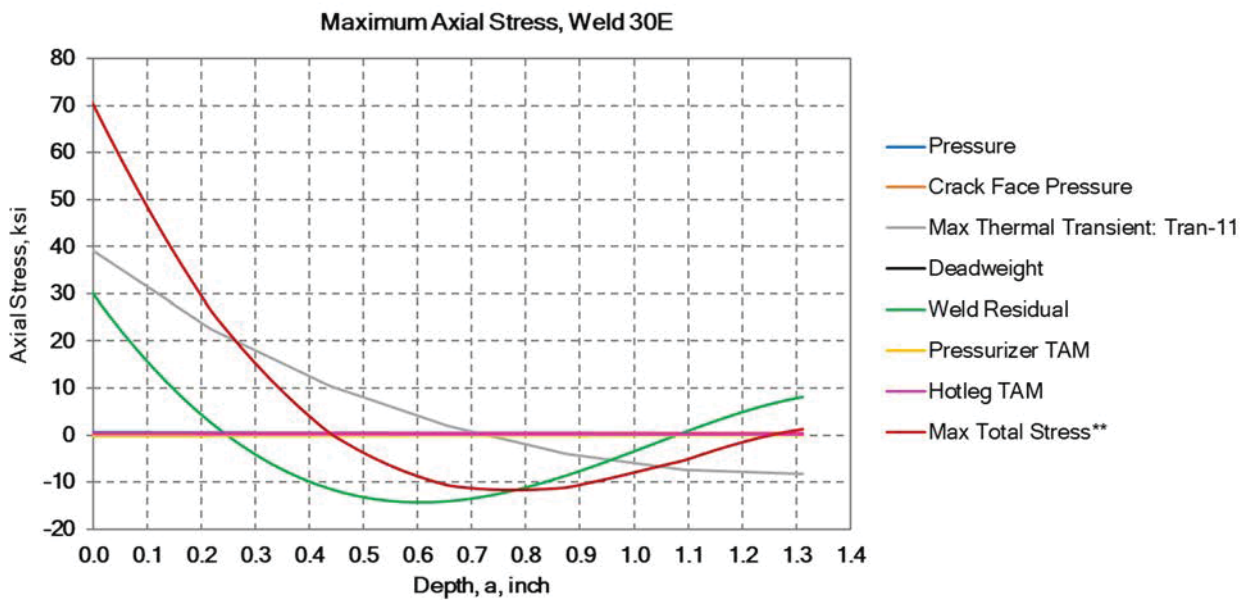
Figure 4-28. Maximum Axial Stress at Weld 30E

Notes:
Figures above were obtained from Reference [6]
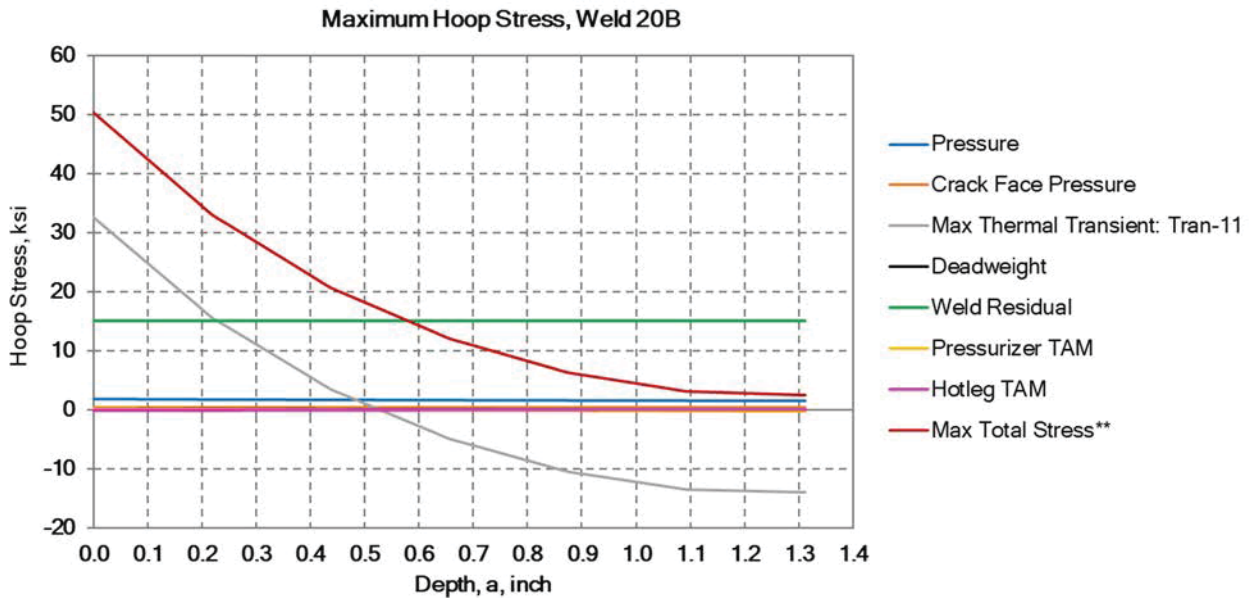** - Maximum total stress is the sum of the stress plotted in the figure.

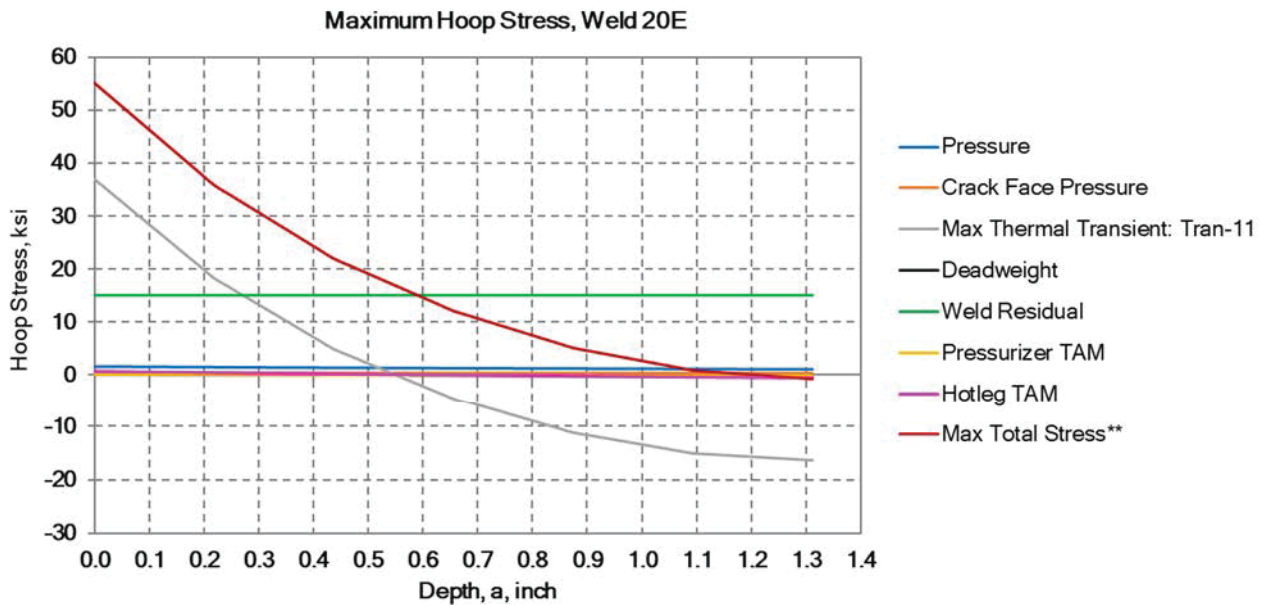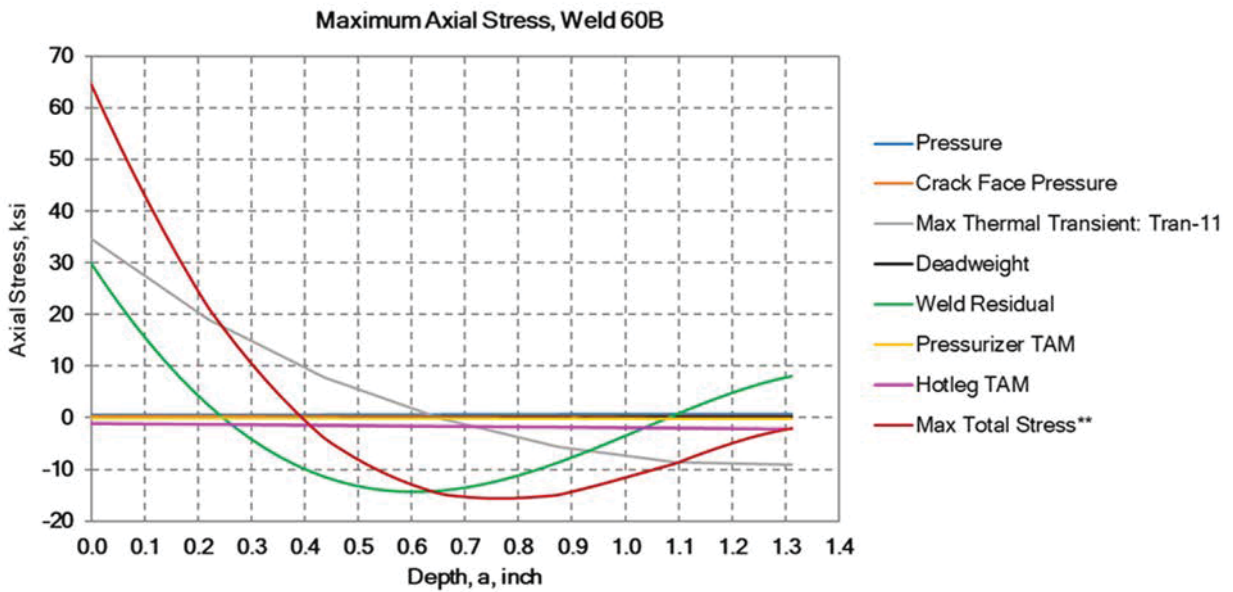**Figure 4-29. Maximum Axial Stress at Weld 60B**
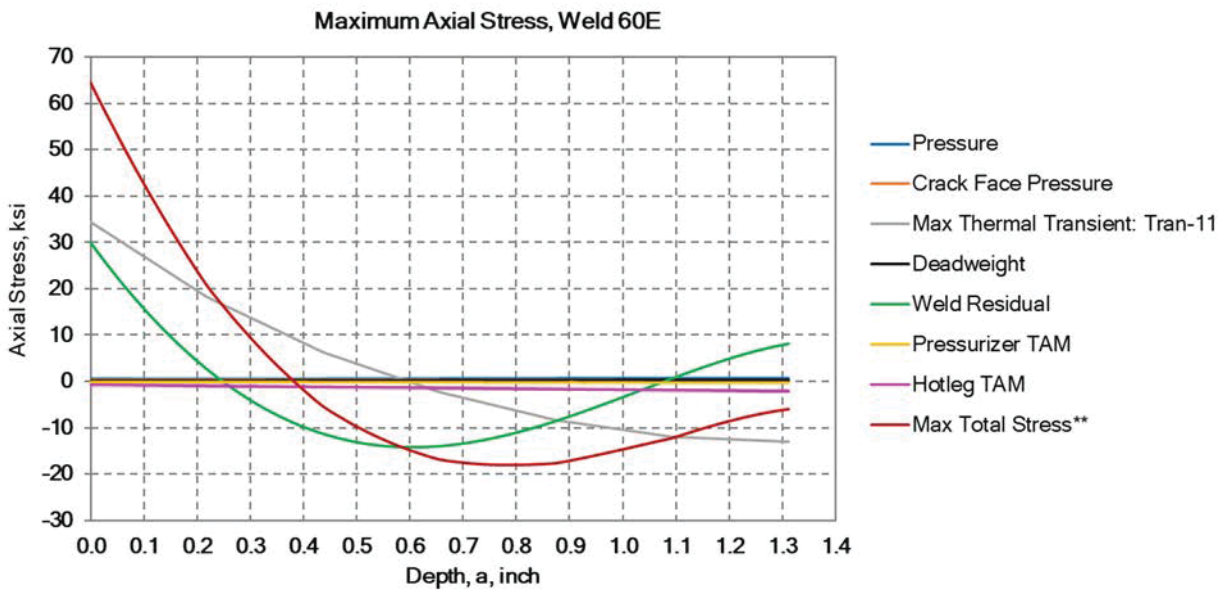
Figure 4-30. Maximum Axial Stress at Weld 60E

Notes:
Figures above were obtained from Reference [6]
** - Maximum total stress is the sum of the stress plotted in the figure.
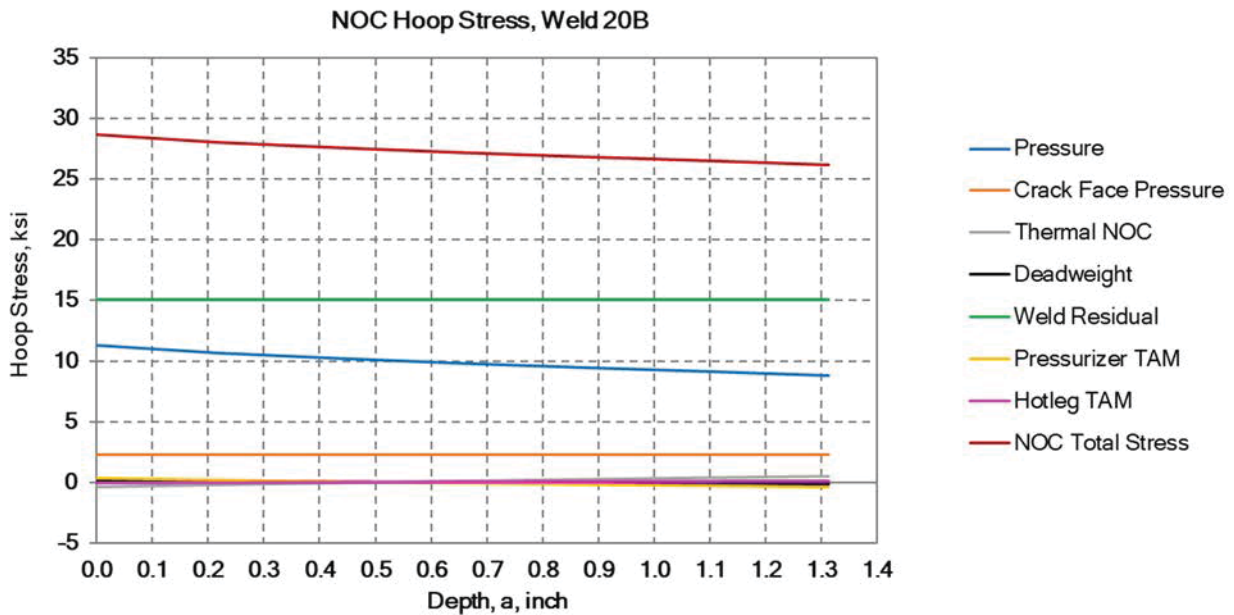
Figure 4-31. Hoop Stress under Normal Operating Conditions at Weld 20B
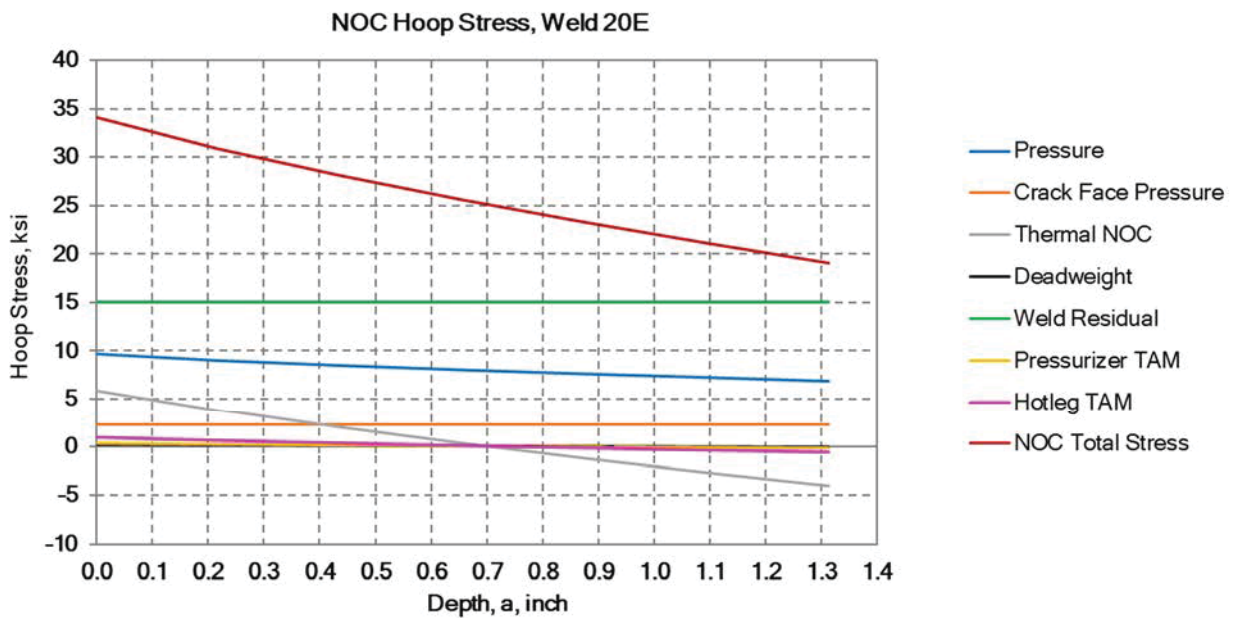
Figure 4-32. Hoop Stress under Normal Operating Conditions at Weld 20E

Note:
Figures above were obtained from Reference [6]
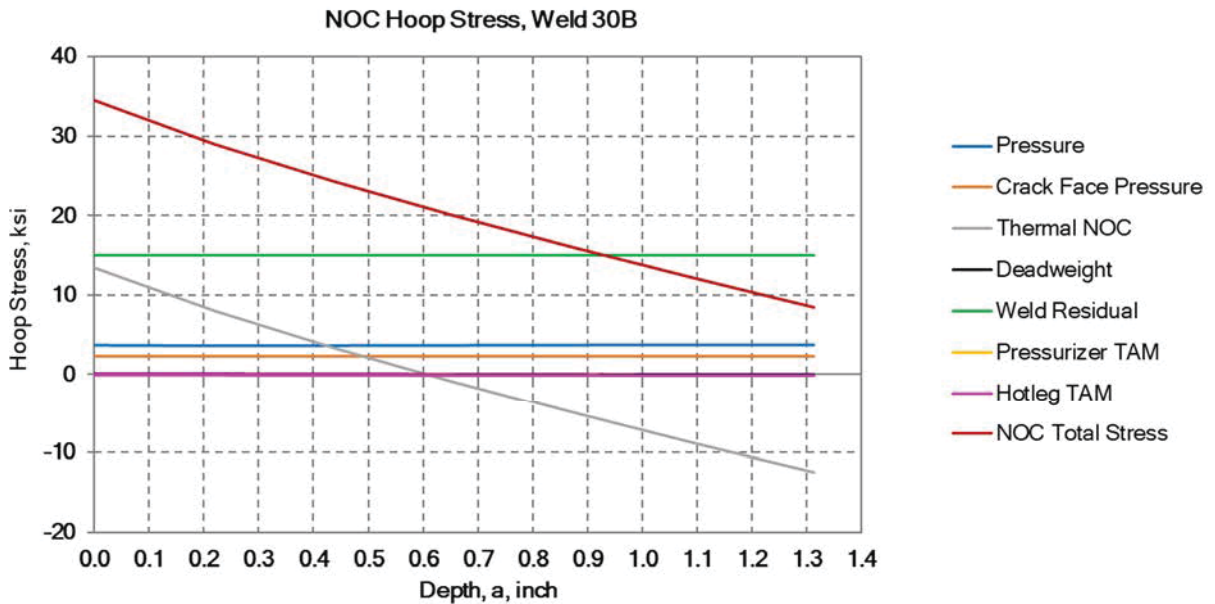
Figure 4-33. Hoop Stress under Normal Operating Conditions at Weld 30B
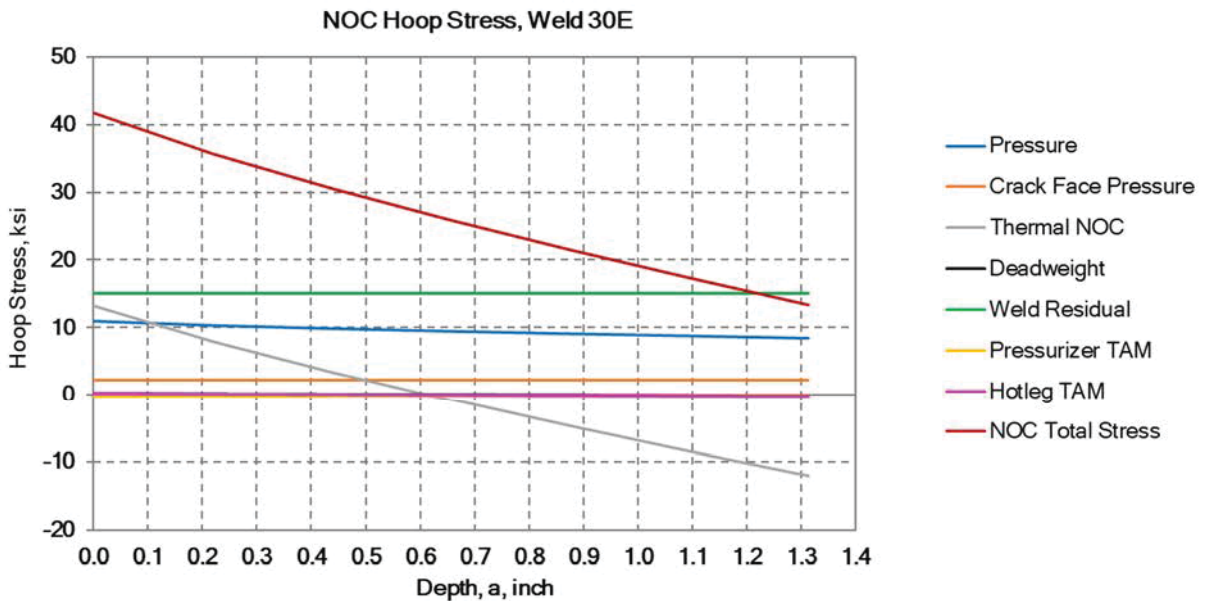
Figure 4-34. Hoop Stress under Normal Operating Conditions at Weld 30E

Note:
Figures above were obtained from Reference [6]
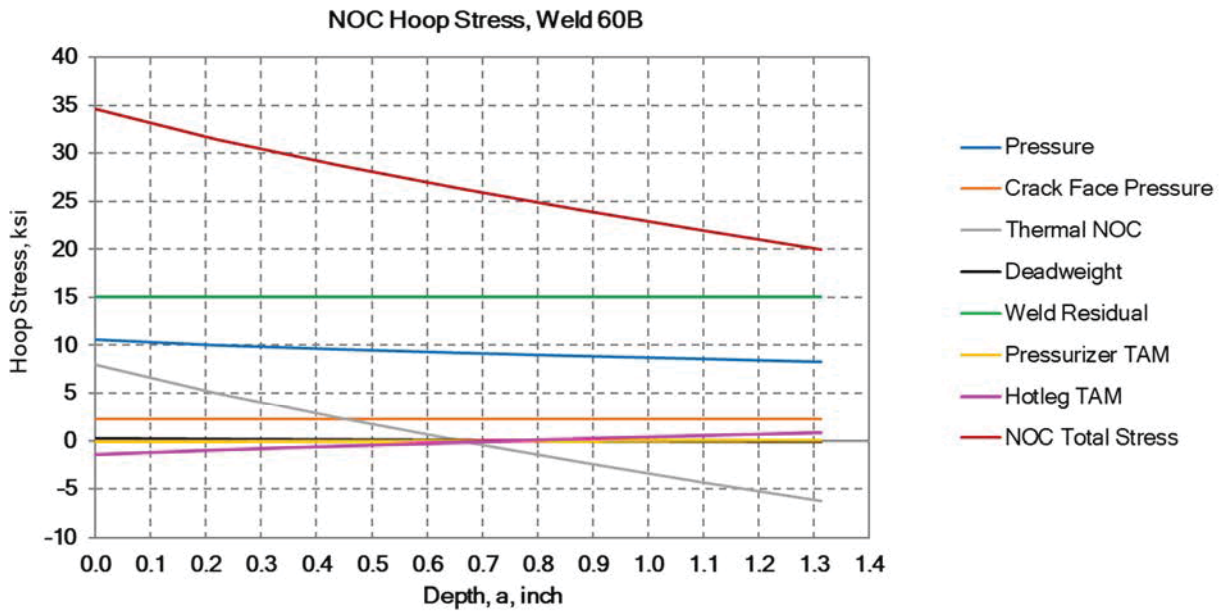
Figure 4-35. Hoop Stress under Normal Operating Conditions at Weld 60B
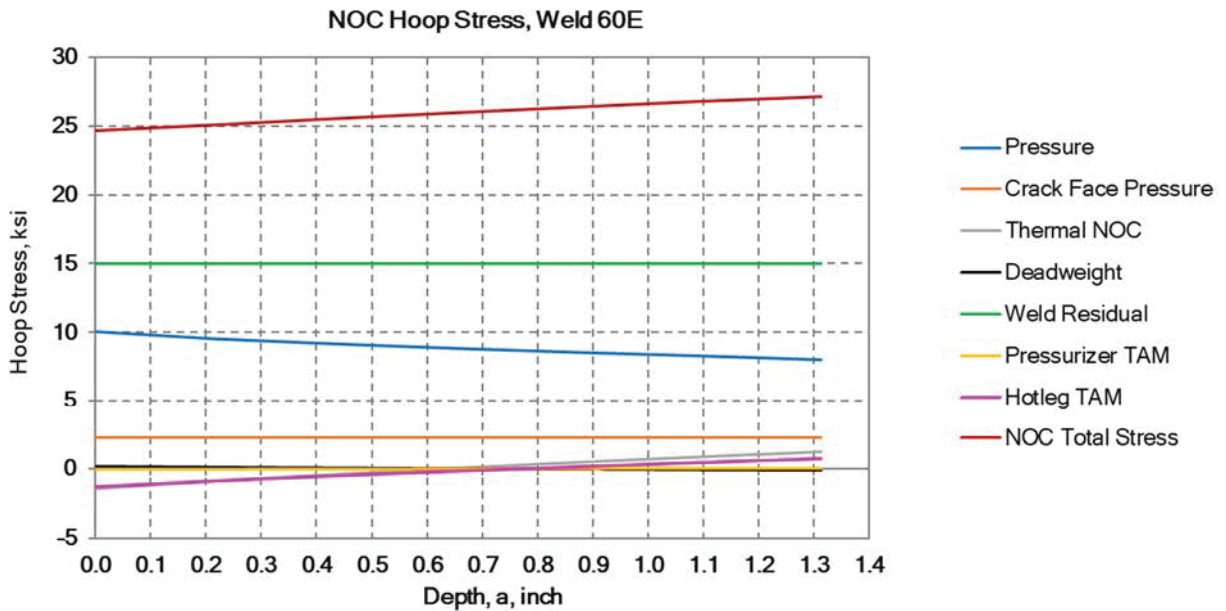
Figure 4-36. Hoop Stress under Normal Operating Conditions at Weld 60E

Note:
Figures above were obtained from Reference [6]
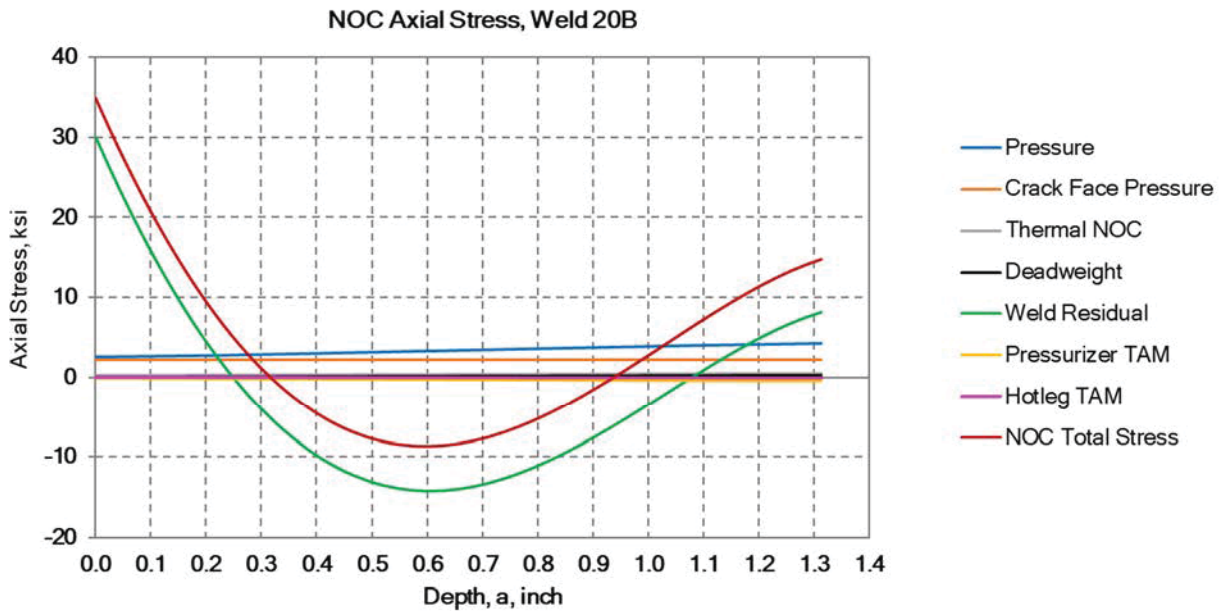
Figure 4-37. Axial Stress under Normal Operating Conditions at Weld 20B
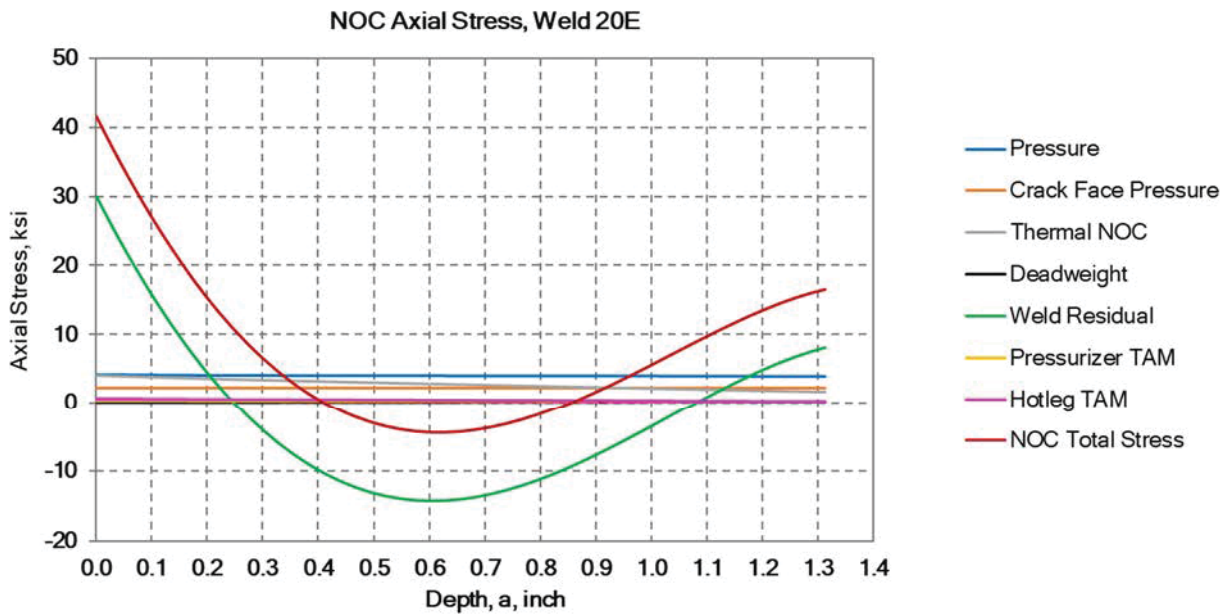
Figure 4-38. Axial Stress under Normal Operating Conditions at Weld 20E

Note:
Figures above were obtained from Reference [6]
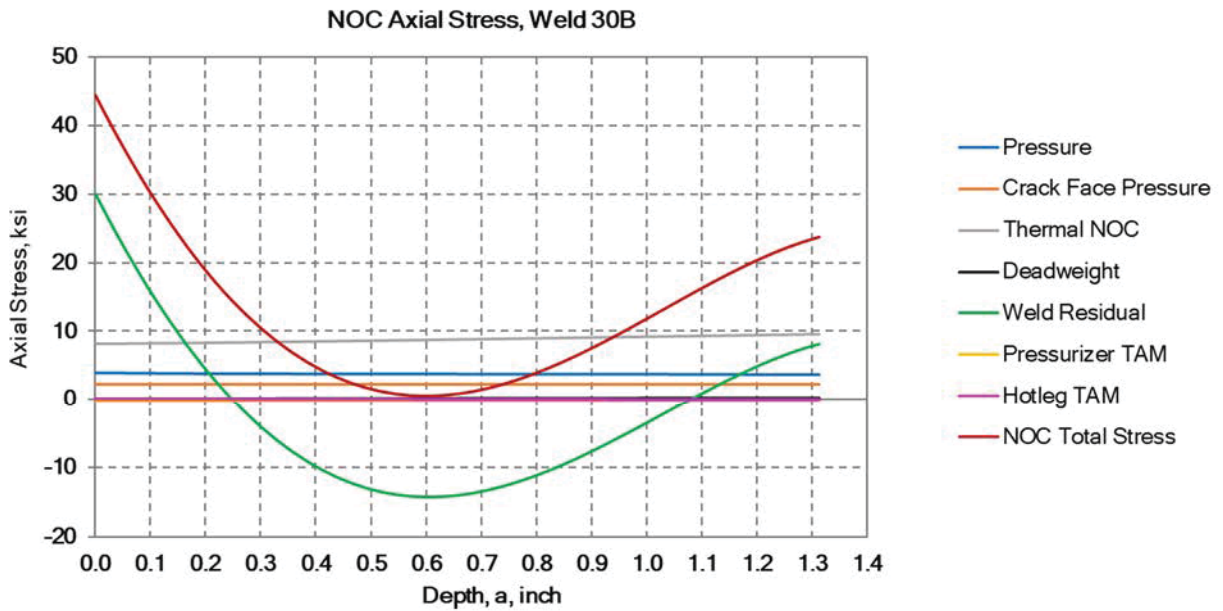
Figure 4-39. Axial Stress under Normal Operating Conditions at Weld 30B
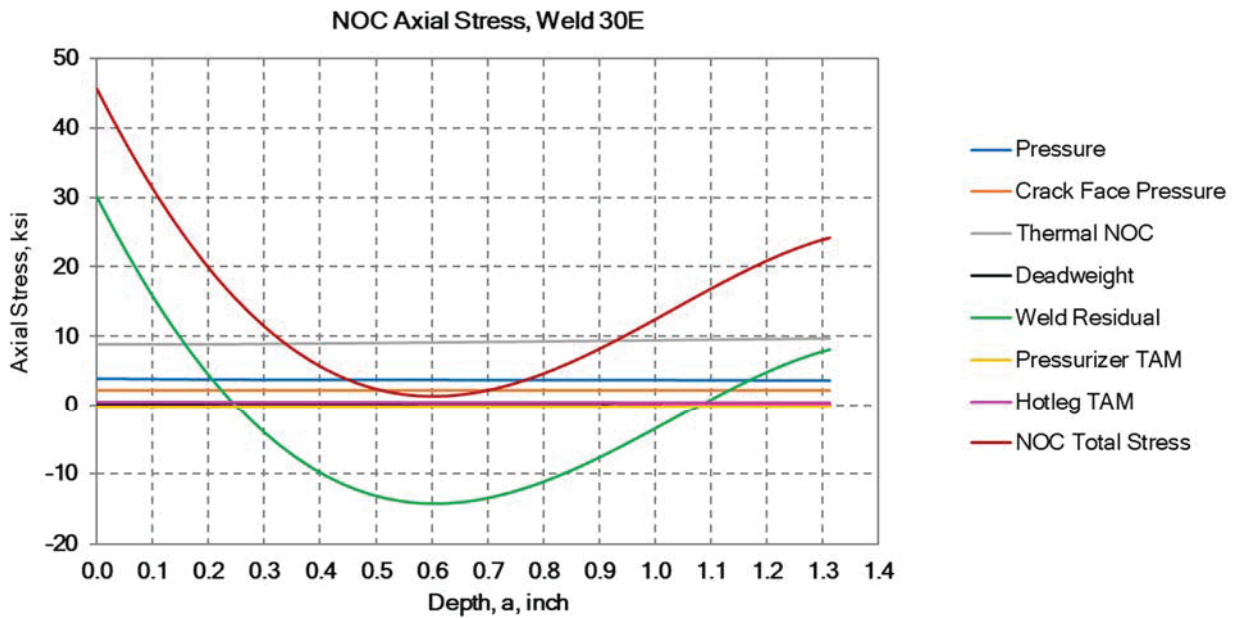
Figure 4-40. Axial Stress under Normal Operating Conditions at Weld 30E

Note:
Figures above were obtained from Reference [6]
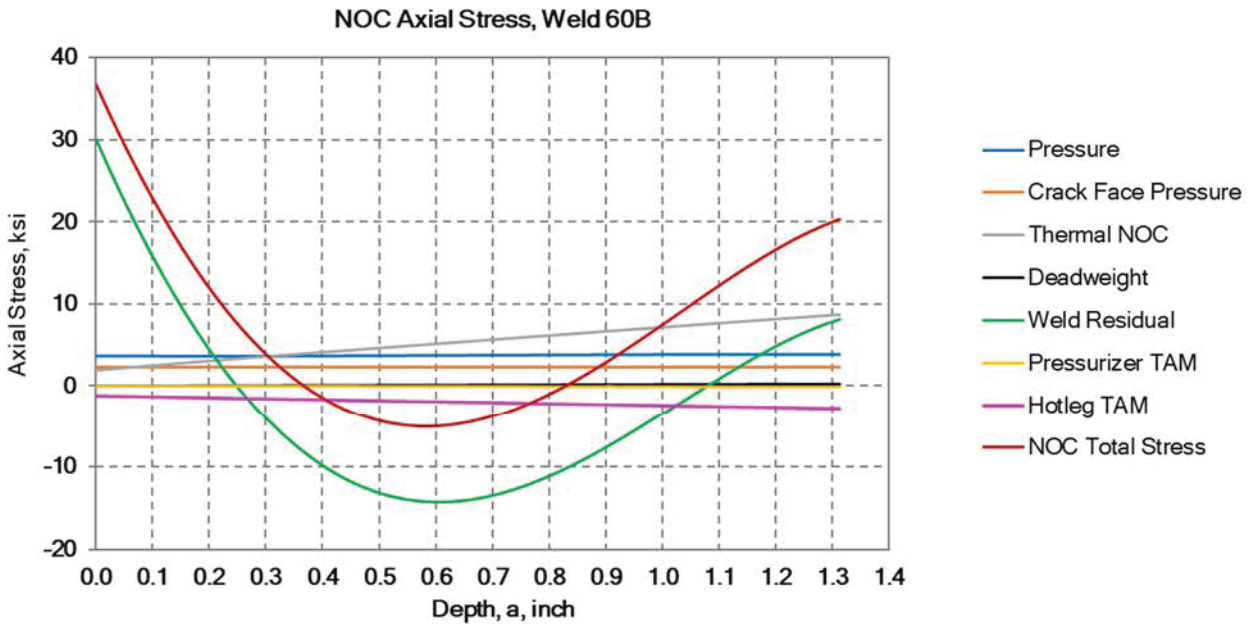
Figure 4-41. Axial Stress under Normal Operating Conditions at Weld 60B
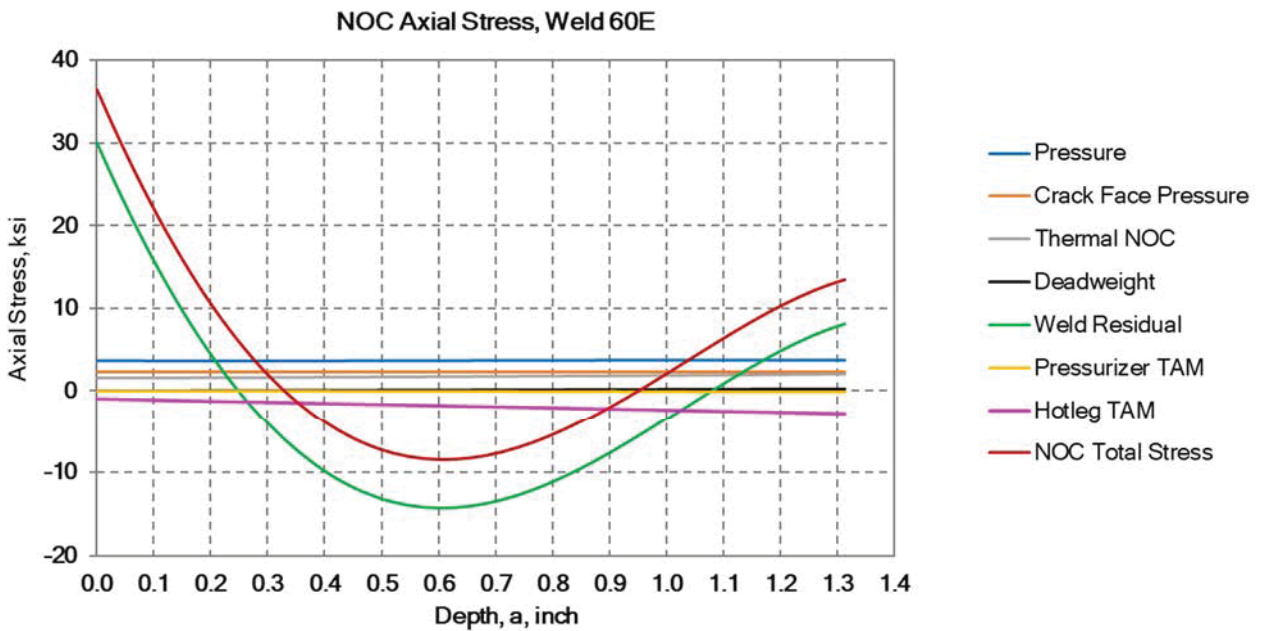
Figure 4-42. Axial Stress under Normal Operating Conditions at Weld 60E

Note:
Figures above were obtained from Reference [6]

5.0 ALLOWABLE FLAW SIZE EVALUATION

Allowable flaw sizes are calculated for circumferential and axial part through-wall flaws in the following sections.

5.1 Allowable Flaw Size Determination

One important aspect of a flaw tolerance evaluation is the determination of the allowable flaw sizes. These are the flaw sizes that cannot be exceeded when the Code structural factors are applied under the applied loads. As required by Appendix L of the ASME B&PV Code, Section XI [1], the flaw evaluation procedures of IWB-3640 are used in the determination of the allowable flaw sizes.

For the weld metal and adjacent base metal, guidance for calculation of allowable flaw sizes at the surge line piping welds is provided in ASME B&PV Code, Section XI, Appendix L (L-3000) [1]. The allowable flaw sizes (circumferential depth/length) for the welds are determined based on the rules in ASME B&PV Code, Section XI, Subsections IWB-3640 and Appendix C [1], which contains the screening criteria procedure to determine the applicable failure mode and evaluation for allowable flaw sizes with appropriate structural factors.

A crack growth evaluation presented in Section 6.0 determines the allowable operating periods based on postulated initial flaw sizes and the allowable flaw sizes calculated herein.

5.2 Assumptions

The following are assumptions used in this calculation:

1. Guidance for determining allowable axial flaw lengths is provided in the ASME B&PV Code, Section XI, Appendix C-5400 [1]. The Code is intended for analysis of straight pipes and the stress equations in Appendix C are for straight pipe components. As allowable flaw sizes will be determined for welds that connect elbows, there could be axial flaws that extend into the elbow itself. The hoop stress in the elbow can be larger than the hoop stress in the straight pipe section [20]. Because the ASME B&PV Code does not provide guidance for the elbow hoop stress, a conservative approach is used to determine the hoop stress that can be used for the allowable axial flaw determination.

The maximum hoop stress in the elbow, shown to be at the 45° azimuth (center) of the elbow's intrados [20], is used to determine the axial stress ratios which are subsequently used to determine allowable flaw lengths. Although procedures for analyzing allowable axial flaws in pipe elbows have been developed by external sources, none have been officially accepted by the ASME. Thus, the approach used in this calculation, and documented in Reference [7], is conservative and is used for all the butt welds connected to elbows.

2. The surge line welds are conservatively assumed to be shielded metal arc welds (SMAW), as both gas tungsten arc welding (GTAW) and SMAW may have been used in the fabrication. The assumption of SMAW (a flux welding process) is conservative as it has more stringent requirements (Z-factor > 1.0) for allowable circumferential flaw size determination.

3. Appendix C of the ASME B&PV Code [1] does not provide guidance for evaluating the Z-factor for axial flaws in austenitic materials. Since an axial flaw is assumed to grow primarily into the austenitic pipe (non-flux) and not only in the flux based welds, a Z-factor of 1.0 is used [21, Equation 17]. In other words, once an axial flaw in the flux butt weld propagates further (axially) past the butt weld, it is now growing into the austenitic base metal of the pipe. This piping base metal has increased ductility, and thus a Z-factor of 1.0 can be used.

4. A single load analysis was conducted by APS for all three units [22]; thus the results from the allowable flaw calculation are bounding for all three units.

5. The calculated hoop stress value for the Node 27 butt weld (a straight pipe-to-pipe weld) used in the allowable axial flaw determination was calculated using a conservative thick wall cylinder formula [20], rather than the Appendix C equation ($\sigma_h = PR_m/t$).

5.3 Interface Loads

The piping interface loads are listed in Section 3.0, Table 3-2.

5.4   Load Combinations

The load combinations represent the normal conditions (Service Level A), upset conditions (Service Level B), and emergency/faulted conditions (Service Level D). Service Level C loads are not evaluated as they are not present in the piping stress analysis [23]. Within each service level, loads are broken into primary and secondary bending loads to appropriately apply structural factors for the allowable flaw calculation. Each separate Service Level load case (Primary or Secondary) is developed by adding the individual moment values (Mx, My, and Mz) from the individual load cases (Deadweight, OBE, Thermal, etc.) to obtain a combined Mx, My, and Mz. These are then combined by the square-root-sum-of-the-squares method to develop a single moment term.

Service Level A Primary Bending
This load combination only includes deadweight loads.
Service Level A Secondary Bending
This load combination includes only thermal loads.

Service Level B Primary Bending
This load combination includes deadweight plus OBE loads (absolute summed).
Service Level B Secondary Bending
This load combination includes thermal plus OBE SAM loads (absolute summed).

Service Level D Primary Bending
This load combination includes deadweight plus the SRSS of SSE and LOCA loads (absolute summed).
Service Level D Secondary Bending
This load combination includes thermal plus SSE SAM loads (absolute summed).

For example, the calculation of Service Level loads at Node 20B is shown in Table 5-1 and Table 5-2.

For Service Level A Primary loads, only deadweight is included. The Deadweight Mx (-2251 ft-lb), My (6 ft-lb), and Mz (1706 ft-lb) are SRSS'd to develop a single moment term (34 in-kip).

For Service Level A Secondary loads, only thermal is included. The Thermal Mx (-6887 ft-lb), My (159231 ft-lb), and Mz (-519 ft-lb) are SRSS'd to develop a single moment term (1913 in-kip).

For Service Level B Primary loads, deadweight and OBE inertial are combined. Deadweight Mx (-2251 ft-lb) is absolute summed with OBE Mx (5097 ft-lb), resulting in a total Mx of 7348 ft-lb. This is repeated for My and Mz, and the resultant three moments are SRSS'd to develop a single moment term (116 in-kip).

For Service Level B Secondary, thermal and OBE SAM are combined. Thermal Mx (-6887 ft-lb) is absolute summed with OBE SAM Mx (1097 ft-lb), resulting in a total Mx of 7984 ft-lb. This is repeated for My and Mz, and the resultant three moments are SRSS'd to develop a single moment term (1950 in-kip).

There are no Service Level C loadings [14].

For Service Level D Primary loads, deadweight is combined absolutely with the SRSS of SSE inertial and LOCA. Deadweight Mx (-2251 ft-lb) is absolute summed with the SRSS of SSE inertial (9522 ft-lb) and LOCA (16952 ft-lb) (SRSS = 19443 ft-lb), resulting in a total Mx of 21694 ft-lb. This is repeated for My and Mz, and the resultant three moments are SRSS'd to develop a single moment term (354 in-kip).

For Service Level D Secondary loads, thermal and SSE SAM are combined. Thermal Mx (-6887 ft-lb) is absolute summed with SSE SAM Mx (2404 ft-lb), resulting in a total Mx of 9291 ft-lb. This is repeated for My and Mz, and the resultant three moments are SRSS'd to develop a single moment term (1997 in-kip).

5.5   Material Properties for Allowable Flaw Size Determination

Material strength data for the base metal use ASME Code minimum properties [18] for both the axial and circumferential flaws. The yield stress, σ_y, and ultimate tensile stress, σ_u, at operating temperatures are shown in Section 4.3. The material properties are applicable to both the base metal and weld metal.

5.6   Welding Process

As stated earlier, the use of a flux process (SMAW or SAW) is conservatively selected for the weldments.

5.7   Z-Factor

As stated earlier, the use of a flux process (SMAW or SAW) is conservatively assumed for the weldments. Per ASME B&PV Code, Section XI, Appendix C (C-6330) [1], Z-factors (load factors) are calculated to account for the use of limit load as a failure criterion for the lower toughness welds fabricated using SMAW or SAW welding processes (flux processes) in the determination of the allowable flaw size for austenitic weldments:

$$Z = 1.30\,[1 + 0.010\,(NPS - 4)] \qquad \text{for NPS} > 4 \qquad (5\text{-}1)$$

where,

$$NPS = \text{Nominal pipe size (in)}$$

The calculated Z-factor for the 12-inch NPS surge line piping is 1.404 and applies for circumferential flaws only. The Z-factor for axial flaws is 1.0 as stated in Section 5.2.

5.8   Allowable Circumferential Part Through-Wall Flaw

For flux welds such as SMAW/SAW, the elastic-plastic fracture mechanics (EPFM) methodology described in ASME B&PV Code, Section XI, Appendix C (per the screening criteria of Figure C-6200-1) should be applied [1]. The technical approach consists of determining the allowable flaw size (circumferential extent and through-wall depth) in the pipe that will not result in fracture by crack extension, including the necessary structural factors (SFs).

For circumferential flaws, the stress ratio for combined loading is calculated as:

$$\text{Stress Ratio} = \frac{Z}{\sigma_f}(\sigma_m + \sigma_b + \frac{\sigma_e}{SF_b}) \tag{5-2}$$

and the stress ratio for pure membrane stress only is calculated as:

$$\text{Stress Ratio} = \frac{ZSF_m\sigma_m}{\sigma_f} \tag{5-3}$$

where,

σ_m		= Primary membrane stress, ksi, due to pressure for all service levels
		= $PD_o/(4t)$, from [1, C-2500], where P is the internal pressure
σ_b		= Primary bending stress, ksi
		= $D_oM_{b1}/(2I)$, from [1, C-2500], where M_{b1} is the primary bending moment in inch-lbf and I is the moment of inertia in inch⁴.
σ_e		= Secondary bending stress, ksi
		= $D_oM_{b2}/(2I)$, from [1, C-2500], where M_{b2} is the secondary bending moment in inch-lb_f and I is the moment of inertia in inch⁴.
σ_f		= Flow stress, ksi, which is equal to the average of the yield strength and ultimate tensile strength
SF_b		= Structural factor for bending stress, depending on service level [1, Table C-2621]
SF_m		= Structural factor for membrane stress, depending on service level [1, Table C-2621]
Z		= Z-factor for flux welds (see Section 5.7)

Based on the calculated stress ratios, the allowable flaw depth-to-thickness ratio due to combined loading for Service Levels A, B, and D are obtained from Tables C-5310-1, C-5310-2, and C-5310-4 of ASME B&PV Code, Section XI, Appendix C [1]. Stress ratios are used in Table C-5310-5 [1] to determine the allowable flaw depth-to-thickness ratio for membrane loading only. The allowable flaw sizes for combined loading and for membrane only loading are compared, and the smaller value is reported as the allowable flaw size for the weld. Table 5-3 lists the resulting allowable circumferential flaw sizes for the surge line butt welds.

5.9   Allowable Axial Part Through-Wall Flaw

The allowable axial flaw size is also determined in accordance with ASME B&PV Code, Section XI, Appendix C [1]. The allowable flaw depth is determined using Table C-5410-1. The stress ratio is calculated as follows:

$$\text{Stress Ratio} = \frac{ZSF_m\sigma_h}{\sigma_f} \tag{5-4}$$

where,

σ_h = Hoop stress (ksi) = PR_m/t (ksi)
P = Internal pressure (ksi)
R_m = Mean radius (inch)
t = Wall thickness (inch)
σ_f = Flow stress, ksi, which is equal to the average of yield strength and ultimate tensile strength
Z = Z-factor for flux welds (Section 5.7)
SF_m = Structural factor for membrane stress depending on Service Level [1, Table C-2621]

The allowable flaw length for stability of a through-wall flaw is calculated as:

$$l_{allow} = 1.58(R_mt)^{1/2}\left[\left(\frac{\sigma_f}{Z\sigma_h}\right)^2 - 1\right]^{1/2} \tag{5-5}$$

where,

σ_h = Hoop stress = PR_m/t (ksi)
P = Internal pressure (ksi)
R_m = Mean radius (inch)
t = Wall thickness (inch)
σ_f = Flow stress, ksi, which is equal to the average of yield strength and ultimate tensile strength
Z = Z-factor for flux welds (Section 5.7)

In both Equation 5-4 and 5-5, the value for hoop stress, σ_h, which is defined in Appendix C as $\sigma_h = PR_m/t$, is conservatively taken as the hoop stress for the elbows (Section 5.10), and a conservative thick wall cylinder hoop stress value for Node 27 (Section 5.11). The end-of-evaluation-period flaw length shall be limited to less than the allowable flaw length. Table 5-4 lists the resulting allowable axial flaw sizes for the surge line butt welds.

5.10 Hoop Stress in Thick-walled 90° Elbows

For thick walled 90° elbows with attached pipe under internal pressure, the hoop stress at the center of an elbow (as a function of radial distance from the pipe axis) [20] is calculated as follows:

$$\sigma_h = P \left[\frac{(r_o/r)^2 + 1}{(r_o/r_i)^2 - 1} \right] \left(\frac{2R + r_m \cos\theta}{2R + 2r_m \cos\theta} \right) \tag{5-6}$$

where,

P = Internal pressure (ksi)

r_o = Outside radius (inch)

r = Radial distance from pipe axis (inch), evaluated at $r = r_i$ for maximum stress

r_m = Mean radius (inch)

r_i = Inside radius (inch)

R = Pipe bend radius (inch)

θ = Polar coordinate (radians) of the pipe cross section evaluated at $\theta = \pi$ for the intrados

5.11 Hoop Stress in Thick-walled Straight Pipes

The hoop stress for thick-walled straight pipes under internal pressure (as a function of radial distance from the pipe axis) [20] is calculated as follows:

$$\sigma_h = P \left[\frac{(r_o/r)^2 + 1}{(r_o/r_i)^2 - 1} \right] \tag{5-7}$$

where,

P = Internal pressure (ksi)

r_o = Outside radius (inch)

r = Radial distance from pipe axis (inch), evaluated at $r = r_i$ for maximum stress

r_i = Inside radius (inch)

Table 5-1: Node 20B Surge Line Loads [14]

Load Cases	Mx (ft-lb)	My (ft-lb)	Mz (ft-lb)
Deadweight1	-2251	6	1706
Therm1	-6887	159231	-519
OBE	5097	3597	3494
OBE SAM	1097	3040	979
SSE	9522	6045	6523
SSE SAM	2404	6890	2174
LOCA	16952	14353	8821

Note: Table 5-1 is a copy of the Node 20B terms in Table 3-1.

Table 5-2: Node 20B Service Level Loads

Service Level	Mx (ft-lb)	My (ft-lb)	Mz (ft-lb)	Msrss (in-kip)
Level A Primary	-2251	6	1706	34
Level A Secondary	-6887	159231	-519	1,913
Level B Primary	7348	3603	5200	116
Level B Secondary	7984	162271	1498	1,950
Level D Primary	21694	15580	12677	354
Level D Secondary	9291	166121	2693	1,997

This table is based on Table 3 of Reference [7].

Table 5-3: Allowable Circumferential Flaw Depth for Units 1, 2 and 3 [1]

Node	Service Level	Ratio of Flaw Length to Pipe Circumference ($l/\pi D_o$)[2, 3]							
		0	0.1	0.2	0.3	0.4	0.5	0.6	0.75 or greater
		Flaw Length (degrees)							
		0	36	72	108	144	180	216	270
20B	Level A	0.984	0.984	0.794	0.562	0.452	0.405	0.379	0.369
	Level B	0.984	0.984	0.702	0.490	0.397	0.357	0.331	0.331
	Level D	0.984	0.984	0.894	0.622	0.500	0.429	0.394	0.372
20E	Level A	0.984	0.984	0.909	0.677	0.547	0.484	0.452	0.439
	Level B	0.984	0.984	0.903	0.632	0.516	0.452	0.426	0.414
	Level D	0.984	0.984	0.984	0.782	0.630	0.544	0.497	0.464
27	Level A	0.984	0.984	0.984	0.923	0.736	0.647	0.597	0.583
	Level B	0.984	0.984	0.984	0.886	0.714	0.621	0.582	0.562
	Level D	0.984	0.984	0.984	0.953	0.802	0.691	0.629	0.580
30B	Level A	0.984	0.984	0.890	0.652	0.526	0.467	0.437	0.423
	Level B	0.984	0.984	0.891	0.624	0.509	0.446	0.420	0.409
	Level D	0.984	0.984	0.984	0.768	0.618	0.534	0.488	0.456
30E	Level A	0.984	0.984	0.882	0.641	0.517	0.459	0.430	0.417
	Level B	0.984	0.984	0.840	0.588	0.479	0.423	0.396	0.388
	Level D	0.984	0.984	0.984	0.687	0.555	0.476	0.436	0.410
50B	Level A	0.984	0.984	0.984	0.958	0.809	0.708	0.651	0.592
	Level B	0.984	0.984	0.984	0.958	0.776	0.671	0.631	0.605
	Level D	0.984	0.984	0.984	0.923	0.765	0.660	0.602	0.556
50E	Level A	0.984	0.984	0.984	0.958	0.796	0.698	0.642	0.592
	Level B	0.984	0.984	0.984	0.954	0.771	0.667	0.627	0.601
	Level D	0.984	0.984	0.984	0.984	0.788	0.680	0.614	0.566
60B	Level A	0.984	0.984	0.984	0.958	0.841	0.723	0.651	0.592
	Level B	0.984	0.984	0.984	0.964	0.807	0.702	0.655	0.606
	Level D	0.984	0.984	0.984	0.979	0.834	0.717	0.652	0.600
60E	Level A	0.984	0.984	0.984	0.958	0.841	0.723	0.651	0.592
	Level B	0.984	0.984	0.984	0.964	0.812	0.707	0.658	0.606
	Level D	0.984	0.984	0.984	0.917	0.758	0.655	0.597	0.552

Notes:
1. This table is based on Table 4 of Reference [7].
2. Values given in Tables C-5310-1, 2, 4, and 5 are converted from a/t to a using t = 1.312 inch
3. Using D = 12.75 inch

Table 5-4: Allowable Axial Flaw Depth for Units 1, 2, and 3 [1][5]

Node	Service Level	Flaw Length, l_f (inch)[3, 4]									Allowable Flaw Length (l_{allow})[2] (inch)
		0.0	1.4	2.7	5.5	8.2	11.0	13.7	16.4	21.9	(inch)
All Excl. 27	Level A	0.984	0.984	0.964	0.727	0.609	0.556	0.530	0.504	*0.488*	16.68
	Level B	0.984	0.984	0.967	0.746	0.628	0.576	0.550	*0.523*	*0.506*	15.01
	Level D	0.984	0.984	0.984	0.984	0.981	0.967	0.960	0.956	*0.940*	16.68
27	Level A	0.984	0.984	0.984	0.892	0.787	0.735	0.708	0.682	*0.656*	20.80
	Level B	0.984	0.984	0.984	0.904	0.802	0.749	0.723	0.697	*0.670*	18.77
	Level D	0.984	0.984	0.984	0.984	0.984	0.984	0.984	0.984	*0.975*	20.80

Notes:

1. Values given in Table C-5410-1 are converted from a/t to a using t = 1.312 inch.
2. Based on r_m = 5.719 inch and t = 1.312 inch.
3. Values in red and italics are beyond the allowable flaw length. The allowable flaw depth can be interpolated up to the allowable flaw length based on the calculation from Section 5.9.
4. Table C-5410-1 goes beyond this flaw length, but values are omitted for brevity and because they are prohibited based on calculation of maximum allowable flaw length from Section 5.9.
5. This table is based on Table 5 of Reference [7].

6.0   CRACK GROWTH EVALUATION

The crack growth evaluations are performed in the surge line butt weld locations, as identified in the stress analyses [5], and are shown in Figure 6-1. The fatigue crack growth is computed using linear elastic fracture mechanics (LEFM) techniques in computing the stress intensity factor. The results of the crack growth evaluations are used in conjunction with the calculated allowable flaw sizes [7, Table 2 & Table 3] to determine the required inspection interval for a postulated flaw.

For a postulated initial flaw, crack growth is simulated until the flaw has reached the allowable flaw size based on the ASME B&PV Code, Section XI, Appendix C [1] procedures. The required inspection frequency is equal to the time to reach the allowable flaw size.

The crack growth evaluations are performed using the **pc-CRACK** [13] software, with stress intensity factor (K) calculations performed using the **SI-TIFFANY** [24] software. **pc-CRACK** and **SI-TIFFANY** are both fracture mechanics software verified under Structural Integrity Associates' Quality Assurance (QA) program [25].

6.1   Loads

The following loads are applied to the crack growth evaluation:

6.1.1   Mechanical Interface Loads

Table 6-1 tabulates the bounding deadweight, operating basis earthquake (OBE), and Seismic Anchor Movement (SAM) axial forces and bending moments for the pressurizer surge line welds (in the local axis coordinate system), which were compiled in Reference [7, 14].

For the elbow-to-straight pipe butt welds, such as nodes 20B, 20E, 30B, 30E, 50B, 50E, 60B, and 60E, the through-wall stress distributions due to the unit axial force (1000 lb$_f$) and unit bending moment (1000 inch- lbf) were extracted from the stress paths from the finite element analysis [5]. These stress distributions from the unit loads are scaled to the actual values of the axial forces (FX) and moments (SRSS of MY and MZ) from Table 6-1 [7, Table 1].

For the straight pipe butt weld, node 27, closed form solutions in calculating the unit axial stress and unit bending moment stress are used as follows:

Straight Pipe Unit Axial Stress:

$$\sigma_a = \frac{F_x}{A}$$

(6-1)

where: F_x = unit axial force, 1000 lb$_f$
                   A = pipe cross sectional area, $\pi(R_o^2 - R_i^2)$, inch²

Straight Pipe Unit Bending Stress:

$$\sigma_b = \frac{D_o M_b}{2I}$$

(6-2)

where:

M_b =   unit bending moment due to mechanical load, 1000 inch-lb$_f$

I =   moment of inertia, $\frac{\pi}{4}(R_o^4 - R_i^4)$, inch⁴.

Do =   pipe OD, inch

For node 27, the stress distributions obtained from Equation 6-1 and Equation 6-2 are scaled to the actual values of the axial forces (FX) and moments (SRSS of MY and MZ) from Table 6-1.

There are 200 OBE full cycles over the designed 40-year plant lifetime [26, page 12] which equates to 200/40 = 5 annual cycles (using a 40-year plant life duration).

6.1.2 Thermal Transient and Thermal Expansion

Thermal transients and thermal expansion are performed in the stress analysis of the surge line [5]. Through-wall stress distributions due to the combined thermal transients and thermal expansion are extracted for each path at the weld locations. The annual cycles of each transient are summarized in Table 6-2.

6.1.3 Thermal Anchor Movement

Thermal anchor movement (TAM) analysis, both at the pressurizer end and hot leg end, are performed in the stress analysis of the surge line [5] based on the associated displacement load of each end. Thermal displacements are applied at 653°F (conservative lower value of normal operating pressurizer temperature [7, Section 2.2] and 553°F (conservative lower value of normal operating hot leg temperature [5, Table 2] for the pressurizer end and hot leg end, respectively. Use of a lower value for scaling (denominator) is conservative as it increases the scaling factor and thus the resultant loading. To account for the minimum and maximum TAM for each thermal event, the minimum and maximum temperatures listed in Table 6-2 are used to scale the stress distribution due to TAM. The scaling factors are calculated as follows:

Thermal Scale Factor for Hot Leg Side, TSF_{HL}:

$$TSF_{HL} = \frac{T_{HL} - 70}{553 - 70} \tag{6-3}$$

where T_{HL} is temperature in the hot leg.

Thermal Scale Factor for Pressurizer Side, TSF_{PRZ}:

$$TSF_{PRZ} = \frac{T_{PZR} - 70}{653 - 70} \tag{6-4}$$

where T_{PZR} is temperature in the pressurizer.

6.1.4 Thermal Stratification

The through-wall stress distribution due to thermal stratification for the paths at each weld are obtained from the stress analyses [5, Table 7]. Based on the finite element analyses [5, Section 3.4], the thermal displacements were already applied to the cut-boundaries of the model and the temperature distributions from the stratification thermal solutions are also applied for a combined stress result.

6.1.5 Weld Residual Stress

The weld residual stresses are calculated as a function of flaw depth. The distribution is reproduced from NUREG-0313 [27, Figure 3 in Appendix A] and shown in Figure 6-2 The through-wall residual stress distribution in the axial direction obtained from laboratory-measured data is given as:

$$\sigma\left(\frac{x}{t}\right) = \sigma_i\left[1 - 6.91\left(\frac{x}{t}\right) + 8.69\left(\frac{x}{t}\right)^2 - 0.48\left(\frac{x}{t}\right)^3 - 2.03\left(\frac{x}{t}\right)^4\right] \qquad (6\text{-}5)$$

where:

   σ_i = inside surface stress, given as the yield stress of the weld metal (ksi)

   x = distance into pipe wall from inside diameter (inch)

   t = wall thickness (1.312 inch)

The yield strength of 30.0 ksi for SA-376, Type 304 stainless steel, obtained from the ASME Code, Section II [18, Table Y-1], is used for the inside surface stress. For crack growth analysis, a stress table is used to input the weld residual stress distribution in **pc-CRACK** [13].

6.1.6 Internal Pressure

The stress due to internal pressure is calculated based on the unit pressure evaluated from the stress analysis [5]. To obtain the maximum and minimum stresses, the unit stresses are multiplied by the maximum and minimum internal pressure for each transient [5].

6.1.7 Crack Face Pressure

The internal pressure analysis and thermal transient analyses assume an un-cracked structure to develop the stress results that are used in the closed-form solution of the crack model. However, initiation of the crack introduces a new surface for pressure loading. This new crack surface pressure loading is assumed to be a far-field loading. A unit pressure value of 1 ksi is scaled to the minimum and maximum operating pressures of each thermal transient (pressures shown in Table 6-2), and then applied as an additional membrane stress in **pc-CRACK** [13].

6.2   Assumptions

The following assumptions are used in this evaluation:

1. The use of Appendix L in this capacity is contingent upon the absence of an initial flaw as per Table IWB-3410-1 [1].

2. The material properties for the surge line butt welds are assumed to be equivalent to SA-376, TP 304 stainless steel, which is the base metal of the surge line piping. This is reasonable because the weld metal is stronger than the base material which adds conservatism to the crack growth calculation.

3. A full 360° circumferential flaw model is used to calculate the increase in crack depth. This is conservative as compared to a semi-elliptical crack model with the same depth because the flaw depth increases faster with a 360° flaw than it does with a semi-elliptical flaw of any length.

4. For the OBE event, the internal pressure, crack face pressure, thermal expansion, and normal operation thermal stresses are taken at normal operating pressure and temperature, since the OBE event is most likely to occur during steady-state normal operating conditions.

5. Emergency and faulted loadings are not considered in the crack growth evaluation. Appendix L [1] states in L-3110 that end-of-period flaw sizes shall be determined using the rules of L-3300. L-3300 states in L-3330 that Appendix C, C-3200 rules are to be used to calculate flaw growth. C-3200 does not contain specific guidance on which Service Level loading to be used. However, Non-Mandatory Appendix A [1] for ferritic components is of similar scope as Appendix C. Nonmandatory Appendix A, A-5200, states: Cumulative fatigue crack growth analysis of components need not include emergency and faulted conditions. Therefore, only Service Level A (Normal) and Service Level B (Upset) loadings are used in the crack growth evaluations. In addition to the exclusion of A-5200, these emergency and faulted events are limited in the number of cycles and are used only to determine crack stability. Note that all Service Level loadings are used to calculate allowable flaw sizes [7], and the end-of-life flaw sizes are checked against allowable flaw sizes for all Service Levels.

Structural Integrity
Associates, Inc.®

info@structint.com   1-877-4SI-POWER   structint.com

6.3   Stress Intensity Factors

Stress analyses of unit internal pressure and thermal transients have been performed in the stress analysis calculation [5]. For these loadings, **SI-TIFFANY** [24] generates tables of the maximum and minimum stress intensity factors, K_{max} and K_{min}, respectively, for various flaw depths and aspect ratios for the unit internal pressure case and thermal transients. The fracture mechanics models are shown in Figure 6-3.

SI-TIFFANY reads in the time history of through-wall hoop and axial stresses for each transient. The program then determines K's for every time point and for every flaw depth, and for a range of defined aspect ratios. The program also selects the largest K and smallest K for each flaw depth and each flaw aspect ratio for all time points and produces two files for each flaw orientation.

The circumferential flaw "*.mnn" file tabulates the wall thickness versus smallest K_{min} for the given path length evaluated. In the case of the axial flaw, the "*.mnn" file provides the wall thickness versus smallest K_{min} for each designated aspect ratio. The "*.mxn" file is the same as the "*.mnn" file, except that the K_{max} values are tabulated.

The stress intensity factors for the weld residual stress, deadweight, OBE, crack face pressure, and thermal expansion loads are calculated within **pc-CRACK** [13]. The axial flaws are evaluated using the **pc-CRACK** crack model 305 (semi-elliptical longitudinal crack in cylinder on the inside surface (API 579) [28]). The circumferential flaws are evaluated using the **pc-CRACK** crack model 301 (full circumferential crack in cylinder on the inside surface (API 579) [28]).

The K through-wall distributions for both the semi-elliptical axial crack and 360-degree circumferential crack were plotted for Weld 20B, 20E, 30B, 30E, 60B, and 60E. The through-wall distributions of K are based on TRAN11 which is the loading block that generates the most severe growth. The total stress intensity factor distributions are combinations of pressure, deadweight, thermal transient and thermal expansion, thermal anchor movement, and weld residual stress.

The through-wall K distributions are plotted in Figure 6-4 through Figure 6-9 for the semi-elliptical axial crack and 360-degree circumferential crack.

6.4   Postulated Initial Surface Flaw

Per ASME B&PV Code, Section XI, Appendix L (L-3210) [1], the postulated initial flaw for austenitic piping is a semi-elliptical circumferential or axial flaw on the inside surface. The initial flaw depth of the postulated flaw is determined from the applicable inservice inspection acceptance standard in Table IWB-3410-1 [1] using a flaw aspect ratio (a/l = flaw depth/flaw total length) of 0.167 per ASME B&PV Code, Section XI, Appendix L-3212 [1]. See Figure 6-10 for a schematic of flaw aspect ratio.

Since the surge line butt welds are considered as "metal welds in piping" from Table IWB-3410-1 [1], the flaw depth-to-thickness ratio (a/t) is determined from IWB-3514 [1] using the component thickness of 1.312 inches and the prescribed hypothetical flaw aspect ratio (a/l) of 0.167. A linear interpolation is employed from Table IWB-3514-1 for austenitic piping to calculate the initial a/t (0.1437). The a/t is used to calculate the actual initial flaw depth (a = 0.1437 x 1.312 inch = 0.1885 inch), to be used in the fatigue crack growth evaluation.

For the circumferential flaw, the initial flaw is assumed to be 360 degrees in extent and with a depth of 0.1885 inch and is used for the crack growth evaluation at the surge line butt welds locations.

For the semi-elliptical axial crack, using the initial axial flaw depth of 0.1885 inch, the initial axial flaw length assumed using an aspect ratio of 6-to-1 is therefore:

l = (0.1885 inch) × 6 = 1.131 inch.

These postulated initial axial flaw sizes (depth and length) are used for the crack growth evaluation at the surge line butt welds and the elbow flank locations.

6.5   Stainless Steel Fatigue Crack Growth Law

The reference fatigue crack growth rate curves taken from Code Case N-809 [8] for Type 304 and Type 316 stainless steels and associated weld metals in a PWR environment are:

$$da/dN = C_0 \cdot \Delta K^n, \text{ units of inch/cycle} \qquad (6\text{-}6)$$

where:

C_0	= scaling parameter that accounts for the effect of loading rate and environment on fatigue crack growth rate
	= C S_T S_R S_{ENV}
n	= slope of the log (da/dN) versus log (ΔK) curve = 2.25
C	= nominal fatigue crack growth rate constant
	= 4.43 x 10^{-7} for $\Delta K \geq \Delta K_{th}$
	= 0 for $\Delta K < \Delta K_{th}$
ΔK	= stress intensity factor range, ksi$\sqrt{\text{in}}$
ΔK_{th}	= 1.00 ksi$\sqrt{\text{in}}$
S_T	= parameter defining effect of temperature on FCG rate
	= e^{-2516/T_K} for 300°F $\leq$ T $\leq$ 650°F
	= 3.39x10^5 $e^{[(-2516/T_K)-0.0301T_K]}$ for 70°F $\leq$ T < 300°F
T	= metal temperature, °F
S_R	= parameter defining the effect of R-ratio on FCG rate
	= 1.0 for R < 0
	= 1 + $e^{8.02(R-0.748)}$ for 0 $\leq$ R < 1.0
R	= K_{min}/K_{max} = R ratio
S_{ENV}	= parameter defining the environmental effects on FCG rate
	= $T_R^{0.3}$
T_R	= rise time, sec
T_K	= [(T-32)/1.8+273.15], (Temperature in Kelvin, K)

This crack growth rate curve is available within **pc-CRACK** [13, Table 1]. The material for the surge line welds is assumed to be equivalent to SA-376, Type 304 stainless steel, which is the base metal of the surge line [5]. The crack growth law "CC809304316" is chosen for crack growth analysis in **pc-CRACK**.

6.6   Crack Growth Analysis

The crack growth analyses use the representative fracture mechanics models in Figure 6-3, which are incorporated into **pc-CRACK** [13] and **SI-TIFFANY** [24].

The fatigue crack growth law used in this calculation is discussed in Section 6.5. The sequence of events for fatigue crack growth is computed on a yearly basis. The **pc-CRACK** runs calculate the incremental growth for each transient (multiplied by the number/fraction of cycles per year) within one-year blocks. The one-year block includes all transients. The sequence of transients is not a concern given the small amount of FCG per year even for the most significant transient, e.g., rearranging the order of transients would not alter the end crack duration. Thus, the annual cycles shown in Table 6-2 are used in a yearly crack growth calculation. In fatigue crack growth, there is no requirement for load pairing between transients per ASME B&PV Code, Section XI [1]. Therefore, each thermal transient that was analyzed in the stress analysis calculation [5] is analyzed in an arbitrary sequential sequence as listed in Table 6-2. The crack growth is calculated, and the crack size is updated after each transient event within the **pc-CRACK** program during the analysis. This approach is consistent with Subparagraph C-3210 of ASME B&PV Code, Section XI [1].

The stress intensity factors for internal pressure and the thermal transients are calculated using **SI-TIFFANY** [24] and are computed as a function of crack depth, and can thus be superimposed for the various operating states.

For each event, the individual stress intensity factors that contribute to the nominal maximum applied stress intensity factor, K_{max}, and the minimum applied stress intensity factor, K_{min}, are summarized in the tabulation below. The stress intensity factor range, ΔK, is computed by taking the difference of the summed K_{max} and K_{min}. $K_{residual}$ and $K_{deadweight}$ are from constant loads and do not contribute to the ΔK range but affect the R-ratio (K_{min}/K_{max}), which accounts for mean stress effects. The internal pressure and crack face pressures, $K_{pressure\ max}$, $K_{pressure\ min}$, $K_{crack\ face\ pressure\ max}$ and $K_{crack\ face\ pressure\ min}$, are the minimum and maximum operating pressures during the transient in Table 6-2.

K_{max}	K_{min}
$K_{deadweight}$	$K_{deadweight}$
$K_{residual}$	$K_{residual}$
$K_{crack\ face\ pressure\ max}$	$K_{crack\ face\ pressure\ min}$
$K_{pressure\ max}$	$K_{pressure\ min}$
$K_{thermal\ anchor\ max}$	$K_{thermal\ anchor\ min}$
$K_{thermal\ transient\ max}$	$K_{thermal\ transient\ min}$

For the OBE event, K_{max} and K_{min} are taken as the positive and negative seismic bending stress. The internal pressure, crack face pressure, thermal expansion, and normal operation thermal stresses are taken at normal operating pressure and temperature, since the OBE event is assumed to most likely occur during steady-state normal operating conditions with 5 events yearly.

The OBE with normal operation K values shown below were obtained using the approximate steady-state thermal stress.

K_{max}	K_{min}
$K_{deadweight}$	$K_{deadweight}$
$K_{residual}$	$K_{residual}$
$K_{pressure\ (normal\ operating\ pressure)}$	$K_{pressure\ (normal\ operating\ pressure)}$
$K_{crack\ face\ pressure\ (normal\ operating\ pressure)}$	$K_{crack\ face\ pressure\ (normal\ operating\ pressure)}$
$K_{thermal\ anchor\ (normal\ operation)}$	$K_{thermal\ anchor\ (normal\ operation)}$
$K_{OBE,\ positive}$	$K_{OBE,\ negative}$

From Reference [5], thermal stratification takes place during 'insurge' and 'outsurge' events. Stratifications that occurred at low pressure, such as S1 through S3 (see Reference [5, Table 7]) are combined with the bounding insurge/outsurge event Trans11 at low pressure state, and Stratification S4 is combined with the next bounding insurge/outsurge event Trans12 at low pressure state. Similarly, stratifications that occurred at high pressure, such as S5 through S6 (see Reference [5, Table 7]) are combined with the bounding insurge/outsurge event Trans14 at high pressure state. For S9 (Hot-Standby [5, Table 7]), thermal expansion and piping interface loads (Table 6-1) are combined with the remaining stratification loads.

K_{max}	K_{min}
$K_{deadweight}$	$K_{deadweight}$
$K_{residual}$	$K_{residual}$
$K_{pressure\ max}$	$K_{pressure\ min}$
$K_{crack\ face\ pressure\ max}$	$K_{crack\ face\ pressure\ min}$
$K_{thermal\ transient}$	$K_{thermal\ transient}$
$K_{startification\ max}$	$K_{stratification\ min}$

For the fatigue crack growth, "CC809304316" is the stainless-steel crack growth law built into **pc-CRACK** (see Section 6.5). The temperature for crack growth is taken as the average temperature of each thermal transient. The rise time for each transient is obtained from the **SI-TIFFANY** report file.

6.7 Crack Growth for Elbow at Bounding Locations – Nodes 30 and 60

Reference [6] evaluated the elbow flank (see Figure 6-11) for crack growth and determined the examination duration for the elbow component. The evaluation results considered the stresses at the flank of the elbows, to determine the bounding locations, for inspection under the ASME B&PV Code, Section XI, Appendix L criteria. The analyses were performed in Reference [6, Appendix B], where it was demonstrated that the axial stresses and corresponding stress intensities, used to determine fatigue crack growth in the circumferential direction at the butt welds, are higher than at the 45-degree flank plane of the elbow. Similarly, the hoop stresses at the elbow flank plane are higher than at the butt welds, but the projected service life for the elbow flank axial flaw is several times (50 years versus 13 years) that of the projected life for the circumferential flaw in the butt welds. Thus, the inspection criteria periodicity under the ASME B&PV Code, Section XI criteria for the surge line piping, elbows and welds are bounded by the butt weld circumferential fatigue service life.

6.8 Crack Growth Results

The fatigue crack growth calculations are performed for pressurizer surge line welds of PVGS as part of the flaw tolerance evaluation. Table 6-3 summarizes the crack growth results for the postulated semi-elliptical axial and 360-degree circumferential flaws.

The allowable flaw size for each path is linearly interpolated using the final flaw length. As shown in Table 6-3, both the axial and circumferential flaws are acceptable for 10 years of operation, with the a/t ratio below the allowable values.

The bounding locations which resulted in the shortest number of years are Weld 30B (Path 1) for the axial crack and Weld 30E (Path 3) for the 360-degree circumferential crack. Plots of flaw depth versus number cycles in years are illustrated in Figure 6-12 and Figure 6-13, for the axial crack and the 360-degree circumferential crack, respectively.

The additional analysis for the elbow flank [6] showed that the hoop stress at the elbow flank due to thermal stratification bounds the hoop stress at the butt weld. From the additional axial crack growth analysis for the elbow flank performed in Reference [6], the result showed 50 years before the axial crack reaches the allowable flaw size. From this result, the limiting axial crack duration at the elbow flank region of 50 years is still bounded by the 360-degree circumferential crack duration at the butt weld at Weld 30E of 13 years (before the initial flaw reaches the allowable flaw limit).

Relative to the acceptance criteria for future flaw tolerance volumetric inspections, the inspection frequency has been shown to be at least 10 years.

Therefore, a subsequent inspection that identifies no circumferential flaws or flaws that have a depth greater than 0.1885 inch may be considered acceptable for the next ten (10) years.

Similarly, a subsequent inspection that identifies no axial flaw that has a depth greater than 0.1885 inch OR an aspect ratio greater than 1:6 may be considered acceptable for the next ten (10) years.

Table 6-1: Piping Interface Loads [4, 5]

Location, Node	Load Type[1]	FX[2, 3], lb$_f$	MY[2], ft-lb$_f$	MZ[2], ft-lb$_f$	SRSS(MY, MZ), inch-kip
Weld 20B	Deadweight	-1	6	1706	20.5
	OBE	1164	3597	3494	60.2
	OBE SAM	584	3040	979	38.3
	Total OBE	1748	6637	4473	98.5
Weld 20E	Deadweight	-6	8	-958	11.5
	OBE	1679	2382	3855	54.4
	OBE SAM	1028	2650	486	32.3
	Total OBE	2707	5032	4341	86.7
Weld 27	Deadweight	6	-42	-2898	34.8
	OBE	966	1920	3877	51.9
	OBE SAM	1028	3100	95	37.2
	Total OBE	1994	5020	3972	89.1
Weld 30B	Deadweight	6	-49	-1140	13.7
	OBE	732	2839	776	35.3
	OBE SAM	1030	3653	155	43.9
	Total OBE	1762	6492	931	79.2
Weld 30E	Deadweight	-2	-43	1446	17.4
	OBE	838	1498	1100	22.3
	OBE SAM	6160	9401	238	112.8
	Total OBE	6998	10899	1338	135.2
Weld 50B	Deadweight	2	-74	-2047	24.6
	OBE	541	1342	505	17.2
	OBE SAM	6160	12308	2242	150.1
	Total OBE	6701	13650	2747	167.3
Weld 50E	Deadweight	1	80	811	9.8
	OBE	556	1549	806	21.0
	OBE SAM	4836	9108	2066	112.1
	Total OBE	5392	10657	2872	133.0
Weld 60B	Deadweight	-1	-84	-811	9.8
	OBE	629	1916	806	24.9
	OBE SAM	4836	6189	2066	78.3
	Total OBE	5465	8105	2872	103.2
Weld 60E	Deadweight	1	86	809	9.8
	OBE	762	2709	1061	34.9
	OBE SAM	4836	12733	5207	165.1
	Total OBE	5598	15442	6268	200.0

Notes:

1. Total OBE = OBE + OBE SAM
2. FX is the axial force in the local direction of the pipe. MY and MZ are the in-plane moments in the local direction of the pipe, respectively. Values from [7, 14].
3. Negative values of FX are considered 0 for the FCG calculation since their compressive nature does not contribute as a crack driving force.
4. Values shown in the table are the magnitudes to be used in scaling the unit load analysis. SSE and LOCA loadings are not included (See Section 6.2).
5. This table is based on Table 1 of Reference [6].

Table 6-2: Transient Events [5]

Transient	ANSYS ID	Pressure[1] (ksig)		Temperature[1] (°F)			Annual Cycles[1]	Rise Time[4], sec.
		Max.	Min.	Max.	Min.	Ave.		
Plant Heatup	Tran1	2.235	0.000	540	70	305	1.398	16356
Plant Cooldown	Tran2	2.235	0.000	540	70	305	1.39	16008
Loss of Flow, Loss of Load	Tran3	2.535	1.685	621	551	586	0.531	100
Reactor Trip – Revised Transient[2]	Tran4	2.385	2.180	621	572	597	3.06	600
Plant Unloading, 10% Step Down	Tran6	2.235	2.235	653	593	623	2.695	29
Plant Unloading, 10% Step Up	Tran7	2.235	2.235	653	593	623	2.695	1303
Leak Test, 2250 psia, Down	Tran9	2.235	0.385	400	160	280	0.042	10800
Leak Test, 2250 psia, Up	Tran10	2.235	0.385	400	160	280	0.042	10080
I/O Heatup, ΔT = 300°F	Tran11	0.366	0.366	440	140	290	19.4	2350
I/O Heatup, ΔT = 250°F	Tran12	0.366	0.366	440	190	315	52.3	2320
I/O Heatup, ΔT = 150°F	Tran13	0.366	0.366	440	290	365	35.93	2100
I/O Heatup, ΔT = 100°F	Tran14	2.235	2.235	653	553	603	69.17	1989
I/O Cooldown, ΔT = 250°F	Tran15	0.366	0.366	440	190	315	7.4	2300
I/O Cooldown, ΔT = 150°F	Tran16	0.366	0.366	440	290	365	3.7	2100
I/O Cooldown, ΔT = 100°F	Tran17	2.235	2.235	653	553	603	6.73	2000
5% Loading – New Transient[3]	Trans18	2.298	2.242	653	572	613	250	4389
5% Unloading – New Transient[3]	Trans19	2.299	2.207	651	572	612	250	822

Notes:
1. Values are extracted from Table 2 of Reference [2] except for Tran4, Trans18, and Trans19.
2. Values are extracted from Table 3 of Reference [2].
3. Values are extracted from Table 4 of Reference [2].
4. Values are extracted from the **SI-TIFFANY** report file. The bounding (maximum) rise-times between the transient events for each stress path are conservatively used.
5. This table is based on Table 2 of Reference [6].

Table 6-3: Fatigue Crack Growth Results [3]

| Weld ID | Paths | Semi-Elliptical Axial Flaw | | | | | 360-Degree Circumferential Flaw | | | |
| | | Flaw size in 10 Years | | | Allowable a/t [1] | N, years | Flaw size in 10 Years | | Allowable a/t [1] | N, years |
		a, inch	c, inch[2]	a/t			a, inch	a/t		
20B	P1	0.2336	0.5972	0.1781	0.75	≥100	0.2500	0.1906	0.2523	22
	P2	0.2321	0.5963	0.1769	0.75	≥100	0.2513	0.1915	0.2523	21
	P3	0.2443	0.6037	0.1862	0.75	≥100	0.2660	0.2027	0.2523	17
	P4	0.2332	0.5966	0.1778	0.75	≥100	0.2475	0.1886	0.2523	22
20E	P1	0.2575	0.6158	0.1963	0.75	≥100	0.2466	0.1879	0.3155	34
	P2	0.2324	0.5978	0.1772	0.75	≥100	0.2702	0.2059	0.3155	24
	P3	0.2537	0.6128	0.1934	0.75	≥100	0.3173	0.2418	0.3155	15
	P4	0.2603	0.6183	0.1984	0.75	≥100	0.3296	0.2512	0.3155	14
27	P1	0.2302	0.5953	0.1755	0.75	≥100	0.2505	0.1909	0.4282	52
	P2	0.2304	0.5954	0.1756	0.75	≥100	0.2474	0.1885	0.4282	57
	P3	0.2274	0.5930	0.1733	0.75	≥100	0.2474	0.1885	0.4282	57
	P4	0.2316	0.5962	0.1765	0.75	≥100	0.2833	0.2159	0.4282	29
30B	P1	0.2635	0.6213	0.2008	0.75	99	0.2487	0.1896	0.3117	32
	P2	0.2455	0.6068	0.1871	0.75	≥100	0.2474	0.1886	0.3117	34
	P3	0.2447	0.6057	0.1865	0.75	≥100	0.2474	0.1886	0.3117	34
	P4	0.2469	0.6074	0.1882	0.75	≥100	0.3236	0.2466	0.3117	14
30E	P1	0.2623	0.6203	0.1999	0.75	≥100	0.2485	0.1894	0.2957	29
	P2	0.2456	0.6068	0.1872	0.75	≥100	0.2661	0.2028	0.2957	23
	P3	0.2471	0.6076	0.1883	0.75	≥100	0.3191	0.2432	0.2957	13
	P4	0.2490	0.6091	0.1898	0.75	≥100	0.3206	0.2444	0.2957	13
50B	P1	0.2389	0.6009	0.1821	0.75	≥100	0.2464	0.1878	0.4238	56
	P2	0.2357	0.5994	0.1796	0.75	≥100	0.2537	0.1934	0.4238	49
	P3	0.2511	0.6102	0.1914	0.75	≥100	0.2487	0.1896	0.4238	52
	P4	0.2471	0.6074	0.1884	0.75	≥100	0.2978	0.2270	0.4238	25
50E	P1	0.2437	0.6042	0.1858	0.75	≥100	0.2468	0.1881	0.4314	57
	P2	0.2358	0.5994	0.1797	0.75	≥100	0.2474	0.1886	0.4314	57
	P3	0.2517	0.6107	0.1918	0.75	≥100	0.2482	0.1891	0.4314	55
	P4	0.2469	0.6073	0.1882	0.75	≥100	0.2999	0.2286	0.4314	25
60B	P1	0.2415	0.6029	0.1841	0.75	≥100	0.2539	0.1935	0.4512	51
	P2	0.2373	0.6000	0.1808	0.75	≥100	0.2522	0.1922	0.4512	55
	P3	0.2385	0.6009	0.1818	0.75	≥100	0.2488	0.1896	0.4512	60
	P4	0.2304	0.5949	0.1756	0.75	≥100	0.2808	0.2141	0.4512	30
60E	P1	0.2317	0.5964	0.1766	0.75	≥100	0.2543	0.1938	0.4207	47
	P2	0.2315	0.5959	0.1764	0.75	≥100	0.2609	0.1989	0.4207	38
	P3	0.2453	0.6052	0.1870	0.75	≥100	0.2504	0.1909	0.4207	51
	P4	0.2406	0.6022	0.1834	0.75	≥100	0.2584	0.1969	0.4207	40

Notes:
1. Allowable flaw sizes: depth-to-thickness ratio (a/t), see Reference [7]
2. c equals half flaw length = l/2.
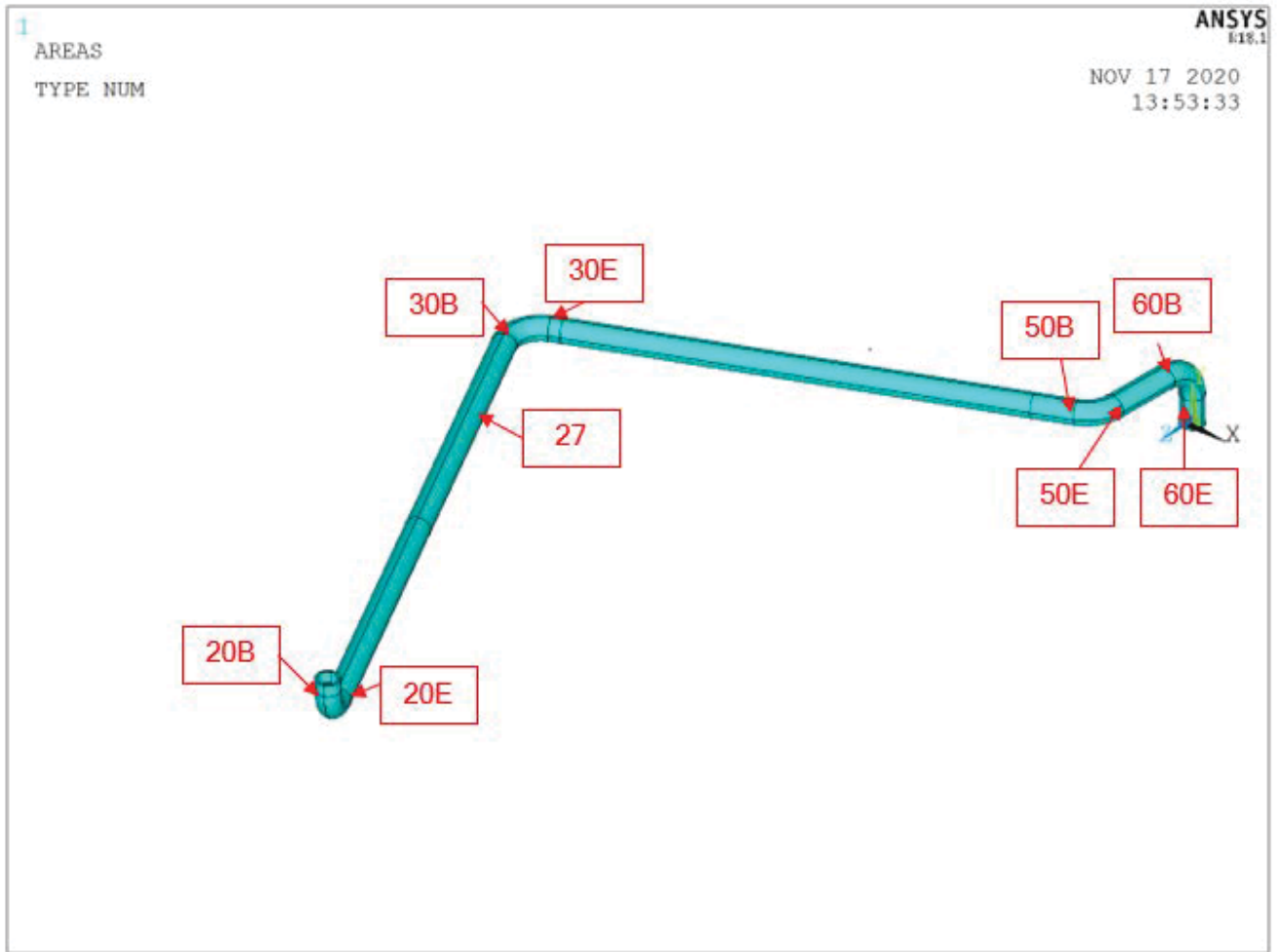3. This table is based on Table 3 of Reference [6].

4.

Figure 6-1. Pressurizer Surge Line Weld Locations

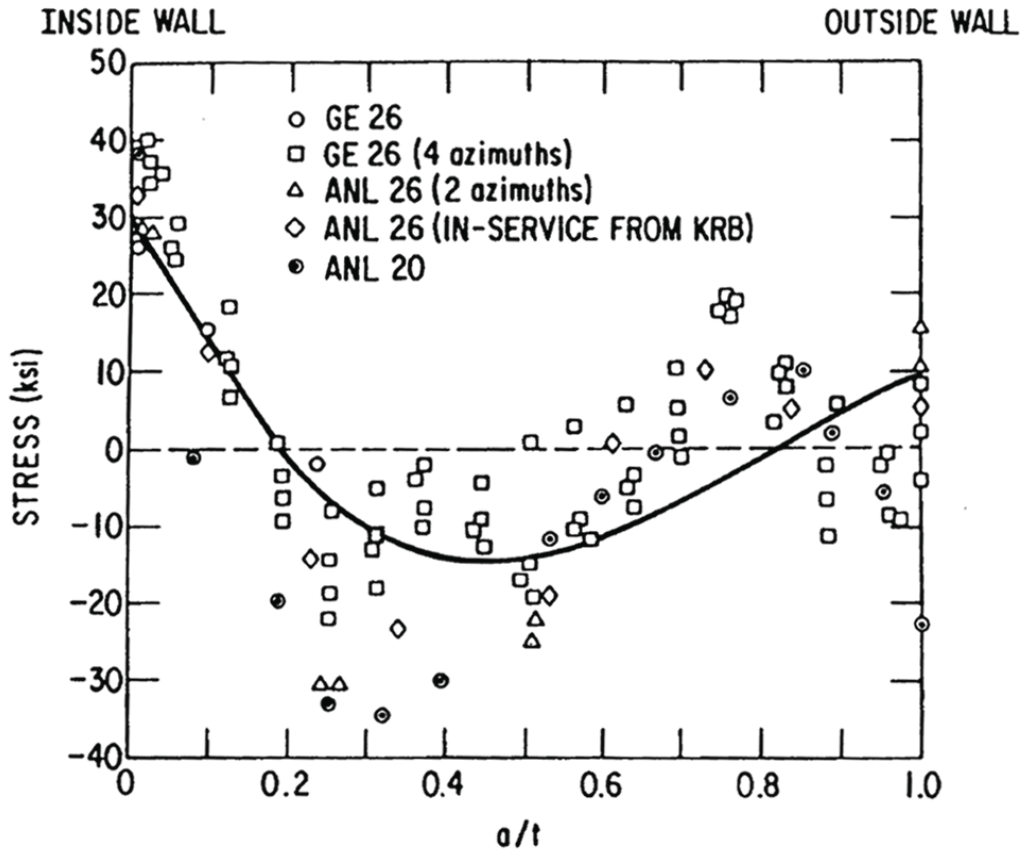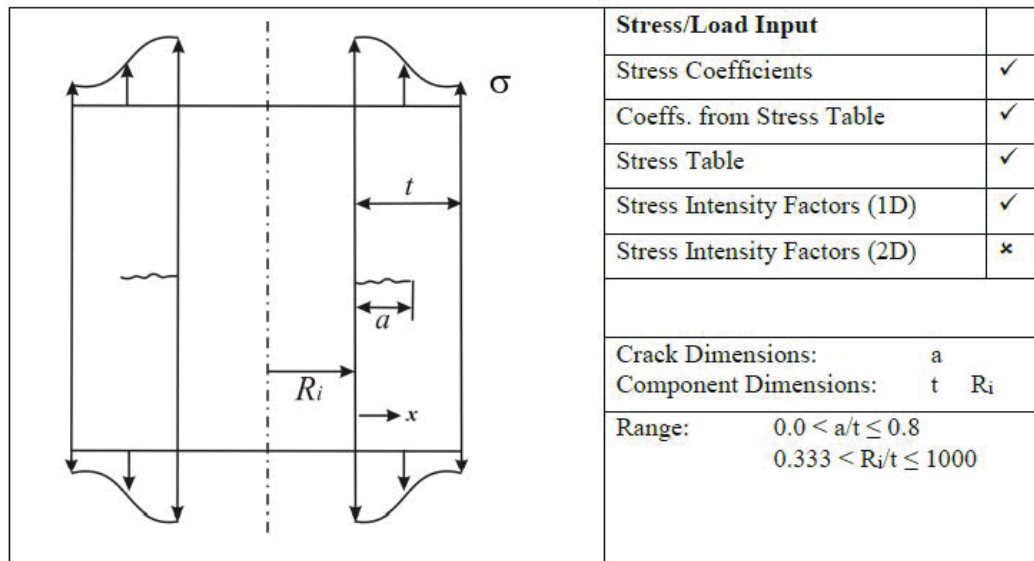This figure is based on Figure 1 of Reference [6].

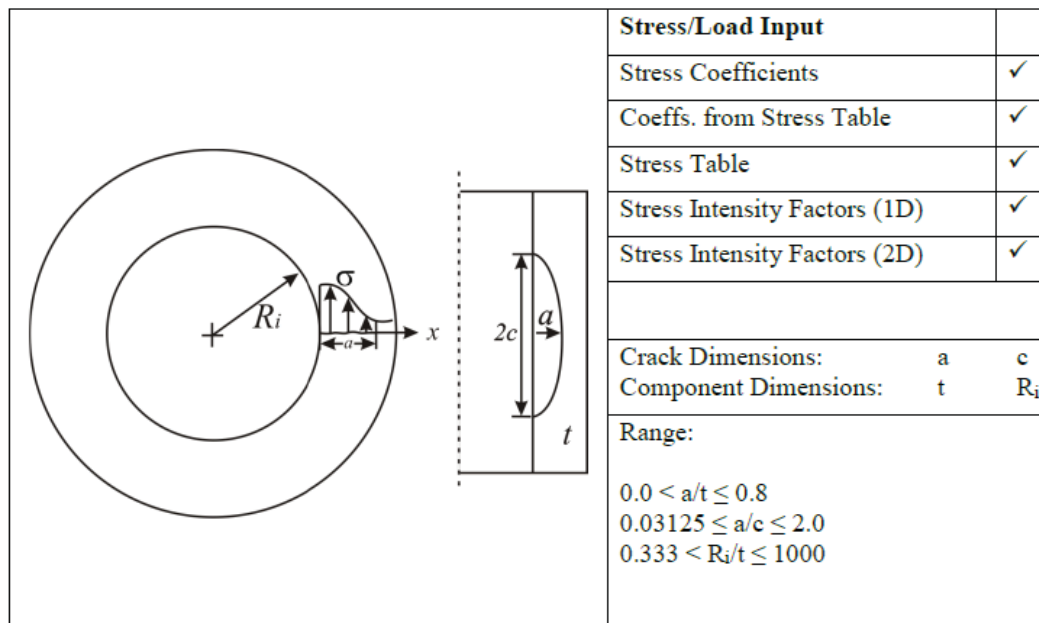Figure 6-2. Through-Wall Residual Stress as a Function of Depth

This figure is based on Figure 2 of Reference [6].

Crack Model: 301 - Full-Circumferential Crack in Cylinder on the Inside Surface

| Stress/Load Input	
Stress Coefficients	✓
Coeffs. from Stress Table	✓
Stress Table	✓
Stress Intensity Factors (1D)	✓
Stress Intensity Factors (2D)	✗
Crack Dimensions: a	
Component Dimensions: t R_i	
Range: $0.0 < a/t \leq 0.8$ $0.333 < R_i/t \leq 1000$	

(a) Full Circumferential Flaw

Crack Model: 305 - Semi-Elliptical Longitudinal Crack in Cylinder on the Inside Surface (API 579)

Stress/Load Input	
Stress Coefficients	✓
Coeffs. from Stress Table	✓
Stress Table	✓
Stress Intensity Factors (1D)	✓
Stress Intensity Factors (2D)	✓
Crack Dimensions: a c	
Component Dimensions: t R_i	
Range: $0.0 < a/t \leq 0.8$ $0.03125 \leq a/c \leq 2.0$ $0.333 < R_i/t \leq 1000$	

(b) Axial Flaw

Figure 6-3. Flaw Models on the Inside Surface of a Cylinder

This figure is based on Figure 27 of Reference [6].
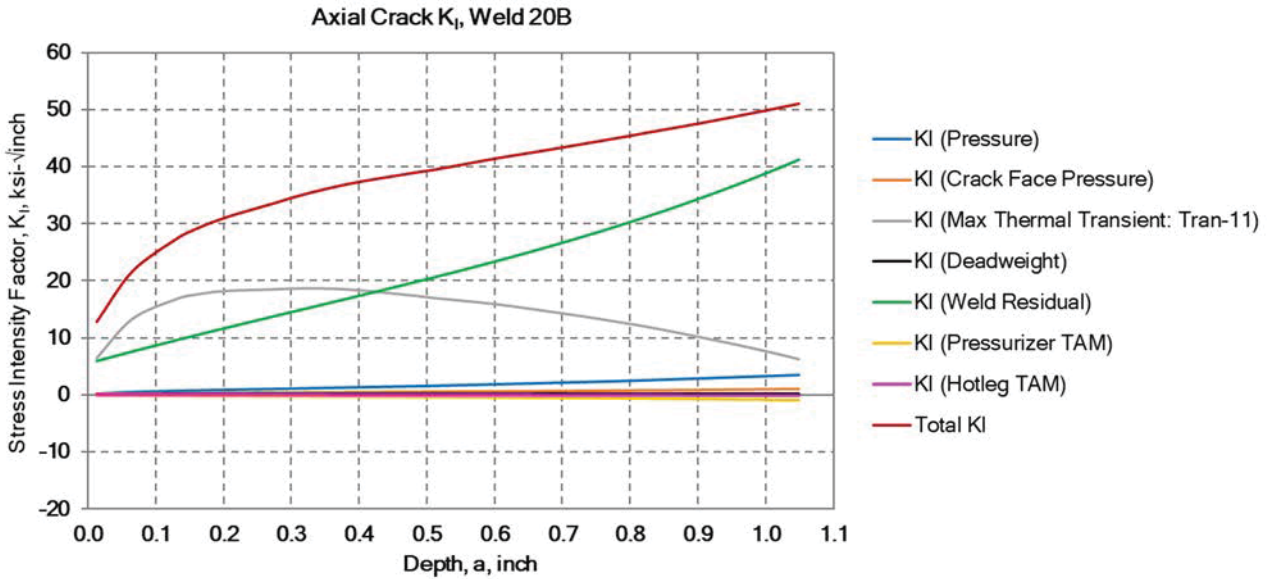
(a) Semi-elliptical Axial Crack
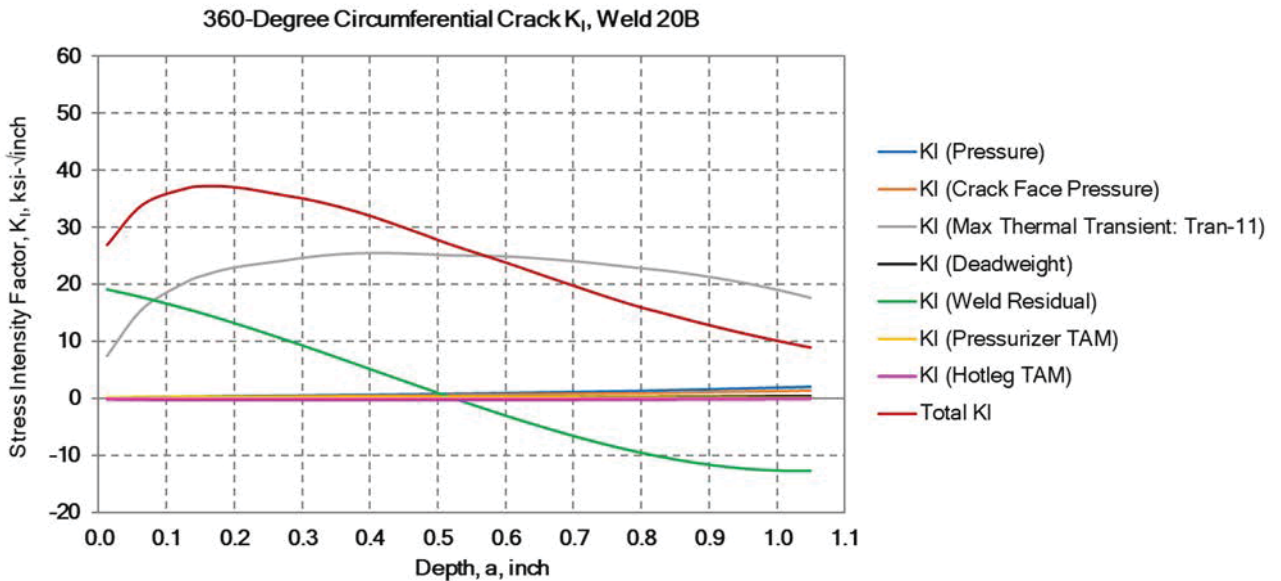
(b) 360-Degree Circumferential Crack

Figure 6-4. Maximum Stress Intensity Factor of Weld 20B

Note:
Figures above were obtained from Reference [6]
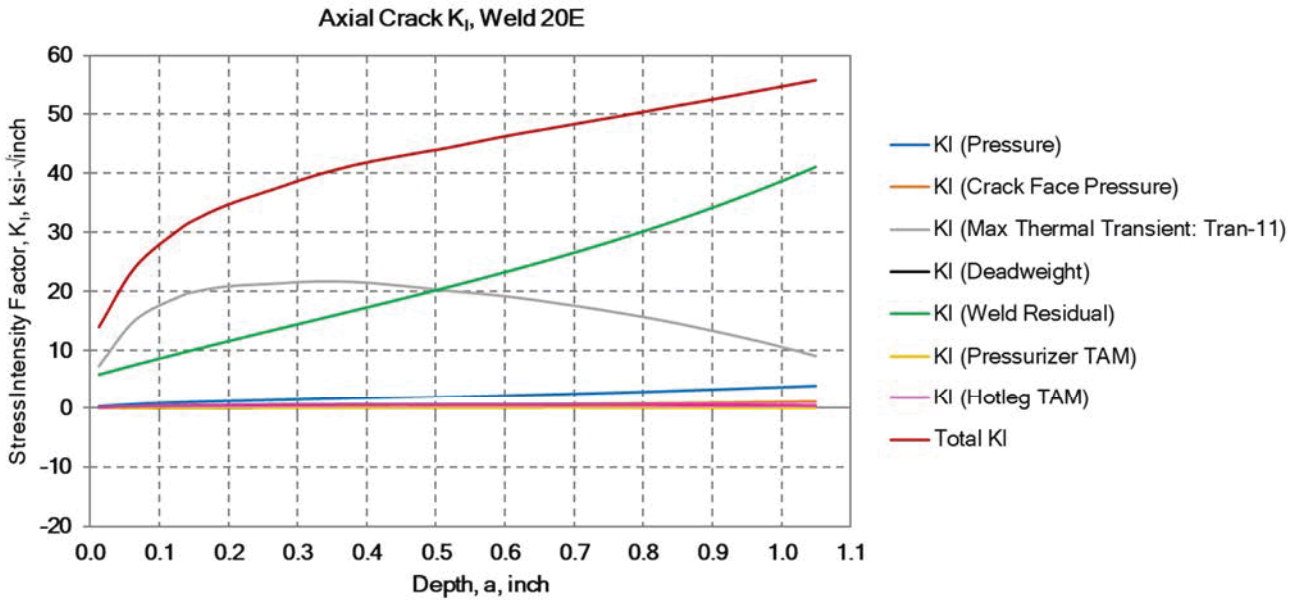
(a) Semi-elliptical Axial Crack
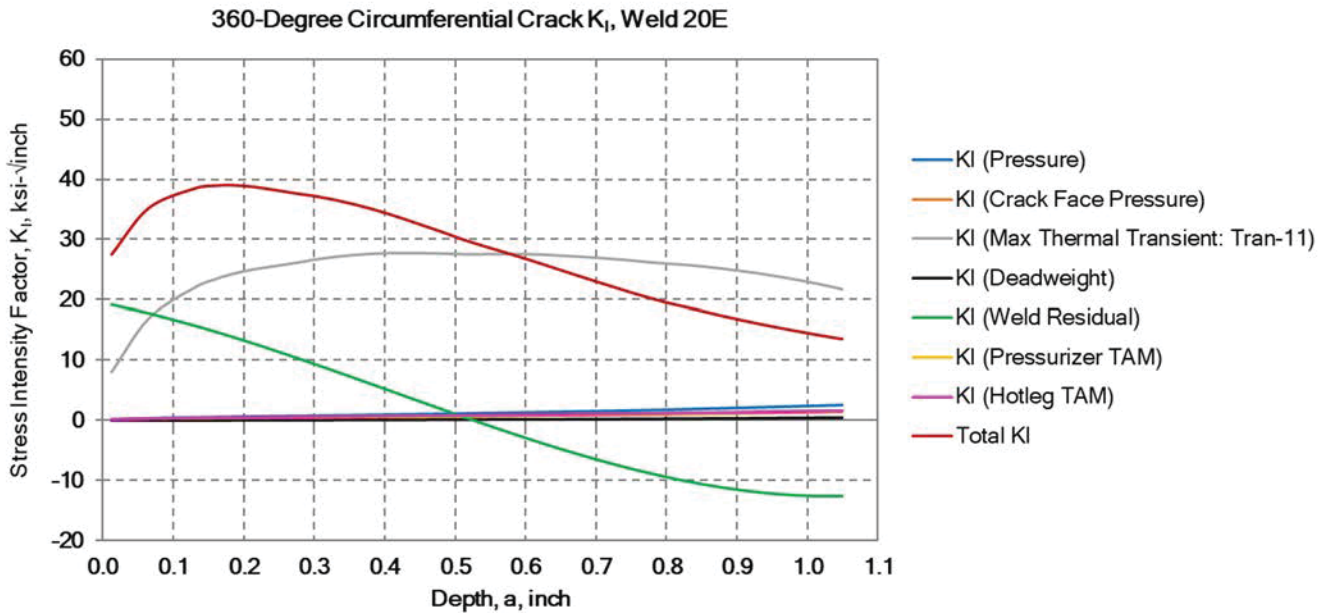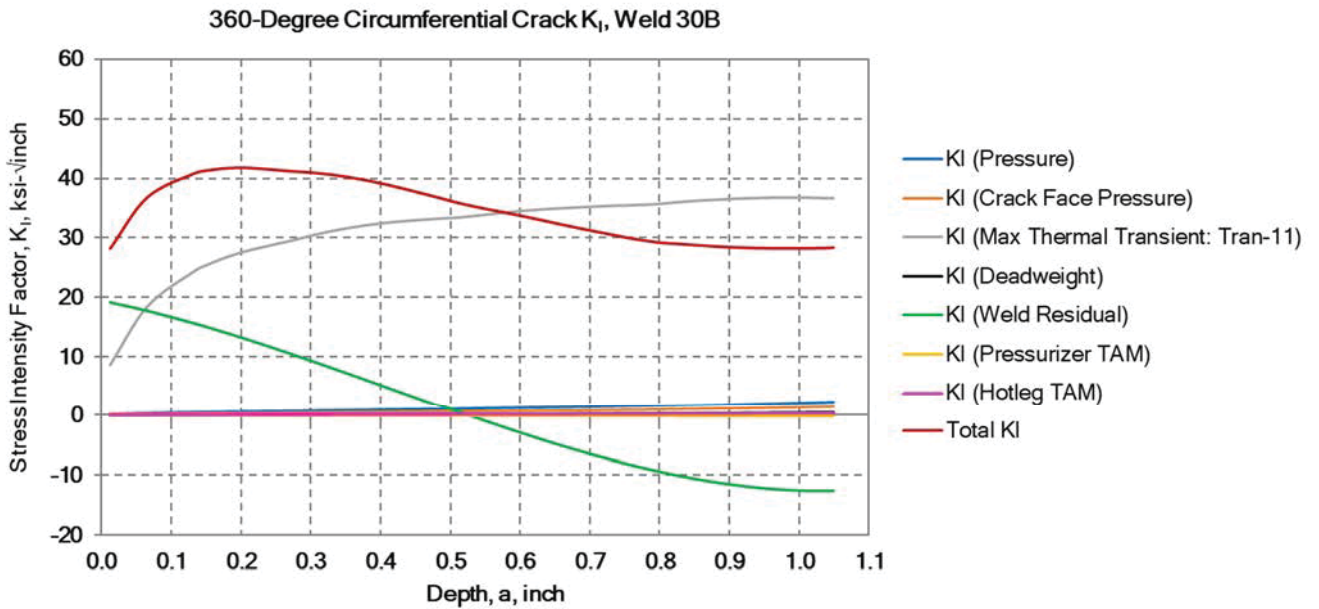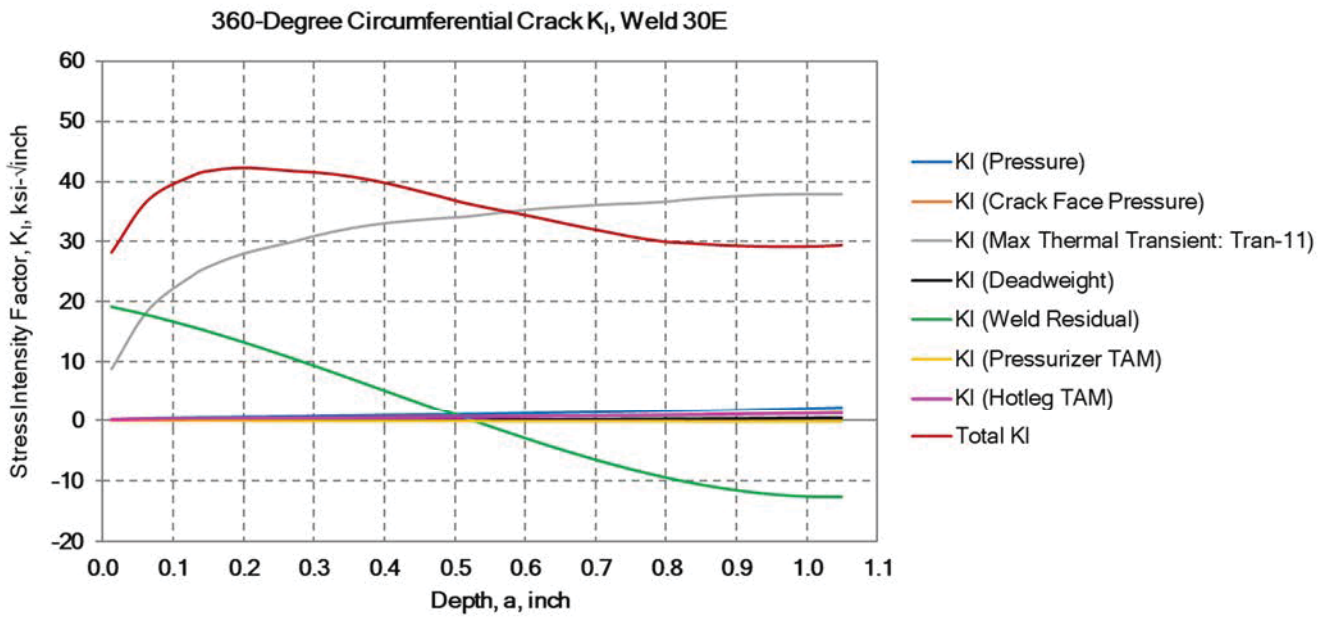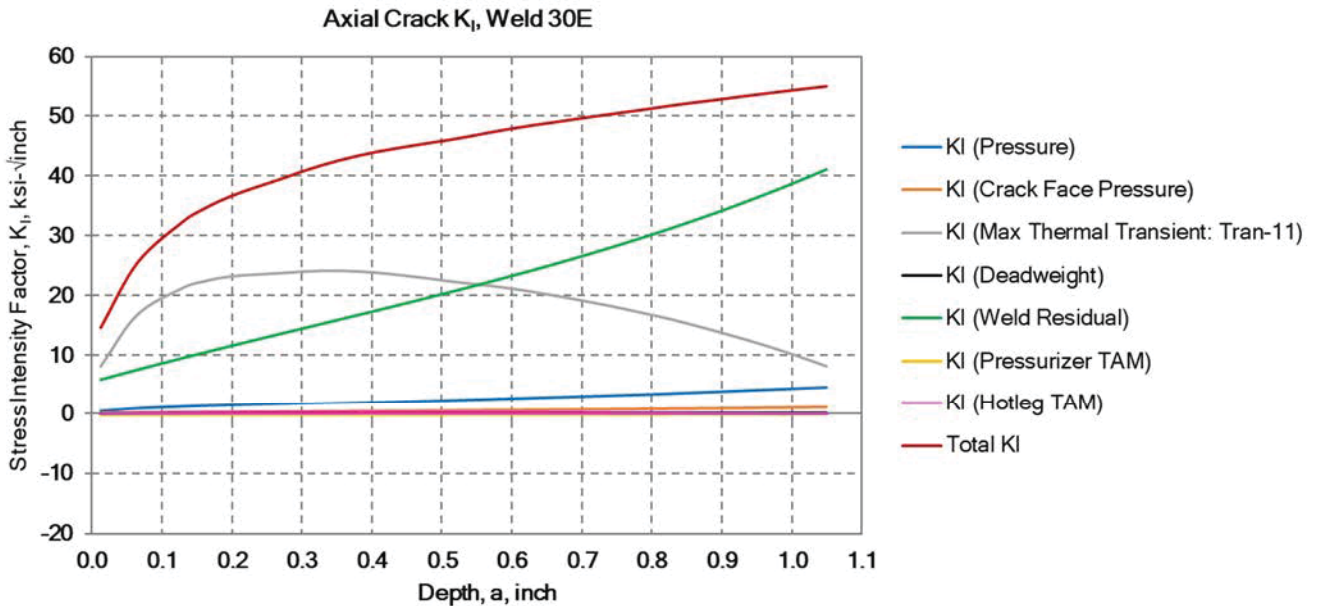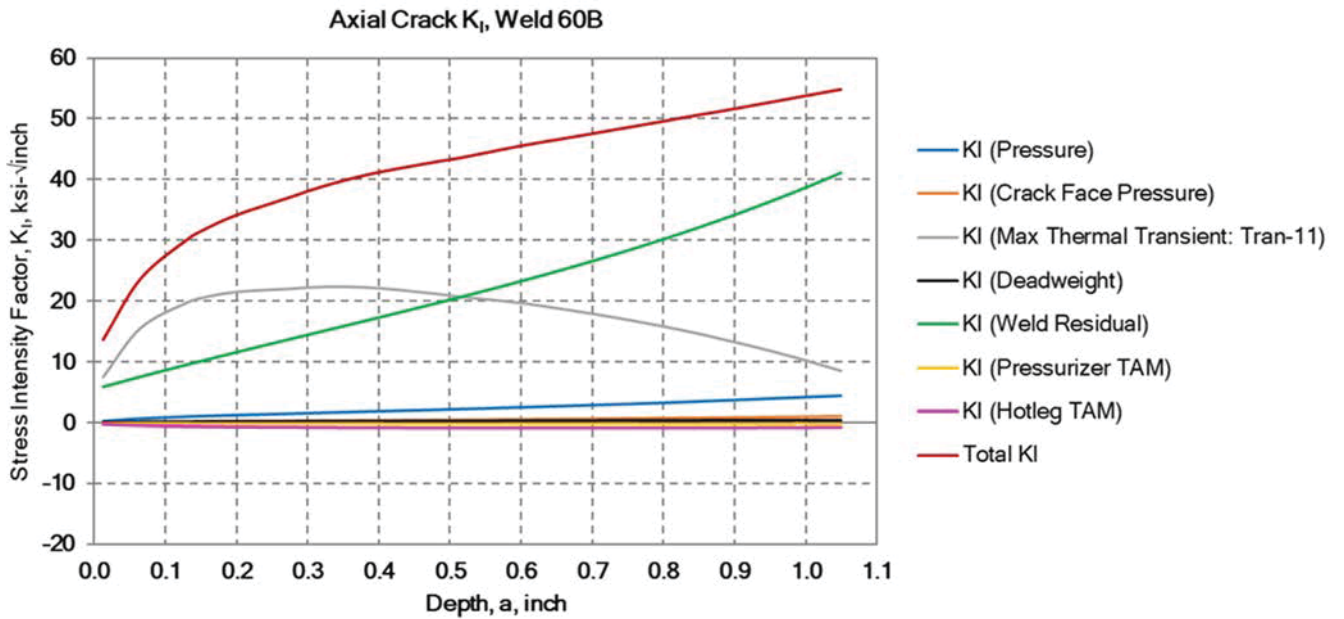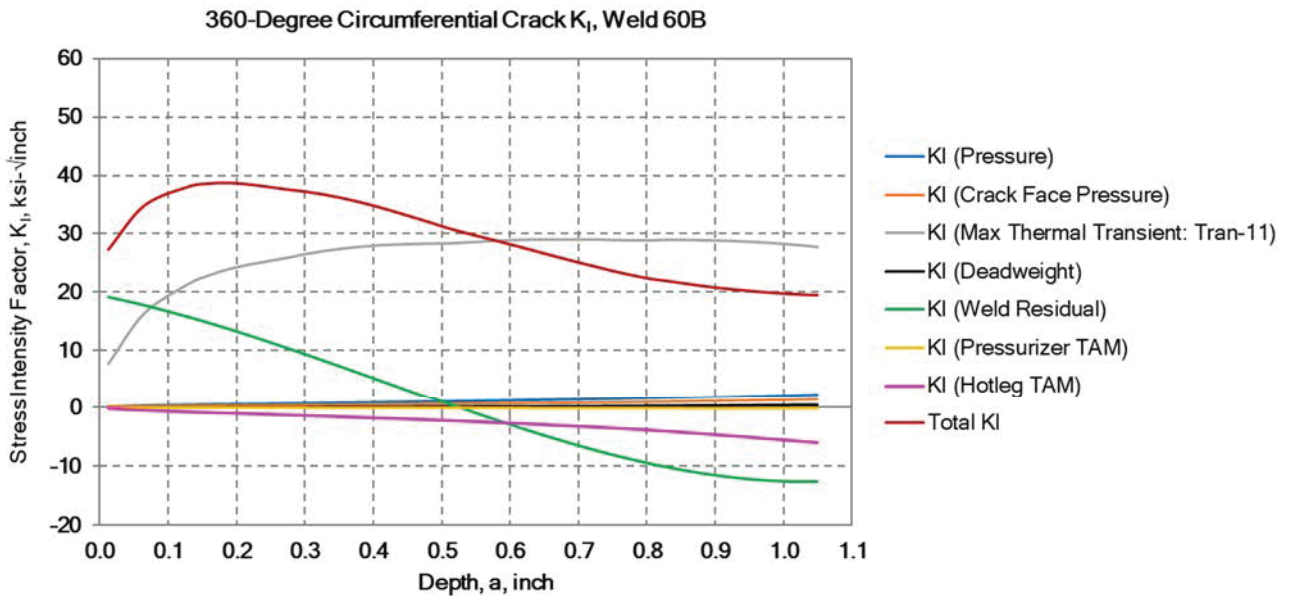

(b) 360-Degree Circumferential Crack

Figure 6-5. Maximum Stress Intensity Factor of Weld 20E

Note:
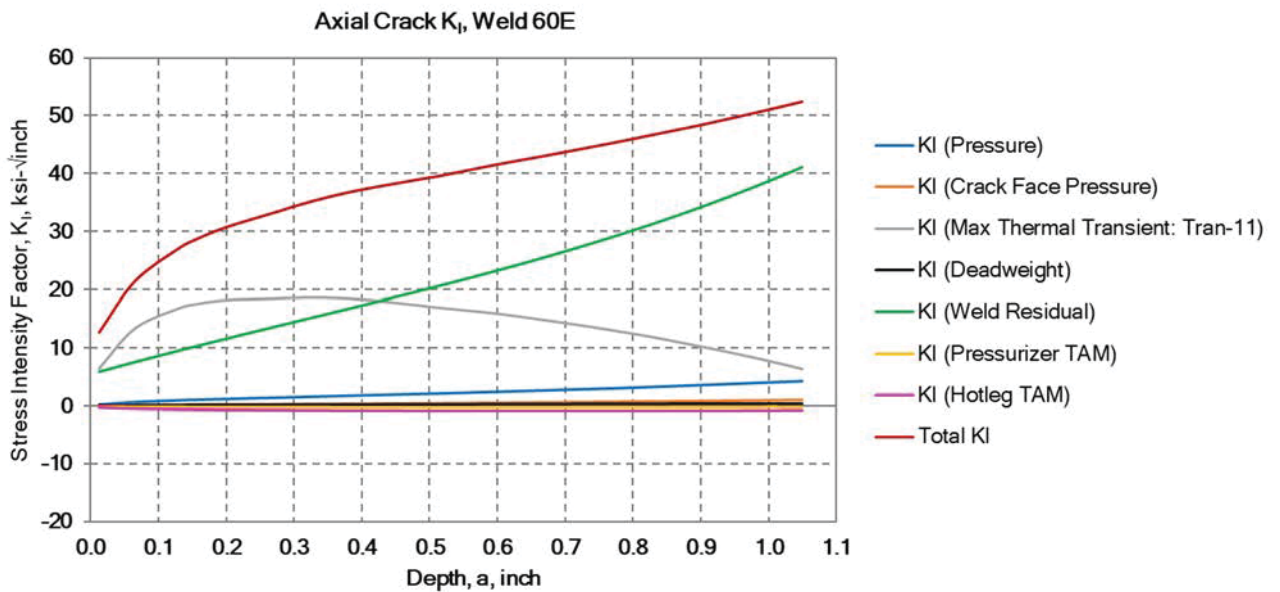Figures above were obtained from Reference [6]
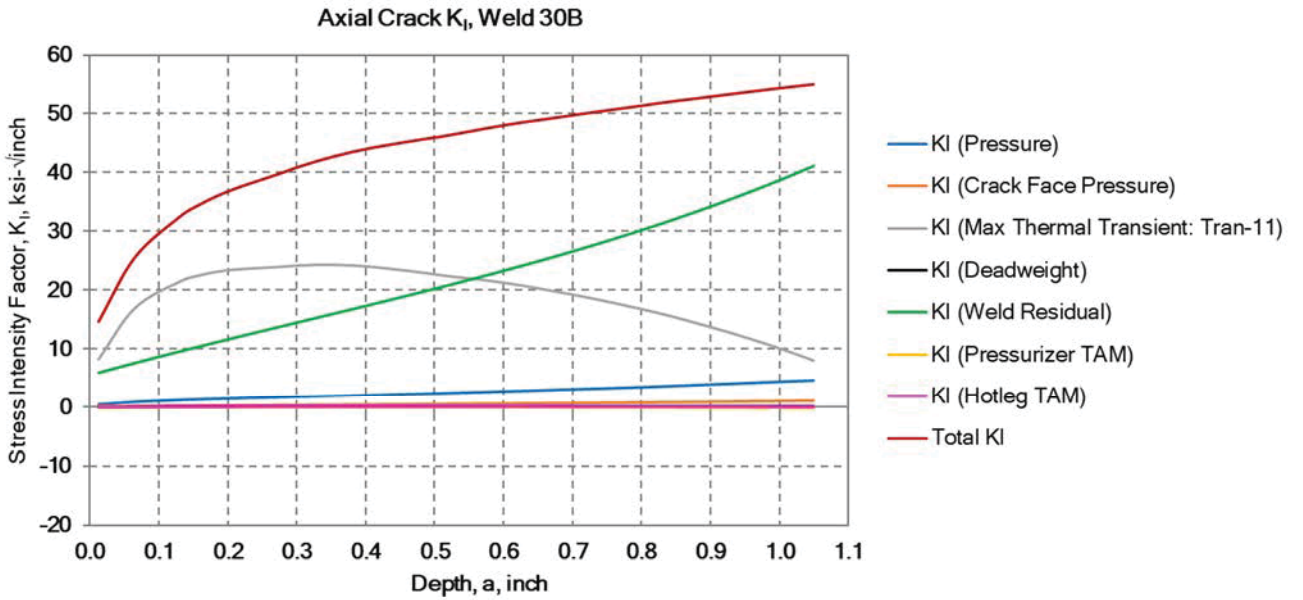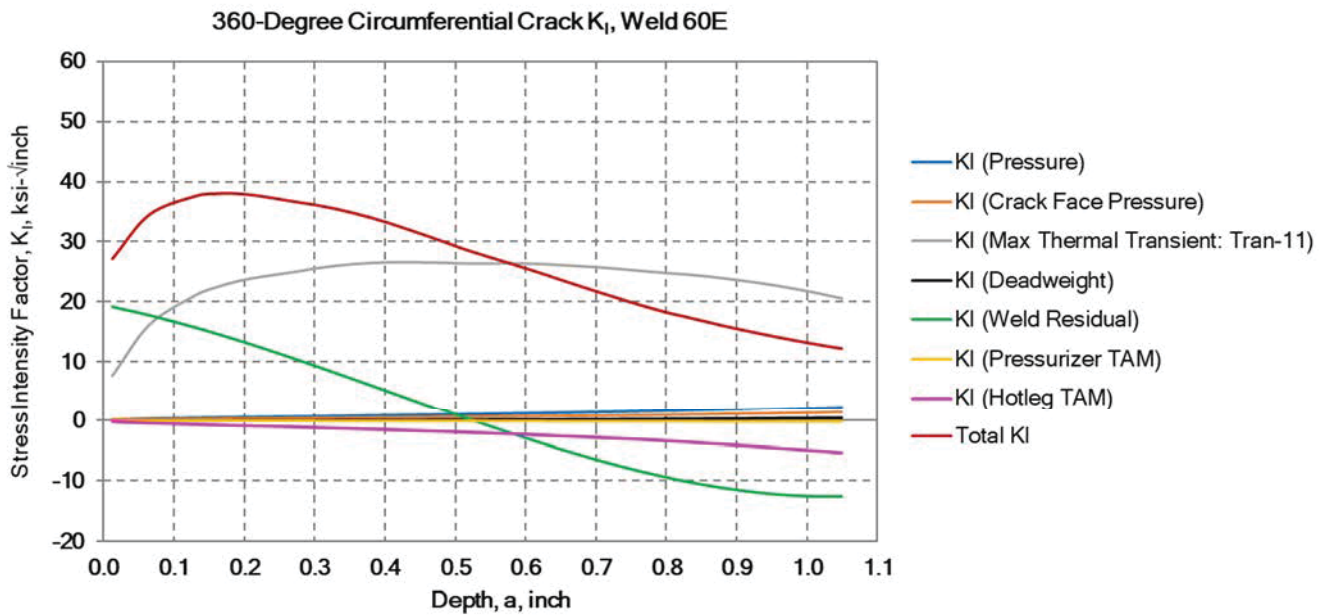
(a) Semi-elliptical Axial Crack

(b) 360-Degree Circumferential Crack

Figure 6-6. Maximum Stress Intensity Factor of Weld 30B

Note:
Figures above were obtained from Reference [6]

(a) Semi-elliptical Axial Crack

(b) 360-Degree Circumferential Crack

Figure 6-7. Maximum Stress Intensity Factor of Weld 30E

Note:

Figures above were obtained from Reference [6]

(a) Semi-elliptical Axial Crack

(b) 360-Degree Circumferential Crack

Figure 6-8. Maximum Stress Intensity Factor of Weld 60B

Note:
Figures above were obtained from Reference [6]

(a) Semi-elliptical Axial Crack

(b) 360-Degree Circumferential Crack

Figure 6-9. Maximum Stress Intensity Factor of Weld 60E

Note:
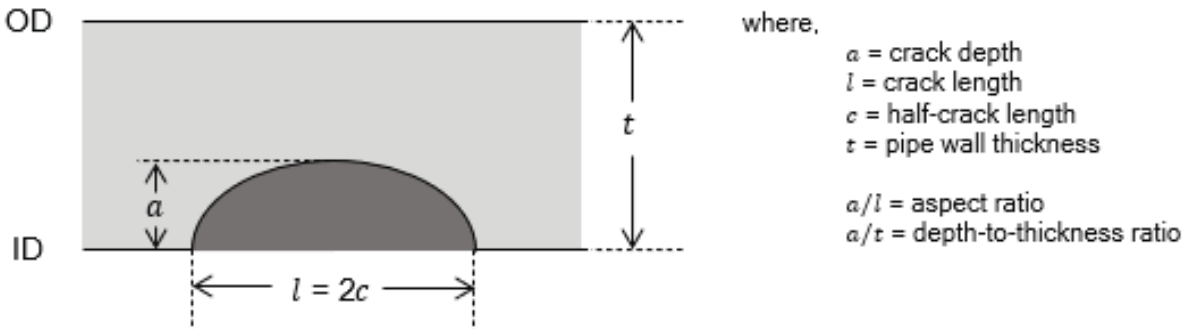Figures above were obtained from Reference [6]

where,

a = crack depth
l = crack length
c = half-crack length
t = pipe wall thickness

a/l = aspect ratio
a/t = depth-to-thickness ratio

Figure 6-10. Flaw Description

This figure is extracted from Reference [6, Section 5.2]

Weld 60B or Weld 30B

Elbow Extrados

Elbow 60 or Elbow 30 Flank

Elbow Intrados
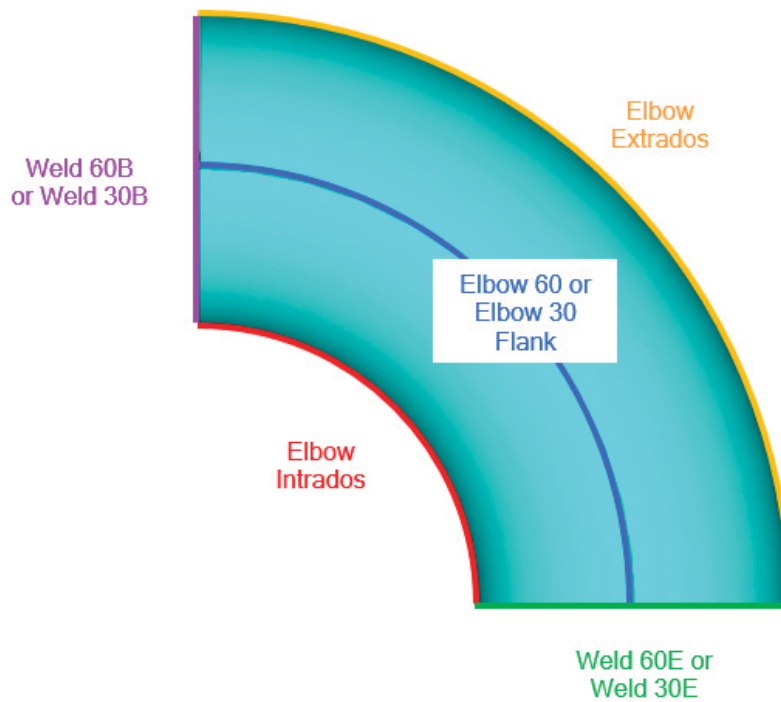
Weld 60E or Weld 30E

Figure 6-11. Surge Line Elbow

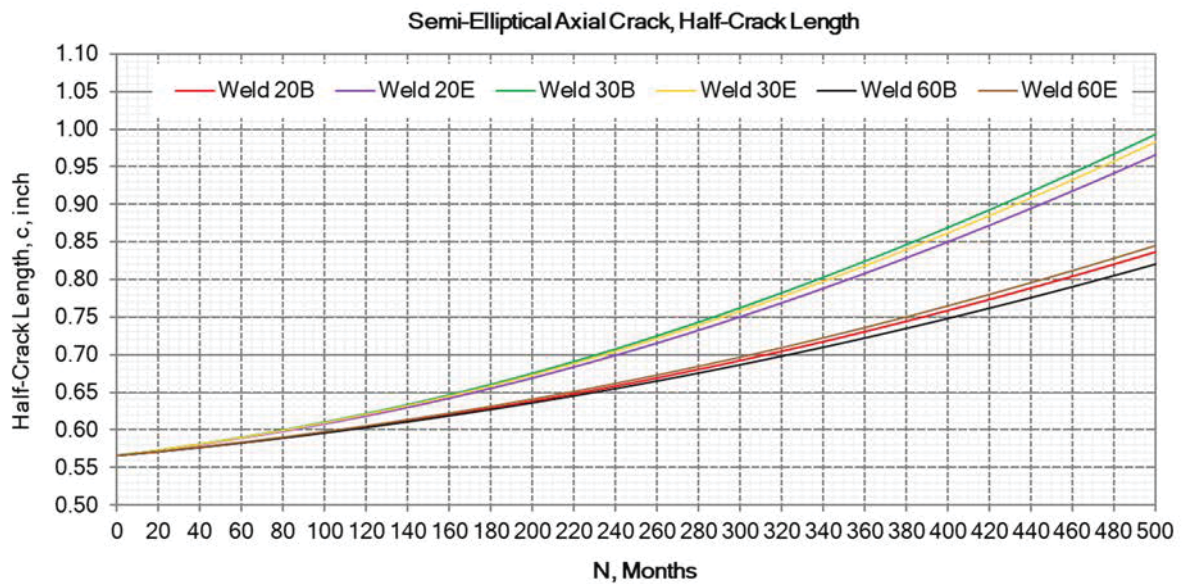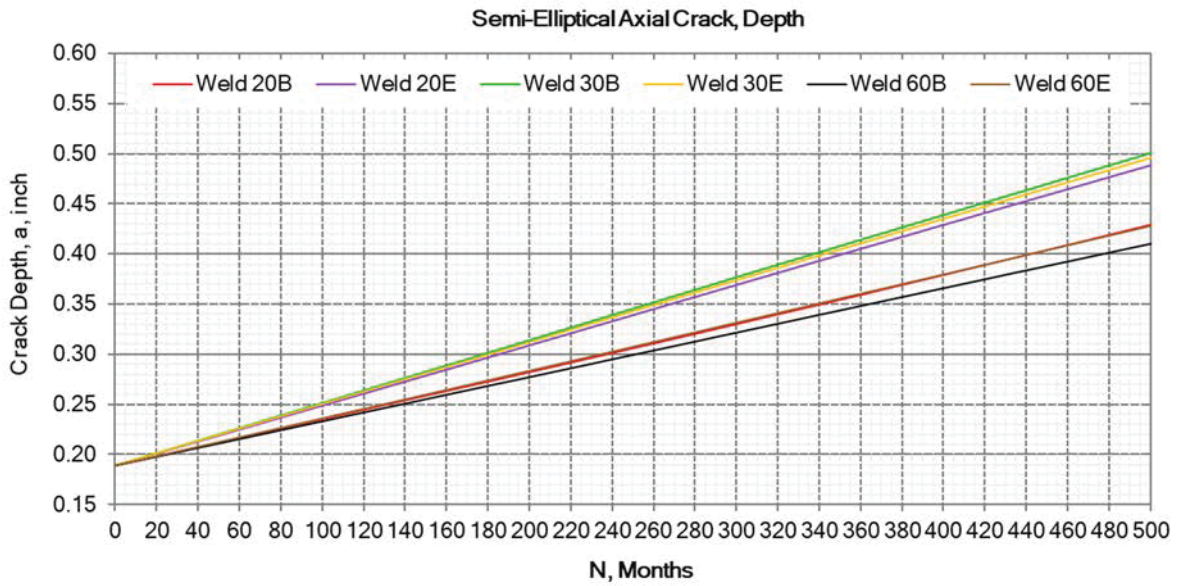This figure is extracted from Reference [6, Figure B-1]

Figure 6-12. Axial Crack: Crack Dimension (Crack Depth and Half-Crack Length) versus Number of Months

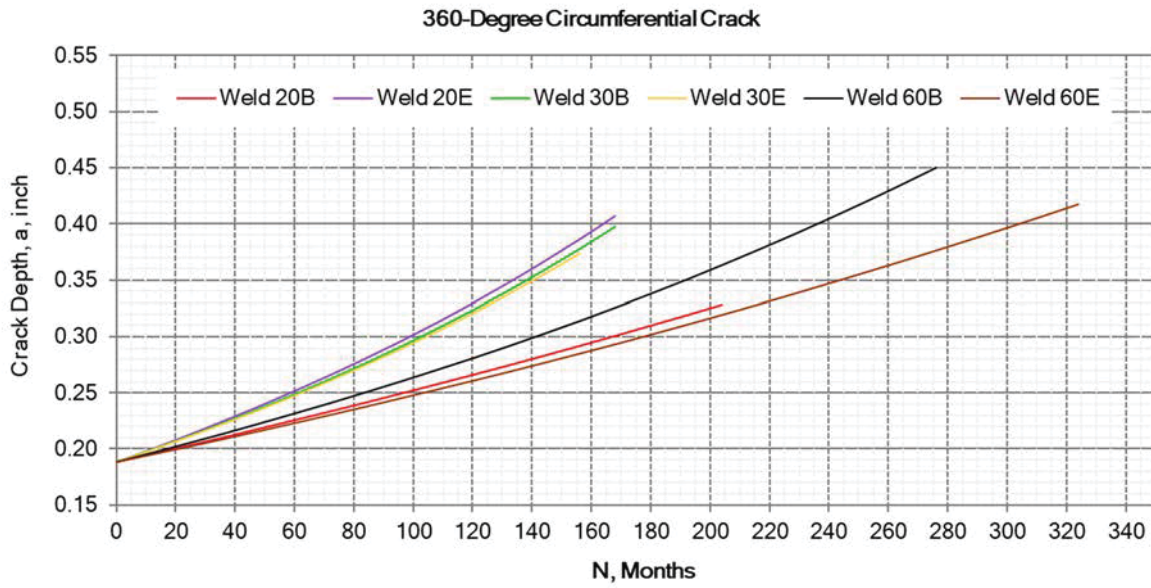This figure is extracted from Reference [6, Figure 34]

Figure 6-13. 360-Degree Circumferential Crack: Crack Depth versus Number of Months

This figure is extracted from Reference [6, Figure 35]

7.0   SUMMARY AND CONCLUSIONS

The flaw tolerance of the pressurizer surge line, at PVGS Units 1, 2, and 3, has been evaluated and the required successive inspection schedule has been determined for postulated flaws per the requirements of ASME B&PV Code, Section XI, Appendix L.

The flaw tolerance evaluation consisted of determining the loads at the bounding locations and performing finite element stress analyses to determine stresses due to thermal transients and other loads. The stresses are used to determine the allowable flaw sizes and perform a crack growth evaluation to determine the allowable operating period based on crack growth of a postulated flaw compared to allowable flaw sizes.

The allowable operating period for the bounding surge line location (Welds No. 30E) is at least 13 years. Therefore, per the guidelines of Table L-3420-1 of ASME B&PV Code, Section XI, Appendix L and IWB-2410 of ASME B&PV Code, Section XI, the successive inspection schedule for the surge line is **ten years**.

8.0 REFERENCES

1. ASME Boiler & Pressure Vessel Code, Section XI, 2013 Edition, "Rules of Inservice Inspection of Nuclear Power Plant Components."

2. Structural Integrity Associates, Inc. Calculation Package, *Updated Crack Growth Analysis of Pressurizer Surge Nozzle Full Structural Weld Overlays*, Revision 0, SI File No. 2000645.316.

3. Structural Integrity Associates, Inc. Calculation Package, *Updated Crack Growth Analysis of Hot Leg Surge Nozzle Full Structural Weld Overlays*, Revision 0, SI File No. 2000645.346.

4. Structural Integrity Associates, Inc. Calculation Package, *Transient Loads Definition for Updated Surge Line Analyses,* Revision 2, SI File No. 2000645.301.

5. Structural Integrity Associates, Inc. Calculation Package , *Palo Verde Pressurizer Surge Line Finite Element Analysis for Appendix L Evaluation,* Revision 0, SI File No. 2000645.302.

6. Structural Integrity Associates, Inc. Calculation Package, *Fatigue Crack Growth Calculation for the Palo Verde (Units 1, 2, and 3) Surge Line Appendix L Evaluation*, Revision 1, SI File No. 2000645.304.

7. Structural Integrity Associates, Inc. Calculation Package, *Allowable Flaw Size Determination for the Palo Verde (Units 1, 2, and 3) Surge Line Appendix L Evaluation*, Revision 1, SI File No. 2000645.303.

8. ASME Code Case N-809, "Reference Fatigue Crack Growth Rate Curves for Austenitic Stainless Steels in Pressurized Water Reactor Environments, Section XI, Division 1," Cases of the ASME Boiler and Pressure Vessel Code, June 23, 2015.

9. Palo Verde Nuclear Generating Station Calculation No. 13-MC-ZZ-595, Revision 7, "RCS Pressurizer Surge Line Nuclear Class 1 Analysis", SI File No. 2000645.214.

10. Structural Integrity Associates, Inc. Calculation Package, *Surge Line Elbow Finite Element Model,* Revision 2, SI File No. PV-30Q-311.

11. Structural Integrity Associates, Inc. Calculation Package, *Structural Analysis of Surge Line*, Revision 0, SI File No. PV-21Q-311.

12. Structural Integrity Associates, Inc. Calculation Package, *Surge Line Elbow Stress Analysis*, Revision 3, SI File No. PV-30Q-313.

13. pc-CRACK 5.0, Version Control No. 5.0.0 CS, Structural Integrity Associates, Inc. Jan. 7, 2021.

14. Piping Loads for the PV Surge Line, ME101 Run 7/10/2015, FILENAME: RC501-NGF-BOL.INP, APS CALCULATION 13-MC-RC-0501, PROBLEM RC-501, SI File No. 2000645.217 and File: psurg loads.xlsx, SI File 2000645.204.

15. **ANSYS** Mechanical APDL, (UP20170403) and Workbench (March 31, 2017) Release 18.1 SAS IP, Inc.

16. Palo Verde Nuclear Generating Station Calculation No. 13-MC-RC-0501 Addendum 1, Rev. 21, "Reactor Coolant System – Pressurizer Surge Line", Excerpt, July 2005, SI File No. 2000645.214.

17. Bechtel Power Corporation Isometric Sketch Sheet 13-P-RCF-101, and Unit specific Isometrics, Containment Building Reactor Coolant Isometric Pressurizer Surge Line, SI File No. 2000645.204.

   6a. Isometric Drawing 01-P-RCF-101, Revision 6

   6b. Isometric Drawing 02-P-RCF-101, Revision 5

   6c. Isometric Drawing 03-P-RCF-101, Revision 4

18. ASME Boiler and Pressure Vessel Code, Section II, Part D – Material Properties, 2001 Edition with Addenda through 2003.

19. PVGS Calculation 13-MC-ZZ-0595, Revision 7, Technical Report TR-4825-1, Teledyne Engineering Services, Class 1 Isometric Surge Line Sketch, SI File No. 2000645.202.

20. *Approximate Elastic Stress Estimates for Elbows Under Internal Pressure*, Hong et al., International Journal of Mechanical Sciences 53 (2011) 546-535.

21. *Development of EPFM Procedure for Axially Flawed Pipe Using Z Factor Based On CVN,* Hasegawa et al., 2006 ASME Pressure Vessels and Piping Division Conference.

22. E-mail from K. James (APS) to J. Axline (SI), Subject: "Changes to loads calc for PV Surge line WOL FCG Redo and Appendix L Eval, SI Project 2000645", Dated 12/9/2020 6:58 AM, SI File No. 2000645.208. Discussion of:

   - CALC 13-MC-RC-0501 Rev. 17 was updated to Rev. 21.
   - CALC 13-MC-ZZ-0595 Rev. 6 was updated to Rev. 7.
   - High Thermal Performance (HTP) fuel - (EWR 17-14728-031)

23. Surge Line Piping Stress Analysis, SNUM AN5824-071015.txt, SI File No. 2000645.211.

24. **SI-TIFFANY** Version 3.2, April 6, 2020.

25. Structural Integrity Associates Quality Assurance Manual, Revision 12.1, February 11, 2022.

26. Structural Integrity Associates, Inc. Calculation Package, *Loads on the Surge Line Elbow Above Hot Leg*, Revision 3, SI File No. PV-30Q-312.

27. NUREG-0313, Rev.2, "Technical Report on Material Selection and Processing Guidelines for BWR Coolant Pressure Boundary Piping," U.S. Nuclear Regulatory Commission, January 1988 (ADAMS Accession No. ML031470422).

28. API 579-1/ASME FFS-1, Fitness-For-Service, June 2016.